1989

Synthesis and Study of N-(4-nitrobenzofurazan)-monoaza-18-crown-6: A Metal Sensitive Fluorophore

Shelley A. Krause
Loyola University Chicago

SYNTHESIS AND STUDY OF N-(4-NITROBENZOFURAZAN)-MONOAZA-18-CROWN-6: A METAL SENSITIVE FLUOROPHORE

by

Shelley A. Krause

A Dissertation Submitted to the Faculty of the Graduate School of Loyola University of Chicago in Partial Fulfillment of the Requirements for the Degree of Doctor of Philosphy

August

1989

ACKNOWLEDGEMENT

I want to thank Dr. Kenneth W. Street for his guidance, advice, and encouragement thoughout my graduate career and my research efforts. I also extend my gratitude to Dr. Bruno Jaselskis for providing extra support and assistance during the last several years.

I am very grateful to the other members of my committee; Dr. Carl E. Moore, Dr. David Crumrine and Dr. John Ferraro, for their extra efforts on my behalf in order to help me complete my requirements.

Special thanks to the other members of the Loyola University Chemistry Department faculty and staff who gave invaluable assistance over the years. This appreciation is also extended to my fellow graduate students, both past and present, who not only provided assistance with my research but moral support as well.

I am grateful to several people outside the Loyola community who provided special services or equipment: Ron Glowinski of OrgSyn who provided additional synthesis, Dennis DeSalvo of Stepan Chemical for use of the Poropak column, Chan Patel of Witco for donating analytical services, and Kathleen Martin for providing FT-IR work.

I acknowledge Loyola University for financial assistance through several teaching assistantships and a University fellowship.

I am grateful to members of the Northeastern Illinois Chemistry department for their support, especially Dr. Howard L. Murray who is probably chiefly responsible for my taking this path in the first place.

VITA

The author, Shelley Ann Krause, is the daughter of Edward Krause and Jessie (Reid) Krause. She was born August 14, 1952, in Chicago, Illinois.

Her elementary education was obtained in the public schools of Chicago, Illinois. Her secondary education was completed in 1970 at Amundsen High School, Chicago, Illinois.

In January, 1975, Ms. Krause entered Wilbur Wright College in Chicago, Illinois, receiving the Associate of Arts Degree in the Physical Sciences, with High Honors, in May, 1976. In May of 1977 she entered Northeastern Illinois University, and received the degree of Bachelor of Arts in Chemistry, with Honors, in August 1979.

In September, 1980, Ms. Krause was granted an assistantship in chemistry at Loyola University of Chicago, and was granted a University Fellowship in 1984, enabling her to complete the Doctor of Philosophy in Chemistry in 1989.

Ms. Krause has been employed as an instructor of chemistry at Northeastern Illinois University since September, 1987.

In April, 1986, Ms. Krause published a paper from her research entitled "A New Metal Sensitive Fluorescence Reagent." in Analytical Letters.

TABLE OF CONTENTS

LIST OF TABLES

LIST OF FIGURES

INTRODUCTION

The alkali and alkaline earth metal cations, especially sodium, potassium, calcium and magnesium, occupy positions of major importance in biological and environmental settings. Aside from classical methods of analysis, most of the determinations of these cations have been performed by atomic absorption and emission methods. Over the years it has not been as easy to analytically determine these cations in comparison to most of the transition metal and heavy metal cations, particularly in the areas of UV-visible spectrophotometry and fluorescence spectrophotometry. Few complexing reagents exist for these groups unlike the colorimetric chelating agents, (dithizone, diphenyldithiocarbazone), and fluorescent chelating agents, (8-hydroxyquinoline, alizarin red, benzoin) frequently used for the transition metal and heavy metal cations. In the last twenty years the synthesis and development of crown ether complexing reagents for alkali and alkaline earth cations has expanded into a major field. The scope of this dissertation is to present the synthesis and analytical applications of a new fluorescent NBD

(4-chloro-7-nitrobenzofurazan) crown reagent for the analytical determination of these and other metal cations.

Complexation and Properties of the Crown Ethers

Natural macrocyclic compounds such as the antibiotic valinomycin (1,2) and the porphyrin rings (1,3) in hemoglobin and cytochrome systems have interested analysts because of their high selectivities and complex stabilities for certain metal cations. The selective complexation observed in the case of potassium ion vis-a-vis sodium in the case of the polyether, valinomycin (4,2) and the extremely strong complexation of iron with the porphyrin heme group (a tetraaza macrocycle) are well known phenomena vital for biological functioning. In the late 1960's Pedersen produced a number of synthetic macrocyclic polyethers that became known as crown ethers (5). The first three structures in Figure 1. are examples of three common crown ethers; 1) 18-crown-6; 2) benzo 15-crown-5; and 3) dibenzo-18-crown-6. Macrocyclic structures such as these typically contain central hydrophilic cavities ringed with electronegative or electropositive binding atoms such as the ether oxygens and exterior flexible frameworks exhibiting hydrophobic behavior characteristic of the repeating ethylene units illustrated in the same examples. They show a remarkable ability to bind a wide variety of cations or anions and in many cases undergo

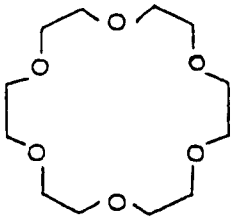

18-CROWN-6

1

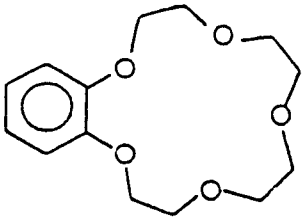

BENZO-15-CROWN-5

2

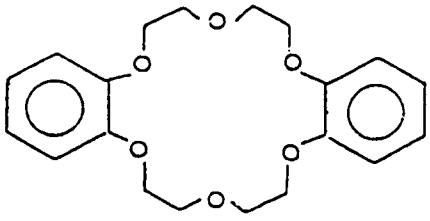

DIBENZO-18-CROWN-6

3

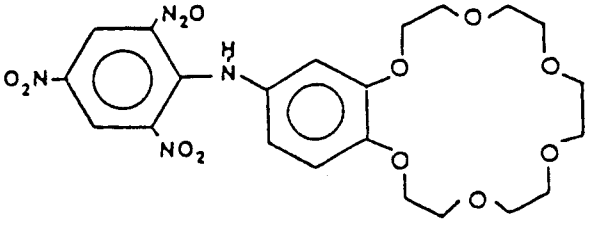

TAKAGI REAGENT

4

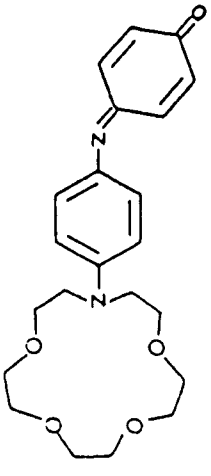

5

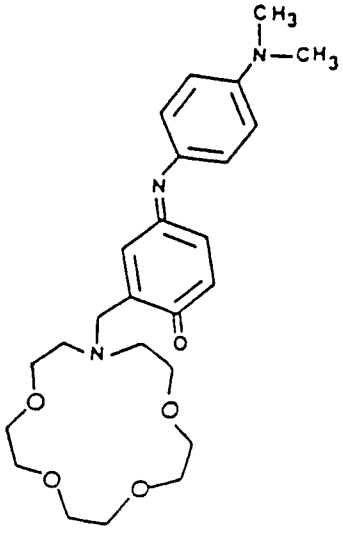

6

FIGURE 1. SOME COMMON CROWN STRUCTURES.

marked conformational changes during complexation. Their hydrophobic exteriors allow them to solubilize ionic substances in both nonaqueous solvents and in membrane media thus making them extremely useful in the fields of organic chemistry and biochemistry (1,6). The most familiar action of the polyethers is their strong affinity for the alkali and the alkaline earth metal cations. Complexes form by the electrostatic interaction occurring between the metal cation and the negatively charged oxygen atoms symmetrically placed in the ring (6). Although the formation of a stable complex is dependent on many factors, the main criterion is that there be a match between the size of the metal cation and the size of the hole in the heterocyclic ring. The ligand 18-crown-6 (Structure 1 of Figure 1) has a cavity that is 2.6 Å - 3.2 Å wide, and K^+, the alkali metal cation forming the most stable complex, has an ionic diameter of 2.7 Å, which conforms to the rule stated above. Other examples of stable complexes of familiar crown ethers with their preferred alkali metals are listed in the following Table 1.

Table 1. Diameters of Selected Cations and Cyclic Polyether Cavities (6).

Cation	Ionic Diameter Å	Polyether	Diameter of Cavity Å
Lithium	1.20	14-Crown-4	1.2 - 1.5
Sodium	1.90	15-Crown-5	1.7 - 2.2
Potassium	2.66	18-Crown-6	2.6 - 3.2
Ammonium	2.84	21-Crown-7	3.4 - 4.3
Silver	2.52		
Barium	2.70		

The crown ethers have been found to form, primarily, 1:1 metal:crown complexes with a large array of metal ions. When the ratio of the diameter of the cavity to the diameter of the metal ion is much smaller than 1.0, the formation of 1:2 and 2:3 "sandwich" and "club-sandwich" complexes have also been observed (7). In many cases, the relative sizes of the polyether cavity and the metal ion control the stoichiometry of the resulting complex.

In addition to the relative sizes of the ion and the hole in the polyether ring, other conditions mediate complex formation. Factors that influence the stability of the complexes are: 1) the number of oxygen atoms in the polyether ring; 2) the co-planarity of the oxygen atoms, (oxygen is considered co-planar if it lies in the same plane as all of the other oxygens in the ring); 3) the symmetrical placement of the oxygen atoms; 4) the basicity

of the oxygen atoms, (the stability of the complex is higher with more basic oxygen atoms - one attached to an aromatic ring being less basic than one attached only to aliphatic carbon atoms); 5) steric hindrance in the polyether ring; 6) the tendency of the ions to associate with the solvent. (The complexes are formed by the following equation:

$$(\text{metal}^{m+})\text{-n solvent} + \text{crown ether} \rightleftharpoons \text{crown ether-}(\text{metal}^{m+}) + \text{n-solvent} \qquad \text{(Eq. 1)}$$

Therefore, the formation of the complex of a particular ion will be minimized or prevented if the ion is too strongly associated with the solvent. In a given group of elements, the solvation energy is usually an inverse function of the ionic diameter.); and finally, 8) the electrical charge density of the ion influences the strength of the complex formed (5).

Pedersen's landmark paper in 1967 presented over thirty macrocyclic ethers of various sizes containing different numbers of donor oxygens in the ring. Since then, several synthetic polyethers, polyamines, polythioethers and other related compounds have been shown to possess interesting and very unusual ion binding properties (1). The donor atoms can be elements other than the usual oxygen atoms. Nitrogen or sulfur have also been

used as donor atoms, and it is not uncommon to have crowns containing two or three different heteroatoms.

The effect of substituting nitrogen for oxygen on the metal binding properties of the cyclic polyethers has been studied and the influence on the complexation of potassium vs. silver ions has been compared. The complexation of potassium was appreciably weakened as nitrogen was substituted into the ring. The stability constant decreased in the order of decreasing electronegativity of the substituent group: O > NR > NH. The effects on silver (I) complexation were exactly the opposite with the stability increasing with substitution. It was concluded that electrostatic bonding exists in potassium complexes whereas the silver complexes have both electrostatic and covalent bonding (8). Because of this phenomenon, the formation of transition metal complexes is more often observed with crown amines and crown amine ethers than with the polyethers.

Thus, it can be easily seen that the synthetic macrocyclic ethers and amines can be extremely useful for complexing various metal cations for analysis. It is obvious, however, that these molecules are not useful to analytical chemists dealing in spectroscopy, because in their existing form they have no chromophores in the UV or visible range. The following sections will review the development of both chromophoric and fluorophoric crown

ether systems which have enabled analytical chemists to spectroscopically determine the presence and concentration of several alkali and alkaline earth metal cations, as well as some transition metal and heavy metal cations.

REVIEW OF RELATED LITERATURE

Complexation and Extraction of Metal Cations with Chromophoric Counter-ions

Early work concerning the complexation of crown ethers with alkali metal cations was limited to two or three methods such as calorimetry (9,10,11), conductance (12) and potentiometry using cation-selective electrodes (8), because most of the cyclic polyethers possessed no ability to absorb or emit light in the UV-visible range. The spectrophotometric measurement of the effect of complexation with alkali metal ions was only possible when the benzo- and dibenzo crowns were used since their aromatic system of electrons made them active in the UV region, generally in the 274-290 nm range of the spectrum. Pedersen first discussed the fact that the main absorbance band of dibenzo-18-crown-6 (DB18C6) appearing at 275 nm in methanol, displayed obvious changes when complexation occurred with alkali metal salts. The principle effect was usually the appearance of a second band at 280 nm (5,13,15). Since the new peak was never clearly separated from the main one, it could not be used for precise quantitative measurements nor for determination of the stability constants of DB18C6 with any of the alkali metal cations. However, it has been used extensively for qualitative evidence of complexation (14).

Pedersen described a new and better means of comparing the relative complexing powers of the different cations. The extraction method, as he named it, had some advantages over the reported spectral method. The complexation efficiencies could actually have values which defined them. Thus, the saturated crown ethers which had no native absorbance at 275 nm could also be evaluated (15). The means of determining the concentration of complexed alkali metal cations was via the formation of an ion-pair-complexed within a crown ether cavity - where the pairing anion was a highly colored dye such as picrate. Once the ion-pair was formed in the aqueous phase, the neutral complex, which formed with the added crown ether, was readily extracted into an organic phase. The absorbance at the λ_{max} of the dye anion in the organic phase was then measured with a UV-visible spectrophotometer. This measurement was easily related to the concentration of the complexed alkali metal ion whose stoichiometry was 1:1:1 metal ion:picrate:crown ether (15).

The extraction method with picrate and other dye anions was further developed and became the major means of spectroscopically determining complexation behavior and stability constants of the crowns with many different metal cations. Most of the research in this area dealt with the picrate anion measured at or near its maximum wavelength of 380 nm: Smid and coworkers investigated the behavior of

K^+-picrate complexes with bis-15-crown-5 ethers (16) and continued the studies with benzo- and dibenzo-15-crown-5 and 18-crown-6 derivatives attached to network polymer resins for Na^+- and K^+-picrates (17). Takeda and his group performed synergistic solvent extractions of Cs^+- and Rb^+-picrates with 15-crown-5 and benzo-15-crown-5 using tributylphosphate (TBPO) to enhance the extraction (18,19). Hasegawa and coworkers performed a similar synergistic extraction of Ag^+-picrate with DB18C6 and trioctyl-phosphineoxide (TOPO) (20). Smid and his group had investigated the fluorenyl anion as a replacement for the picrate anion with the crown compound dimethyl-dibenzo-18-crown-6 to complex Ba^{2+}, Na^+, and to a lesser extent, K^+ and Cs^+ (21,22). The only technique in this category to yield a successful analytical application of the method was the work of Ueno and coworkers using the bromocresol green anion with 18-crown-6 for the determination of K^+ in blood serum (23).

Chromophoric Crown Ethers

This section deals with the development in recent years of crown ethers that have had chromophoric functional groups added to the molecule. These new compounds were designed to bring about a specific color change or a change in the intensity of light absorption or emission upon complexation with a metal cation within the crown ether

ring. The modified crown ethers then could serve as photometric reagents selective for certain metal cations such as alkali and the alkaline earth metals. Most of the crown reagents were modified in two possible ways; either the chromophoric group could contain a dissociable proton or protons, or it could be non-ionic (24). In the first instance, the ion-exchange between proton and the appropriate metal cations causes a color change, while in the latter, the coordination of the metal ion to the chromophoric donor or acceptor of the dye molecule induces a change of the charge-transfer band of the dye. The proton dissociable crown ether dyes are especially suited for extraction photometric determination of alkali and alkaline earth metal ions (4). Similarly, the neutral crown ether dyes are potentially useful for such determinations in lipophilic homogeneous media.

Solvent Extraction with Crown Ethers: Monoprotonic Crown Ether Dyes

In creating alkali metal selective crown ether dyes, a monoprotonic chromophore is introduced into a crown ether skeleton in such a proximity to the ethereal function that the dissociation of the chromophoric proton is assisted by the complexation of the positively charged metal ion with the crown ether macrocycle (25). In theory, the function of the metal binding and the function of its detection may

be separately carried out by the crown ether and the protonic chromophore, respectively. However, the anionic chromophore can more or less contribute to the metal binding ability of the crown ether, and thus, in the actual molecule, the two functions cannot be separated from each other.

The first crown ether dyes designed according to the above principle are 4'-picrylamino-substituted derivatives of benzo-15-crown-5 reported by Takagi, Ueno, and coworkers in 1977 (25). The synthesis is readily attained by first nitrating and then reducing benzo-15-crown-5 leading to 4'-aminobenzo-15-crown-5 (26), which is then reacted with picryl chloride under basic conditions to yield the compound. The reagent is almost insoluble in water unless subjected to basic conditions, and is highly soluble in common organic solvents such as methanol, chloroform and benzene. The compound, HL, is appreciably acidic, and the initial color of the aqueous phase is orange (at 390nm; ϵ = 12,900 $L \cdot M^{-1} \cdot cm^{-1}$) which shifts to a blood red color (at 445nm; ϵ = 20,000 $L \cdot M^{-1} \cdot cm^{-1}$) when the amino proton dissociates under basic conditions leaving the anion form of the crown (L^-). When a chloroform solution of the compound is brought into contact with basic aqueous solution containing the alkali metal salts, potassium and rubidium are extensively extracted into the organic phase which changes from orange to blood red indicating formation

of an L^- species in the chloroform. Sodium is extracted only slightly, and lithium is not extracted at all. The extent of the absorbance of the chloroform solution at 560 nm (the solution is measured at a wavelength higher than the maximum absorbance of the complex to escape interference of the high reagent blank) can be used as a measure of the alkali metal concentration present in the original aqueous solution. Potassium and rubidium were readily extractable from the alkaline solution into $CHCl_3$ as their crown ether complexes in the form of ML·HL. Since underivatized benzo-15-crown-5 was found to form a 1:2 metal: ligand complex with K^+ (27), it is most likely the same phenomenon occurs here. Sodium ion, Na^+, was extracted only to a small extent but was found in both 1:1 (ML) and 1:2 (ML·HL) forms of the complex. This first effort resulted in a successful colorimetric determination of 10-400 ppm potassium in the presence of < 2000 ppm Na^+.

In 1979 and 1980 Takagi, Ueno, and coworkers published papers covering further work on the 4'-picrylamino crown reagents (28,29). They derivatized the 5'-position of the 4'-picrylamino-15-crown-5 with a nitro or bromo group, and they derivatized the 5'-position with a nitro group for the 4'-picrylamino-18-crown-6 structure as well. The photometric determination of 10-800 ppm potassium in seawater was possible in the presence of other alkali and alkaline earth metals using the 5'-nitro-4'-picrylamino-15-crown-5

derivative as long as lithium-EDTA was present to mask the Ca^{2+} and Mg^{2+} that would otherwise precipitate as hydroxides at the operating pH of 11.56. The 5'-nitro derivative of the 4'-picrylamino-18-crown-6 reagent was so effective that they now have Dojindo Laboratories, Inc., in Japan manufacture the compound for commercial use under the name Takagi Reagent (Structure 4 of Figure 1). With the larger sized ring of 18-crown-6 present, the metal ions form 1:1 metal:ligand complexes (except for cesium which forms CsL·HL) and are extracted in the order of $K^+ > Rb^+ > Cs^+ > Na^+ >> Li^+$. The colorimetric determination of 4-40 ppm K^+ in Portland cement was possible in the presence of the other alkali and alkaline earth metal ions as long as Li-EDTA buffered at pH 12.35 was again employed to remove the alkaline earths (29).

Under the above conditions, usually only about 18% K^+ is transferred from the aqueous to the organic solution, and the calibration plots are not entirely linear and often show a curvature. This behavior somewhat violates the traditional concept of colorimetry of metals in which the complete conversion to colored metal complexes is expected. The extraction constants of crown ether dyes are much too small compared to the standard of such traditional extraction photometric reagents for the determination of heavy metals such as dithizone and 8-hydroxyquinoline (24).

Pacey, Bubnis and coworkers made substitutions for the

nitro groups on the picryl portion of Takagi's 4'-picryl-aminobenzo-15-crown-5 reagent and produced 4''-cyano-2'',6''-dinitro-4'-aminobenzo-15-crown-5 (30) and the two trifluoromethyl derivatives: 4'-(2'',6''-dinitro-4''-trifluoromethylphenyl)-aminobenzo-15-crown-5 (4TF) and 4'-(2'',4''-dinitro-6''-trifluoromethylphenyl)-aminobenzo-15-crown-5 (6TF) (31,32). Although all but the 6TF derivatives exhibit lower molar absorptivities for the HL and ML forms in contrast to Takagi and Ueno's reagents, their advantage lies in the feature that the HL and ML absorbance maxima are much more widely separated (80 nm and 150 nm differences for 6TF and 4TF respectively). With less spectral overlap the complex can be measured close to its λ_{max} where the high reagent blank of Takagi's reagents poses no problem. The trifluoromethyl derivatives also showed slightly higher aqueous solubility, but the extraction efficiency of the metal ions remained in the less then 20% range. As with the earlier 4'-aminobenzo-15-crown-5 derivatives, the complex was extracted in the form of a 1:2 metal:ligand ML·HL adduct. For their best results, potassium was able to be determined in the 5-700 ppm range in the presence of 3000 ppm Na^+ with reagent 6TF. Rubidium still caused interference when present in concentration level $\geq$ 1000 ppm. The 6TF also allowed them to effectively determine the levels of potassium in human blood serum within the normal range of 137-207 ppm K^+.

Several other colorimetric benzocrowns and dibenzocrowns were synthesized by Takagi, Ueno, Yamashita and Nakamura. A few of these were additional picrylamino and dipicrylamino derivatives, but they did not prove to be quite as useful for the extraction photometry of alkali metals, for the extraction efficiency was too low (33). The Takagi group also produced p-nitrophenol derivatives of azacrowns, and phenylazo derivatives of both the benzocrowns and azacrowns.

Side-armed Crown Ether Derivatives

It has been observed previously that chromophoric crown ethers were produced by extending the benzocrown systems. In 1982 one of the new types of colorimetric crown ethers - reported by Takagi and Ueno with Nakamura and Nishida - to be used in the solvent extraction and photometric determination of metal cations, were the side-armed crown ether derivatives (34,35). Of these, the most interesting are the dinitrophenol derivatives of 15-crown-6 and 18-crown-6. These have enhanced acidity and water solubility and higher extraction constants than the 4'-picrylamino-benzocrown reagents that they reported earlier. Also unique to the dinitrophenol side-armed crowns in contrast to the earlier reagents, is an important property - unless the metal of the proper size is present for complexation, the reagent will not distribute into the

organic phase even at the required basic pH ≥ 10. The phenolate anion also directly assists in complexation by being able to position itself directly over the metal held within the crown ether cavity. Sodium in a dilute blood serum sample was successfully determined using the (2-hydroxy-3,5-dinitrophenyl)-oxymethyl-15-crown-5 reagent that produced a linear calibration curve for 0-6 ppm Na^+ (24,35).

"Crowned" Phenols and Related Compounds

Some unusual crown ether dyes were synthesized by Kaneda and coworkers in which a phenolic hydroxyl group constitutes an integrated part of the of the crown ether skeleton (36). Rather than a 15-crown-5 or 18-crown-6 ether with side-arms, or even a benzo group springing from one of the ethylene groups between oxygen atoms, a phenolic group is a direct part of the skeleton, and a hydroxyl function extends into the crown ether cavity from a carbon positioned in the place of the expected oxygen atom in that structure. A 2,4-dinitrophenylazo group was attached to the para- position of the phenol. The researchers reported that upon addition of crystalline lithium chloride or perchlorate to a yellow solution of the 15-crown-5 form of the reagent in chloroform, a drastic color change took place when pyridine (800 times the molar excess of the reagent) was simultaneously added. Other alkali metal

salts produced no such change. The color shift process was reported as very selective to Li^+, and the coloration very sensitive to experimental conditions. Later, Nakashima and coworkers (37) performed further studies on this system and reported conditions under which 25 to 250 ppb lithium was determined photometrically in a chloroform:dimethylsulfoxide:triethylamine mixture (95.5:5.0:0.5; v/v). Sodium ions did not interfere, but K^+, Rb^+, Ca^{2+}, Sr^{2+}, Ba^{2+}, and Mg^{2+} did and had to be removed before the determination was performed. They concluded the coloration of the reagent in organic medium is due to deprotonation of the phenolic proton under combined influence of the proton-removing amine and the metal cation stabilizing the resultant phenolate anion, but the complexity of the system does not seem to allow a quantitative approach to the equilibria involved (37). The high sensitivity claimed for this method is remarkable. However, the strict precautions in sample preparation (exclusion of water) seem to limit the use of these "crowned" dinitro-phenylazophenols for general purpose.

Benzocrown Ethers with Azo-linked Side-arm

A unique family of crown ether dyes was reported by Shinkai, Manabe, and coworkers which was photoresponsive and changed complexation and extraction selectivity after exposure to light (38). The benzo-18-crown-6 structure was

not extended with picrylamino groups as in the case of Takagi's reagents, but with phenylazo derivatives which terminated in a p-nitrophenol. These dyes adhere to their thermodynamically stable open chain E-form under normal conditions, and bear no special characteristics other than that typical of benzocrown ethers and phenols. Since the ionizable phenol function is quite remote from the crown cavity, there can be no cooperation within the molecule for enhanced interaction with complexed metal ions. When irradiated with the proper energy light, the E-form is photochemically isomerized to the Z-form at the azo-linkage and folds over on itself, bringing the phenol and crown ring portions of the molecule into close proximity. In this Z-isomer it is possible for the phenolate anion to interact directly with the crown ether bound metal cation from the axial direction.

N-Sidearmed Monoaza Crown Ethers

Chromophoric crown ethers can be produced in other ways in addition to extending the benzocrown systems or adding side-arms. If one of the oxygens in the crown ether ring is replaced with a nitrogen atom, there results a 2° amine that readily permits derivatization of the crown to a spectrally active molecule in the UV-visible range. The resulting monoaza crown ethers behave essentially in the same manner as the crown ethers in respect to their ability

to complex metal cations. However, some differences have been noted. When two oxygens have been replaced by nitrogens, the differences are more marked for these diaza crown ethers.

Early in the research on the new cyclic polyethers, Frensdorff used cation specific electrodes to potentiometrically determine the stability constants for 1:1 complexes with univalent cations in water and methanol for nearly two dozen crown ethers. There were various substituents included in the crowns as well as nitrogen and sulfur atoms in the heterocyclic rings (8). For 18-crown-6, it had been established that potassium was the metal cation most strongly complexed, and if the structure was expanded to benzo- or dibenzo-18-crown-6, or other substituents, potassium was still bound the strongest. When one nitrogen was introduced in place of an oxygen in 18-crown-6 and dibenzo-18-crown-6, the K^+ complex lost in excess of two orders of magnitude in its stability constant. When two nitrogens (at the 1- and 10-positions) were substituted in the ring, K^+ was no longer the cation that formed the strongest complexes. In fact, the metal cation of choice was no longer an alkali metal cation at all, but the monovalent transition metal ion Ag^+. Frensdorff explained that the complexing of potassium is weakened appreciably by nitrogen and sulfur substitution and that the stability constants fall in the order of

decreasing electronegativity, O > NR > NH > S. This is just as one would expect. As the negative charge on the heteroatom drops, the electrostatic attraction between it and the cation is diminished. The effects on Ag^+ complexing from the substitution of N (or S) are exactly the opposite; it is greatly increased. Evidently it is not the electrostatic forces that have the most influence here, but rather the type of covalent bonding which is involved in many of the well known complexes of Ag^+ with amines (6,8).

Later studies performed in the 1970's and early 1980's on monoaza-and diaza-18-crown-6 ethers and their derivatives reported many instances of their strong complexation with alkaline earth metal and other divalent metal cations (39,40). Some additional work has appeared in the literature on the use of monoaza crown ethers with long chain alkyl N-amide side-arms - (Okahara, Nakatsuji, and coworkers (41)) - where Ca^{2+} and Ba^{2+} form the most stable complexes with the 18-crown-6 derivatives, but these were analyzed by potentiometry and not colorimetric methods.

Takagi and Ueno felt that in order to enhance the metal extraction efficiency or to increase the extraction constant, one could introduce a chromophoric side-arm into a crown ether skeleton in such a manner that the deprotonated anionic group could interact directly with or coordinate to the metal ion bound in the crown ether cavity. This modification was most easily achieved via

synthesis using the aza-crown ethers and extending the chromophore from the ring nitrogen (33,42). In this fashion, they produced p-nitrophenol derivatives of monoaza-18-crown-6 and monoaza-15-crown-5 (34,42). (Takagi made similar derivatives with 4-methylumbelliferone side-arms which not only absorbed in the visible range, but were fluorescent as well (43). They will be presented in detail within the section covering fluorescent crown derivatives.) Just as the picrylaminobenzo crowns, these compounds distribute predominantly into organic solvents such as 1,2-dichloroethane, and selectively extract certain alkali and alkaline earth metal ions causing a measurable change in wavelength or intensity of the organic phase solution. These dyes have dissociable protons on the phenolic oxygen and the ammonium nitrogen, but the two proton dissociation constants are fairly far apart, and only the ammonium proton (the weaker acid) takes part in the alkali metal extraction reactions. (24).

Diprotonic Crown Ether and Crown Amine Ether Dyes

The introduction of two of the proton-dissociable chromophores into the crown ether skeleton, according to the similar strategy outlined before, should lead to those dyes which are selective for divalent metal ions-especially the alkaline earths (24). Takagi and Ueno's laboratory tried derivatizing both sides of the dibenzo-18-

crown-6 structure to form the dipicrylamino-substituted crown, but it did not extract alkaline metal earth ions as expected (33). They decided to follow the example of their p-nitrophenol derivatives of side-armed crown ethers mentioned earlier here, where the phenolate ion can interact directly with the complexed metal ion from axial directions (34,35). These types of crown ethers are most easily attained by using the diaza-18-crown-6 structure and similar diaza crowns. The 1,10-diaza-4,7,13,16-tetraoxacyclooctadecane structure, or diaza-18-crown-6, is known as Kosh 22 by Takagi's group and is better known in this country as the commercially available compound Kryptofix 22. (The "22" represents the 2 oxygen atoms for each part of the crown ring that appear between the two nitrogens. Kryptofix 21 is 1,7-diaza-4,10,13-trioxacyclopentadecane, the diaza-15-crown-5 derivative where 2 oxygen atoms and 1 oxygen atom appear between the two nitrogens in the 15-crown-5 ring). Takagi and Ueno's group attached some extremely extended dye systems to both of the nitrogens of the diaza heterocycle. These symmetrical diprotonic dyes are either bound directly to the secondary amine nitrogens of the ring, or to an adjacent carbonyl group creating an amide function. The substituents from that point outward are variations on the p-nitrophenol structures and extended dye systems adjacent to the nitrophenol rings: either p-nitrophenylazo groups, or naphthylazo groups. The

structures with a carbonyl bound to the ring nitrogen were found to be poor extraction vehicles for the alkaline earth metal ions, although a few of them did extract those metals, as well as Li^+, into $CHCl_3$ at high metal ion concentrations near 1 mole/liter. A low coordinating ability of the amide nitrogens is most likely responsible for this behavior (33). On the other hand, those derivatives with no amide functions in the ring unanimously show strong affinity for alkaline earth metal ions and extract them efficiently into 1,2-dichloroethane (40,44). The order for metal extraction selectivity is: $Ca^{2+} > Sr^{2+} > Ba^{2+} >> Mg^{2+}$ for both the diazacrown-18-crown-6 and diaza-15-crown-5 derivatives. Magnesium ion and alkali metal ions are extracted only to a minor extent. An especially high extraction constant is exhibited by the diazacrown-18-crown-6 ether with the p-nitrophenol-chromophore. Unlike the extraction of alkali metal ions with the monoprotonic crown ethers, a spectrophotometric concentration of about 10^{-4} mol/L can extract Ca^{2+} quantitatively into 1,2-dichloroethane if the pH of the aqueous phase is adjusted high enough (pH $\geq$ 10). The determination of Ca^{2+} in blood serum was successfully performed with this reagent. The absorbance of the complex in the organic phase was measured at 406 nm. The calibration plot was linear for 0-0.8 ppm Ca^{2+} and as little as 100 ppb Ca^{2+} was easily determined (24). The molar absorptivity of 81,000 $L \cdot M^{-1} \cdot cm^{-1}$ for the

Ca^{2+} complex is among the highest known for Ca^{2+} determinations. When comparing this extraction photometric reagent and method to others in regard to convenience of calcium determination, however, there does not seem to be any particular advantages over many traditional metallochromic chelating agents such as Calmagite and Eriochrome Black T which allow the determination of ppm to ppb levels of Ca^{2+} in aqueous media. Other divalent metal ions such as Cu^{2+}, Ni^{2+}, Zn^{2+}, Cd^{2+}, and Pb^{2+} are also extracted by the reagent causing interference and resulting error in the determination of Ca^{2+}. The interference from these can be removed by using NTA (nitriloacetic acid) as a masking agent (44). The complexation constants of the reagent have not yet been determined in homogenous solutions, but presumably the complexes of the alkaline earth metal cations are less stable than those of the other divalent metal ions. With ordinary chelating agents, transition metal and related heavy metal ions usually form much more stable complexes than the alkaline earth metals do. However, the presence of the crown ether structure in the reagent and others like it may well be expected to reduce the difference in the stabilities between the two families of metal ions. In fact, the complexation behavior of "crown complexanes" by Takagi, Tazaki, Ueno and coworkers (45,46) have partially supported this expectation.

These crown complexanes refer to the diazacrowns

18-crown-6 and 15-crown-5 where the nitrogens have been derivatized with both alkyl chains ending in a carboxyl group or a phosphate group. Some of the complex formation constants of these with the alkaline earth metal ions come quite close to those with divalent transition metal ions. The diaza-18-crown-6 structure derivatized with acetic acid side-arms forms complexes of almost the same stability with Co^{2+}, Ni^{2+}, Ba^{2+}, Ca^{2+}, Sr^{2+}, and Zn^{2+} (46). The two acetate groups were found to coordinate in a trans-configuration to the Cu^{2+} atom bound in the distorted diazacrown ether ring (47). When observing this phenomenon as well as the size-fit of the Ca^{2+} ion and the crown ether cavity, it is very likely that the calcium complexes of the nitrophenol derivatives of the diazacrowns involve the coordination of the two phenolate anions from the axial directions onto the metal ion held in the crown ether cavity, forming securely an electrically neutral lipophilic skin around the otherwise highly hydrophilic Ca^{2+}. Few synthetic reagents are known to extract Ca^{2+} with appreciable selectivity among common divalent metal ions (including transition and post-transition metals).

Uncharged, Neutral Crown Ethers and Related Dyes

Approximately 40 to 50 chromogenic crown ether dyes have been synthesized by Dix and Vogtle. The main objective of the syntheses has been the attachment of crown

ethers of various ion selectivity to dyes in such a manner that the interaction with the alkali and alkaline earth metal ions cause color changes. The dyes have both electron donor and acceptor sites within the molecule so that the charge transfer from the donor to acceptor according to electronic excitation gives rise to their strong visible light absorption (24). These compounds are based on the similar premise developed independently by Takagi and Ueno's group, but here the interest lies in neutral uncharged crown ether dyes. The chromophores have no dissociable protons and function in homogeneous solvent media - they are not used for solvent extraction.

In 1978, Dix and Vogtle published a report on neutral dye derivatives of monoaza-15-crown-5, monoaza-18-crown-6, and some monoaza-21-crown-7 ethers (48). They started with common dye structures of gentian violet and Michler's hydrol blue and replaced the dimethylamino functions with the monoaza crowns. The most impressive compounds that they created were the p-nitrophenylazo derivatives of the N-phenyl-monoaza crown ether amines. With acetonitrile as the solvent, they added salts of the alkali metals, alkaline earth metals, and a few of the divalent transition metals in a ratio of $\geq$ 10:1 metal salt:ligand. Some of the salts produced drastic hypsochromic shifts in wavelength from the initial λ_{max} of 474 nm before complexation to new maxima that appear as far as 120 nm toward the blue after

complexation. They postulated that the selective inclusion of alkali metal, alkaline earth metal, ammonium and heavy metal cations, as well as H_3O^+ in such crown ether dyes, should exert a selective influence on the chromophore. This influence should include the effect of the nitrogen of the crown ether amine because the lone pair contributing to resonance will be affected to a greater or lesser degree by the positive charge of the guest cation, depending on the nature of the ion concerned (48).

In the next two years they published more extensive work on these types of chromophoric dyes, some additional monoaza crown derivatives, and even some heavily conjugated benzocrown derivatives (49,50,51). In the last paper they worked with two sets of compounds where the monoaza crown nitrogen is either directly adjacent to the dye system (Structure 5 of Figure 1) or the nitrogen is separated by a methyl group which is in turn bound to the dye system (Structure 6 of Figure 1). On complexation with several metal cation salts in acetonitrile, the two types of dyes behave in an entirely opposite manner. In dyes such as Structure 5, the amino nitrogen which is an integral part of the crown ether ring is simultaneously involved in the dye chromophore as a vital electron donor site. Thus the interaction with metal cations tends to localize the electronic charge on the crown ether portion causing a hypsochromic shift of the charge transfer band which

appears as the longest wavelength absorption of these dyes. In comparison, for dyes like Structure 6, the metal cations interact with the acceptor site (the carbonyl oxygen) of the dyes giving rise to a bathochromic shift of the charge transfer band (24,51).

For these dyes of Dix and Vogtle, the extent of the absorption shift depends on 1) the fit between the size of the crown ether and the metal ion, 2) the surface charge density of the metal cations, and 3) the solvent medium. The first point has been stressed throughout this introduction and is exemplified by the result of the complexation of the monoaza-18-crown-6 dyes with K^+ from the alkali metals and Ba^{2+} from the alkaline earth metals where they produce an almost exclusive absorption shift as large as 100 nm or more in both acetonitrile and methanol. Point 2) is easily demonstrated by the behavior of their compounds, Structures 5 and 6 in Figure 1, in acetonitrile. Lithium ion, Li^+, produces the largest spectral shift among the alkali metals ions. Alkaline earth metals ions show even greater changes in wavelength than Li^+. For point 3) the extent of the shifts is considerably diminished on going from acetonitrile to aqueous MeOH; for dyes of Structure 6, the maximum shift is 83 nm with $MgCl_2$ in CH_3CN, but only 39.5 nm in aqueous methanol.

At this time, however, all of the Dix and Vogtle chromophoric dyes have been tested only with large excesses

of the metal salts used in their complexation studies. Their response to low concentrations of metal salts have not been reported. For practical applications a right choice of solvent media must be made, since most of these dyes have either shown, or are expected to show, considerable solvatochromism. The effect of the anion associated with the metal cation should also be carefully assessed.

Fluorescent Crown Compounds

It has now become evident that there are many chromophoric crown reagents useful for the spectrophotometric analysis of metal cations. However, it is important to note that there is a much smaller body of work involving the use of fluorescent crown reagents, or crowns used with fluorescent dyes, for the determination of metal cations. Some of the earliest crown ethers described by Pedersen (5) had benzo and dibenzo groups displaying a native absorbance in the 275-290 nm range, and emission was observed near 300 nm. Variations on the benzo-crowns lead to naphthalene-crown derivatives. In 1977, Sousa and Larson published a communication that reported studies of the effect of alkali metal ions on the emission of two naphthalene derivatives: 2,3-naphtho-20-crown-6 and 1,8-naphtho-21-crown-6 (52). In these two compounds the crown portion of the molecule is basically the 18-crown-6 structure except for the side of the ring that is bound to the naphthalene group. The first

compound, 2,3-naphtho-20-crown-6, has its naphthalene group approaching end-on to share one side with the crown ether ring. The second compound, 1,8-naphtho-21-crown-6, has the two adjacent sides of both napthtalene rings forming two sides of the crown ether. Sousa and Larson measured the change in fluorescence quantum efficiency, phosphorescence quantum efficiency and phosphorescence lifetimes of the complexes with several alkali metal chlorides at 77°K in a 95% EtOH glass. For the first compound the quantum efficiency of fluorescence drops but that of phosphorescence increases with complexation. The second compound behaves in the opposite manner. In each case the Rb^+ and Cs^+ ions had the greatest effect and the heavier the atom the shorter the phosphorescent lifetime in both compounds (52).

In 1980 Shizuka, Takeda and Morita reported studies on the fluorescence enhancement of dibenzo-18-crown-6, DB18C6, by alkali metal cations at several different temperatures between 77°K and room temperature at 300°K, using methanol or methanol/ethanol as the solvent media (53). As Pedersen showed earlier for the absorbance spectra of DB18C6 at 300°K, small bands appear at 274 nm due to complex formation (5). Soon afterwards, Frensdorff proved that DB18C6-M^+ complexes of 1:1 stoichiometry were easily formed in alcohol (8). In this study, they determined that the fluorescence (or lifetime) enhancement of DB18C6 is caused by chelation with alkali metal cations

(M^+) the extent of which depends upon the atomic number of M^+. Their vibrational spectra show the chelating strength of the cations with DB18C6 to be in the order: $K^+ > Na^+ > Rb^+ > Cs^+ > Li^+$. The molar absorptivities of the complexes are almost the same as DB18C6 alone in MeOH. The excitation spectra were very close to those of the corresponding absorptions of the complexes showing that the fluorescence originates from the lowest excited singlet state. There is a heavy atom effect for Cs^+ and Rb^+ causing the rate of intersystem crossing to increase. The rate for quenching of fluorescence occurs in the following order: DB18C6 alone > $Li^+ > Cs^+ > Rb^+ > Na^+ > K^+$ - exactly the opposite of enhancement. This consequence suggests that the order of internal quenching rate constants is due to the dynamic (Browninan) motion of excited DB18C6-M^+ complexes and is the same as that for the quenching rate. Their findings show that a rigid structure of the DB18C6-M^+ complexes is responsible for a decrease in the internal quenching rate constant. Consequently, the fluorescence enhancement occurs in DB18C6-M^+ complexes having a rigid structure, and the fluorescence enhancement is significant at higher temperatures and lower viscosity. It is assumed that DB18C6-M^+ complexes, especially for K^+ and Na^+, have a planar or semi-planar structure both in the ground and the excited states (53). (It is known that the rate constant for internal conversion is markedly enhanced by a conform-

ational change in the excited state.) A conformational change between the bichromophores in DB18C6 in the S_1 state may give rise to an exciton interaction or a charge-transfer interaction leading to the non-radiative decay $S_1 \dashrightarrow S_0$. Complex formation of DB18C6 with M^+ prevents such a conformational change in the excited state. Shikuza et.al. performed the same studies using dibenzo-24-crown-8 with alkali metal cations. The fluorescence enhancement, as seen for DB18C6 was scarcely observed in this system. One possible explanation is the difficulty of forming a planar or semi-planar structure in such large ring sized complexes which wrap around the metal ion with too much flexibility to develop a rigid structure (53).

From both the cited studies, one can see that extensive investigation went into the nature of the systems described. However, no analytical determinations had yet been made using the fluorescent properties of a crown ether-metal ion complex. Benzo- or naphtho- crown ethers fluoresce appreciably, but do not reflect the complex formation with sufficient sensitivity for analytical purposes. There is reference made to studies that monitored the quenching of fluorescence in benzo-(2,2,2)-cryptand by the formation of heavy metal complexes with Pb^{2+}, but no details are published in available journals. The cryptand is also a macrobicyclic ligand, not a single heterocycle (54). (This was work performed by Kina, a

doctoral student in Takagi and Ueno's group). One successful fluorometric determination of K^+ in blood serum using a crown ether reagent appeared in the literature in 1981 by Sanz-Medel, Blanco Gomis and Garcia Alverez (55). The study involved the extraction - with 18-crown-6 - of K^+ associated with the fluorescent counterion, eosin. It did not involve a crown reagent exhibiting its own fluorescence.

Takagi and Ueno's group, as previously described, designed and synthesized a large number of proton-dissociable chromogenic crown ethers which could selectively extract alkali and alkaline earth metal ions and thus serve as a photometric tool for the determination of those metal ions. Several active compounds were based on the incorporation of a side-arm dye system by attaching the side-arm directly to the nitrogen in monoaza and diaza crown ethers. In 1982 they created analogous fluorescent reagents by coupling the indicator dye, 4-methylumbelliferone, to the nitrogen atoms in monoaza-15-crown-5, monoaza-18-crown-6 and diaza-18-crown-6 (Kryptofix 22) (43). The dye portion of the molecule has a hydroxy group which can be deprotonated in basic aqueous media, and after complexation with a metal cation, the complex can be extracted into 1,2-dichloroethane and measured fluorometrically. For both the complexed and uncomplexed forms of the dye, the fluorescence emission at 440 nm remains the same. The excitation

maximum shifts from 326 to 380 nm once the complex forms.

The extraction constants determined for these dyes were a few orders of magnitude lower than for the chromophoric p-nitrophenol derivatives that they obtained of monoaza-15-crown-5 and monoaza-18-crown-6 (33,34,35,42). The two monoaza derivatives with 4-methylumbelliferone were isolated and characterized as oils. Of all the alkali and alkaline earth metal ions tested, the monoaza-15-crown-5 dye gave the best results with Li^+ and the monoaza-18-crown-6 dye gave the best results with Ca^{2+} . The diaza-18-crown-6 derivative formed with 4-methylumbelliferone was isolated as a crystalline product, but no analytical results were reported with it. Takagi et.al. reported that their analytical method for Ca^{2+} - using the monoaza-18-crown-6 derivative of 4-methylumbelliferone - was efficient down to ppb levels, but they neither reported the conditions nor specifics concerning the analysis. They concluded that in order to get this type of reagent to function for solvent extraction, the basic nitrogens must eventually be removed from the ring structure.

Wolfbeis and Offenbacher reported the effects of alkali metal cation complexation on the fluorescence properties of two commercially available crown ethers, dibenzo-18-crown-6 and Kryptofix 5, in 1984 (56). The compound, DB18C6, has been frequently referred to in this introduction, and the structure is familiar, but Kryptofix

5 (K 5) bears little resemblance to the aforementioned Kryptofix structures. Kryptofix 5 is a bis-8-alkoxyquinoline "open" crown compound, similar to an uncyclized 15-crown-5 cavity: 1,13-bis(8-quinolyl)-1,4,7,10,13-pentaoxatridecane. Complexation of DB18C6 with either Na^+ or K^+ leads to fluorescence enhancement (312 nm) and vibrational resolution of the absorbance (or excitation at 280 nm) spectra even at room temperature.

In the investigation of the increase in relative fluorescence intensity with increasing concentrations of the metal cation it was noted that there was a difference in extent of complexation which was dependent on the water content of the solvent medium. When the solvent is predominantly organic in nature - 99% MeOH (1% H_2O) - the formation constant for the complexation of DB18C6 with Na^+ was 2 - 4 $\times$ 10^4. (The value could not be calculated more accurately because DB18C6 was used as a 10^{-4} M solution). When the solvent medium was 50% H_2O in MeOH, K_f was determined to be only 50 - nearly 3 orders of magnitude lower. The plot of relative fluorescence intensity vs. log concentration of metal cation added is an S-shaped curve in both solvent systems. Even though the final fluorescence intensity in 50% MeOH/H_2O is slightly higher than in 99% MeOH, the amount of Na^+ (as sodium acetate) required before any change in emission intensity is seen - signaling the formation of the fluorescent complex - is two orders of

magnitude higher (from 10^{-5} to 10^{-3} M) in the highly aqueous system. Wolfbeis and Offenbacher explain that the enormous difference in the two formation constants reflects the different hydration energies of the ions in the two solvent systems. In the MeOH containing only 1% H_2O, maximum fluorescence is attained at a slight molar excess of sodium ion to DB18C6 concentration. This fact indicates a strong binding of the "naked" ion. Complexation must occur in a time interval much smaller than 0.5 sec (the time-constant of their instrument), since there are no changes in intensity with time reported after mixing the crown ether and the salt solution. Titration curves similar to those for sodium were obtained for potassium.

Depending upon the anion tested, there is a definite difference in the fluorescence response of the DB18C6 in the presence of the metal salt solution once excess concentrations of the salt have been reached. When the titrations were performed with Na^+ and K^+ acetates in 99% MeOH, the fluorescence emission maintained its maximum intensity at high salt concentrations. When sodium chloride or bromide were added, there was a slight drop in intensity once the concentration of the cation was increased ten times more than the concentration required for maximum fluorescence of the complex. If sodium iodide was added, it never quite achieved the fluorescence intensity the other salts attained, and the fluorescence

quickly dropped in intensity as the concentration of NaI increased until the fluorescence fell much lower than the initial fluorescence of the uncomplexed DB18C6. The fluorescence behavior of the crown ether shows similar results with the potassium salts, only the drop in intensities are more accentuated. The decrease in intensity is interpreted in terms of dynamic fluorescence quenching of the DB18C6 fluorophore, since there are almost no changes evident in the absorption spectra at halide concentrations of 10^{-3} M or higher. Small contributions of static fluorescence quenching cannot, however, be excluded (56).

With Kryptofix 5, the 8-alkoxyquinoline chromophores cause its absorption, excitation and emission wavelength maxima to occur at wavelengths distinctly longer than the UV range of DB18C6. The investigators performed effect of pH studies on the polyether and found the absorption λ_{max} to be 312 nm for the uncharged species and 354 nm for the protonated species. The fluorescence emission maximum for the cation occurs quite high, at 495 nm, but the neutral molecule emits at 409 nm. The fluorescence emission of K 5 is solvent dependent and shifts from a λ_{max} of 395 nm in chloroform to 405 nm in methanol. Fluorescence titration of K 5 with alkali and alkaline earth metal cations indicates complex formation in organic solvents, but the interaction is much weaker in mixed organic-aqueous solvent media (56).

There are two possible effects of complex formation on the fluorescence: 1) changes in fluorescence intensity and 2) a shift in wavelength maxima. Several alkali and alkaline earth metal salts (0.1 M concentration) were tested with K 5 (10^{-4} M) in pure MeOH. The Na^+ as acetate or chloride produced the most pronounced effect: a 55% increase in fluorescence intensity and a small bathochromic shift of 4 nm. Enhancement effects were also observed with KCl and $Ca(OAc)_2$ but to a lesser extent. These two salts produced small shifts to shorter wavelengths of -9nm and -3nm respectively. The $MgCl_2$ and NH_4OAc salts caused a drop in fluorescence intensity with no discernable shifts in wavelength. Wolfbeis and Offenbacher interpret the increase in fluorescence intensity as a consequence of the rigidification of the molecule due to strong complexation. The hypsochromic shift of the emission maximum of the K^+ complex indicates a strong interaction of the central metal ion with the nitrogen atom of the heterocyclic fluorophore (56).

The fluorescence intensity of the K 5/Na^+ complex was found to be quite sensitive to the water content of the methanol solution. The intensity was highest in pure solvent, dropped to only 95% of maximum intensity in the presence of 1% H_2O, and only 70% the initial intensity in the presence of 10% H_2O. This change dramatically reflects the decrease in the complexation constants in going from

methanol to aqueous solutions due to high hydration energies. Wolbeis and Offenbacher were unable to detect any alkali cation complexation of K 5 by fluorimetry in pure water at neutral pH.

As in the study described earlier for the effect of different anions - as counterions with DB18C6 - on the fluorescence intensity, K 5 also exhibits similar effects in 1% H_2O in MeOH. Sodium acetate and chloride show no discernable quenching of fluorescence at high concentrations; NaBr shows less initial fluorescence intensity, and sodium with iodide not only quenches the fluorescence intensity almost totally, but it also manifests little fluorescence enhancement even at intermediate concentrations. The ions bromide and iodide act as dynamic quenchers, since there are no changes in the absorption spectra to be observed, and potassium with each of these counterions behaves in the same manner (56).

In 1983, Steger and Pacey presented preliminary research studies on the fluorescent detection of alkali metals utilizing crown ethers at the 15th Regional ACS Meeting in Oxford, Ohio (57). They used the polyether 12-crown-4 to complex the sodium cation which was then extracted into an organic phase in the presence of a highly fluorescent counterion anilinonaphthalenesulfate (ANS). By using flow-injection analysis with this system the need to separate organic and aqueous phases before detection could

be eliminated. By 1984, this system had been further developed as reported in Steger's dissertation. The method allowed determination of the Na^+ ion with a linear range of 4-16 ppm in the presence of 40 ppm K^+ and 2 ppm NH_4^+ for blood serum in the absence of protein (58). A second study in Steger's dissertation involved the synthesis and study of a new class of fluorophoric crown ethers. Two of the three compounds were NBD and DNS derivatives of compounds first introduced by Takagi and Ueno: 4'-NBD-aminobenzo-15-crown-5, 4'-dansyl-aminobenzo-15-crown-5, and NBD-aminomethyl-15-crown-5. These compounds indicated that the changes occurring in the molecule upon complexation also effect the attached fluorophore to produce a change in fluorescence upon complexation (58). Further details are unknown as this information was derived from a dissertation abstract and as yet has not been published.

Photoluminescence Phenomena: Fluorescence Spectrophotometry

The absorption of ultraviolet or visible light of the characteristic energy of a particular substance causes excitation of a bonding electron in the substance to a higher electronic state. Therefore, wavelengths of absorption peaks can be correlated with the type of bonds that exist in the species being studied, and absorption spectroscopy can be valuable for identifying functional groups in a molecule. For a specific compound containing a

particular type of absorbing bond, absorption spectroscopy provides a rather selective method of quantitative analysis. Absorbing species can be organic molecules and ions as well as a number of inorganic anions, but the majority of published work and the focus of this research concerns organic systems.

All organic compounds are capable of absorbing electromagnetic radiation because all contain valence electrons that can be excited to higher energy levels. The excitation energies associated with electrons forming most single (or sigma, σ) bonds are sufficiently high that absorption by them is restricted to the so-called vacuum-UV region ($<$ 185 nm), but experimental difficulties associated with the vacuum-UV are not easily overcome. As a result most spectrophotometric investigations of organic compounds have involved the wavelength region greater than 185 nm. Absorption of longer wavelength UV and visible radiation is restricted to a limited number of functional groups known as chromophores that contain valence electrons with relatively low excitation energies. These generally are aromatic or contain highly conjugated systems with π electrons, many which also have functional groups containing O, N, halogen, or S atoms which have unpaired, or non-bonding (n) electrons (59).

Photoluminescence is the emission of photons from electronically excited states. Chemical systems that

exhibit photoluminescence can be excited by electromagnetic radiation and eventually reemit radiation of either the same or of longer wavelengths. A tremendous body of organic compounds will undergo the first absorption process, but only a fraction of the many substances that absorb will actually undergo photoluminescence; most lose their excitation energy in a manner that will not generate an emitted photon, usually through radiationless phenomena (59,60,61).

Two classes of photoluminescence exist depending upon the nature of the ground and excited states. Most molecules contain an even number of electrons; in their ground state these molecules exist as pairs within the orbital. The Pauli exclusion principle demands that the two electrons in a given orbital have opposing, or paired, spins. A molecular electronic state in which all electron spins are paired is referred to as the singlet state. This means that at room temperature in the absence of radiation, the great majority of molecules will exist in their ground singlet state (59,60).

The singlet excited state occurs when the electron, moved up to the higher energy orbital, retains the opposite spin orientation to the second electron remaining in the lower energy ground singlet state orbital. The triplet excited state occurs when the electron in the higher energy orbital changes its orientation to the same spin as that in

the ground state; the electrons then have unpaired spins. Fluorescence emission results with the return from the singlet excited state. This process has quantumly allowed emission rates of about 10^7 to 10^9 sec^{-1} so the lifetime is in the range of 10^{-8} seconds or 10 nanoseconds. In comparison, absorbance is completed almost instantaneously in 10^{-15} sec. Phosphorescence is emission which results from the transition between states of different multiplicity, generally a triplet excited state, returning to the ground state. Such transitions are not "allowed" and the emissive rates are slow. Typical phosphorescent lifetimes are much longer - 10^{-3} sec to whole seconds - and depend primarily on the importance of the deactivation processes other than emission (59,62).

In 1935, A. Jablonski published a study of the mechanism of photoluminescence of dye materials. Figure 2. (59) is a simplified partial energy level diagram which has come to be known as a Jablonski diagram (59-61,63), that serves as an excellent means of illustrating what happens to a typical photoluminescent molecule undergoing excitation and emission processes. There are four different electronic states shown for the molecule: the ground and first two excited singlet states (S_0, S_1, S_2), and a triplet state, (T_1). Superimposed upon the electronic energy level of each molecular orbital is a series of closely spaced vibrational levels, of which only the first few

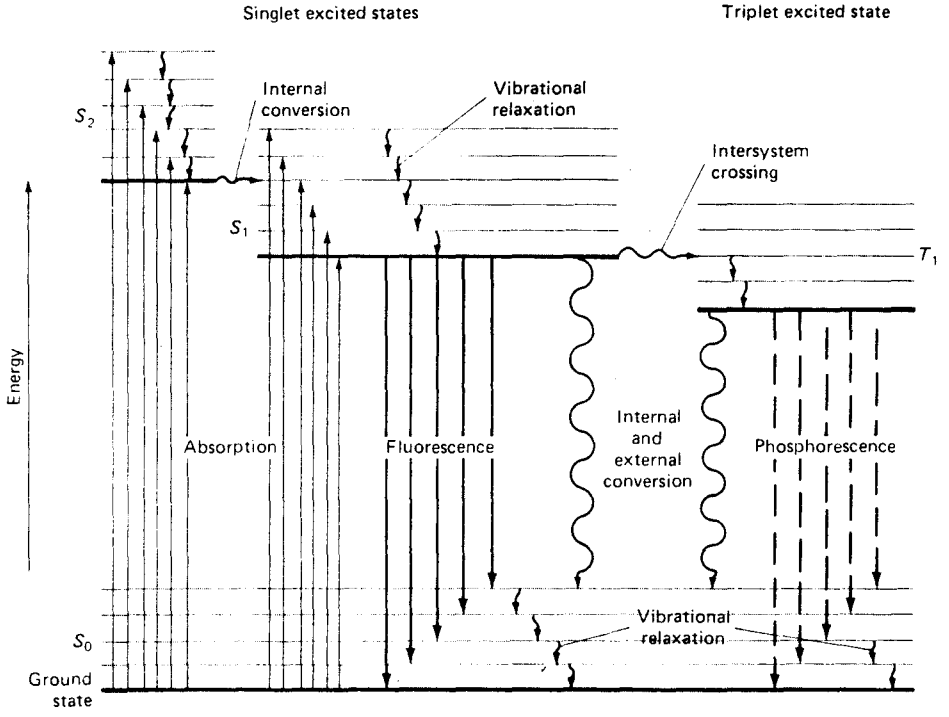

FIGURE 2: Partial Energy-Level Diagram for Photoluminescent System

levels are shown. Excitation occurs in 10^{-15} seconds and produces a fluorophore that is often excited to some higher vibrational energy level of either S_1 or S_2. The time before fluorescence emission takes place is generally 10^{-8} sec and in that time several processes can occur (59,62). For most excited molecules that exist in the condensed, (or liquid) phase, however, they rapidly relax to the lowest vibrational level of the S_1 state. The excess vibrational energy is usually lost through collisions with molecules of the solvent, which generates a very small amount of heat. This deactivation process (illustrated by the wavy lines in the diagram) is called vibrational relaxation within the S_1 state. Internal conversion when the electron drops from the upper S_2 excited state. This phenomenon is possible when the lower vibrational levels of the S_2 state overlap the upper vibrational levels of the S_1 state, and they basically have the same potential energy (59,60,62).

From the lowest vibrational level of the S_1 excited state, the electron drops to some vibrational level within the ground S_0 state and emits a photon. The photon is obviously of less energy than that which caused the original excitation, and therefore the wavelength of emission is longer than the wavelength of excitation. This phenomenon is known as the Stoke's shift (60,61). If the photon is in a higher vibrational level of the ground state, that difference in vibrational energy levels will

also be lost quickly by vibrational relaxation, and most of the electrons will return to the lowest vibrational level of the S_0 ground singlet state (59).

The time for vibrational relaxation and internal conversion from the upper vibrational levels to the lowest vibrational level of S_1 occurs in 10^{-12} seconds, which is more than enough time for the relaxation to be completed before emission of the photon takes place at about 10^{-8} seconds. Emission generally results from the thermally equilibrated excited state, and for this reason almost all fluorescence emission spectra show one band for $S_1 \rightarrow S_0$ irrespective of the number of bands the excitation or absorption spectra show (59,60,61).

Molecules in the lowest vibrational level of the S_1 excited state can sometimes undergo conversion to the first triplet state (T_1). Some of the vibrational levels of T_1 have nearly the same potential energy as the vibrational levels of S_1 and intersystem crossing occurs, $S_1 \rightarrow T_1$, while the spin of the excited electron from the singlet state becomes reversed. Transition from T_1 to the ground state is forbidden and as a result the rate constants for such phosphorescent emissions are several orders of magnitude smaller than those of fluorescence (59).

An excited molecule can return to its ground state by a combination of several mechanistic steps, and does so as soon as possible. The favored route back to the ground

state is simply the one that minimizes the lifetime of the excited state. Thus, if deactivation by fluorescence is rapid with respect to the radiationless processes, such an emission is observed. On the other hand, if a radiationless path has a more favorable rate constant, fluorescence is either absent or much less intense (59).

A factor of primary importance is a quantity known as the quantum yield, (ϕ) or quantum efficiency, for a fluorescent process. Quantum yield can be defined simply as the ratio of the number of photons emitted to the number of photons absorbed (62), or put another way, the number of molecules that fluoresce in a sample divided by the total number of molecules excited in the sample. As seen earlier in this section, the deactivation processes leading to non-radiative transitions are constantly in competition with the processes that result in emission of a photon. Therefore, the fluorescent quantum yield must be determined by the relative rates of the processes by which the lowest excited singlet state is depopulated, namely: fluorescence, intersystem crossing, external and internal conversion, predissociation and dissociation. (The latter two are processes by which the excited molecule breaks apart either due to high vibrational energy within the lower excited state after internal conversion, or the absorbed energy is directly responsible for the rupture of the bond).

The equation representing the fluorescence quantum yield, ϕ, follows:

$$\phi f = \frac{k_f}{k_f + k_{isc} + k_{ec} + k_{ic} + k_{pd} + k_d} \qquad \text{(Eq. 2)}$$

where the k terms are the rate constants for the different deactivation processes. This equation permits a quantitative interpretation of many of the structural and environmental factors that influence fluorescence intensity. Clearly, those variables that lead to high values for the fluorescent rate constant, k_f, and low values for the other k terms enhance fluorescence (59).

For a highly fluorescent molecule such as fluorescein (59), or rhodamine B (60), the quantum efficiency under some conditions approaches unity (~ 1.0). The environment also influences the quantum yield since solvent interactions or the presence of quenching species (other substances which cause the non-emitting pathways to dominate), can inhibit the emission process, thereby allowing the radiationless deactivation processes to prevail. It should be noted that the same type of equation and relationships can be made for the quantum yield of phosphorescence emission.

The fluorescence phenomenon is limited to a relatively small number of systems incorporating structural and environmental features that cause the rate of radiationless relaxation or deactivation processes to be slowed to a

point where the emission reaction can compete favorably. For the chemical systems that meet the criteria for this type of emission, measurement of the fluorescence intensity allows the quantitative determination of many species at trace levels. Many useful fluorometric methods exist, particularly for biological systems (59).

One of the greatest advantages of fluorometry is its inherent sensitivity. The lower limits for the method frequently are less than for an absorption spectroscopy technique by one or more orders of magnitude, and lie in the range between a few ppt and the ppb range. Furthermore, the selectivity is at least as good and often better than many other methods (59). In fluorescence one deals with two wavelengths - excitation and emission - for isolation of a species of interest, whereas absorption spectra have but one maximum wavelength which may be common to many similar species.

Fluorescent Derivatizing Agents and NBD-Chloride

Often there is a chemical system where a great advantage would be gained from using a fluorescence technique, but the component of interest has no intrinsic fluorescence (60,61). Over time, chemists have developed methods of varying the structure of the non-fluorescing substance in order to produce a fluorescent molecule. These modified structures are known as extrinsic

fluorophores (60).

For classes of compounds containing certain functional groups, a number of fluorescent derivatizing agents have been synthesized. These fluorescent derivatives of organic compounds are nearly always aromatic or heterocyclic ring systems which satisfy the requirement that the transition between the excited singlet state and ground state be $\pi^* \rightarrow \pi$ (60). For example, Dansyl chloride (1-dimethylaminonaphthalene-5-sulfonyl chloride) and Dansyl hydrazine (1-dimethylaminenaphthalene-5-sulfonyl hydrazine) are well known fluorescent derivatizing agents for primary amines, phenols, and aldehydes. G. Weber introduced DNS-Cl in 1952 as a reagent for the preparation of fluorescent conjugates of proteins, and used it for the study of protein structure by fluorescence polarization measurements (64,65). Since that time, DNS-Cl has evolved into a frequently used derivatizing agent for the determination of amino acids by TLC and HPLC using a fluorescence detector (66,67). Dansyl hydrazine, a modification of DNS-Cl retaining the fluorophore portion of the molecule, reacts with the carbonyl group of various aldehydes and can be used with the same type of determination methods (68). All dansyl derivatives excite in the range of 335 nm to 365 nm and emit their maximum fluorescence near 520 nm.

Another similar analogue to DNS-Cl is abbreviated BNS-Cl (5-di-n-butylaminonaphthalene-1-sulfonyl chloride),

where the variation in structure involves replacement of the N-dimethyl groups of DNS-Cl with N-dibutyl extensions. The compound BNS-Cl is used to derivatize amino acids in the same manner as the DNS-reagents were used. They have a slightly slower reaction time with amines, but a 10% gain in fluorescence efficiency (64). Naphthalene sulfonic acids have been modified to form anilino- and toluidinyl-fluorescent reagents (ANS and TNS) which non-covalently label proteins and membranes. These reagents are non-fluorescent in water, but are highly fluorescent when in non-polar solvents or bound to macromolecules (61). As mentioned in the section on review of fluorescent crown reagents, ANS has been investigated as a counter-ion with Na^+ complexed with polyether 12-crown-4 (57,58).

Fluorescamine (69,70,71,72,) and o-phthalaldehyde (71,73,74,75) are commonly used fluorescent derivatizing agents for primary amines, particularly the amino acids which are later separated and determined by HPLC. Carboxylic acids can react with 4-bromomethyl-7-methoxy-coumarin (Br-MmC) to produce highly fluorescent esters which can also be analyzed by HPLC (76,77).

Of all of the fluorescent derivatizing agents mentioned above, Dansyl-chloride has been the one most often used, especially for the analysis of amino acids. In 1968, a new fluorescent derivatizing agent appeared in the literature: 7-chloro-4-nitrobenzo-2-oxa-1,3-diazole,

(or 7-chloro-4-nitrobenzofurazan) better known as NBD-Cl (78,79). There are several advantages possessed by NBD-Cl that are making it very popular for the analysis of amino acids. The compound NBD-Cl can react with - not only- primary amines, but secondary amines and imino groups. If a neutral to acidic pH is used for the reaction mixture, it can react with thiols. Thus, it can selectively react with the amino acids containing S-H groups, such as cysteine (81).

Perhaps the most important feature of NBD-Cl, giving it an advantage over Dansyl-Cl, is - although it is a highly absorbant compound - it has no inherent fluorescence of its own which eliminates the disadvantage of a high reagent blank. Once reacted with amines, NBD-Cl produces highly fluorescent derivatives that show their maximum excitation in the range of 465-475 nm, a weaker band near 345 nm, and their emission maxima near 525 nm in organic solvents of low polarity such as chloroform (80). Another advantage lies in the fact that both the excitation and emission of NBD derivatives occur in the visible range. In contrast, DNS derivatives excite at 335 nm or 365 nm requiring the use of quartz cells. NBD-Cl also reacts faster than DNS-Cl, is more stable and dissolves better in an aqueous:organic medium (80,82).

Aside from NBD-Cl assisting in the determination of amino acids, it has also been used for the trace analysis

of drugs that contain the amine functional group. The reagent has been used successfully to determine the presence of amphetamines and their derivatives in human blood and urine samples (82).

Other aspects of the behavior of NBD-Cl derivatives will be presented in the Results and Discussion section of this dissertation where they will be related to the function and properties of MA-NBD as a new metal sensitive fluorophore and the subject of this work.

PROPOSAL

It can be seen from the review of literature and the background on crown ether reagents that few fluorescent crown reagents are available at this time for analytical usage in the determination of both alkali and alkaline earth metal cations. Two crown ether amines, diaza-18-crown-6 and monoaza-18-crown-6, contain secondary amines that seem well suited for derivatization with the reagent NBD-chloride. The resulting compounds should be both highly fluorescent and retain most of the complexing abilities associated with other modified and unmodified aza- and diaza-18-crown-6 species. The purpose of the research to be presented in this dissertation involves 1) the synthesis of new fluorescent crown ether reagents, and 2) the examination of their analytical utility. Alkali and alkaline earth metal ions are of particular interest. The new reagents' selectivity for various mono- and divalent cations as well as anion effects in various nonaqueous solvent systems are to be investigated. Preliminary observations have shown that one cation/anion complex with the ligand in acetonitrile is a novel fluorescence reagent possibly suitable for the determination of water in "anhydrous" organic solvents.

Reagents Used:

Acetonitrile, Aldrich Chemical Gold Label 99+%
Acetonitrile, Aldrich Chemical Sure Seal
Acetonitrile, Burdick and Jackson distilled in glass UV grade
Acetonitrile, Eastman Kodak #488
Acetonitrile, Fisher Scientific HPLC grade
Aluminum chloride, anhydrous, Aldrich Chemical 99.99% 29,471-3
Ammonium thiocyanate, Fisher Scientific,certified grade A-709
Boric acid, Fisher Scientific ACS certified A 73
t-Butanol, Fisher Scientific certified grade #A-401
Cadmium nitrate tetrahydrate, J. T. Baker analyzed reagent grade 1-1226
Calcium carbonate, Fisher Scientific ACS certified C 64
Calcium hydride, Aldrich Chemical 95+% 21,326-8
Calcium nitrate tetrahydrate, Fisher Scientific ACS Grade C-109
Calcium perchlorate tetrahydrate, G. Frederick Smith #12
Chloroform, Fisher Scientific Spectranalyzed #C-574.
4-Chloro-7-nitrobenzo-2-oxa-1,3-diazole, Regis Chemical #065050
Diethanolamine, Fisher Scientific purified grade
p-Dioxane, Aldrich Chemical Gold Label 99+% #15,482-2
p-Dioxane, Burdick and Jackson distilled in glass #AC 806
Filtering aid, Celite, Jones Manville analytical grade F2881-1
Hexane, Burdick and Jackson distilled in glass UV grade
Hydrochloric acid, J.T. Baker analyzed reagent grade 3-9535
Kryptofix 22, Matheson, Coleman and Bell Reagents #KX38
Lithium aluminum hydride, Alfa Products, Thiokol/Ventron Division
Lithium carbonate, Aldrich Chemical 99% 25,582-3
Lithium chloride, anhydrous, Alfa Products, Thiokol/Ventron Division 44139
Lithium hydroxide monohydrate, Aldrich Chemical 21,282-2
Magnesium nitrate hexahydrate, Fisher Scientific ACS certified M 46
Magnesium perchlorate, anhydrous, G. Frederick Smith #54
Magnesium perchlorate hexahydrate, G. Frederick Smith #56
Methanol, Burdick and Jackson distilled in glass # 230
Methanol, Fisher Scientific HPLC grade #A-452
Nitric acid, Fisher Scientific ACS reagent A-200
Pentane, Burdick and Jackson distilled in glass
Phosphoric acid, 85%, J.T. Baker analyzed reagent grade 3-0260
Potassium, metal, Fisher Scientific P 168-1
Potassium bisulfate, Fisher Scientific ACS certified P193
Potassium chloride, Fisher Scientific ACS certified P-217
Potassium nitrate, J.T. Baker analyzed reagent grade 1-3624
Potassium perchlorate, anhydrous, Fisher Scientific ACS certified P-276
Potassium permanganate, Fisher Scientific ACS reagent
Potassium thiocyanate, Fisher Scientific ACS certified P 317
Quinine, Aldrich Chemical #14,590-4
Silver nitrate, D. F. Goldsmith ACS grade
Silver perchlorate, G. Frederick Smith ACS Reagent #86

Reagents Used, Cont:

Sodium chloride, J.T. Baker analyzed reagent grade 1-3624
Sodium hydride, Aldrich Chemical dry 97% #22,344-1
Sodium nitrate, Fisher Scientific ACS certified S 343
Sodium perchlorate, anhydrous, G. Frederick Smith #91
Sodium thiocyanate, Fisher Scientific ACS certified S441
Sulfuric acid, Fisher Scientific ACS reagent A-300
Tetraethylene glycol, Aldrich Chemical #11,0175-5
Tetrahydrofuran, Waters Associates (Non UV) 99% Min. #017198
p-Toluene-sulfonyl chloride, Aldrich Chemical Gold Label 99+% #24,087-7
Water, deionized and distilled
Water, Fisher Scientific #W-5 HPLC grade

Equipment. Ultraviolet and visible spectra were obtained on either a Perkin-Elmer 330 or a Perkin-Elmer Coleman 575 spectrophotometer using matched 1 cm quartz cuvettes, or 1 cm Beckman borosilicate glass cuvettes occasionally for those spectra requiring measurements in only the visible range. Fluorescence spectra were obtained on a Perkin-Elmer LS-5 spectrofluorometer connected to a Perkin-Elmer R-100 recorder, samples were contained in a 1 cm quartz fluorescence cuvette. Infrared spectra were obtained from an IBM Fourier-transform IR 98 spectrophotometer operated by K. Martin. Proton magnetic resonance spectra were obtained on Varian EM360 or EM360A NMR spectrometers. The pH of buffers and solutions were determined with a Corning Model 12 pH meter. Melting points were determined on a Fisher-Johns melting block apparatus. High performance liquid chromatographs of the products and starting materials were obtained from an LC system composed of the following component units: a Beckman Model 100A solvent reservoir and pump with a 20 microliter injection loop, an Ultrasphere ODS-C_{18} 25 cm analytical column connected to an Altex UV detector, 313 nm, with Beckman Model 150 controls. When fluorescence detection of the eluted products was required, the eluent from the UV detector was immediately measured by the Perkin-Elmer LS-5

spectrofluorometer modified with a 20 microliter LC sample cell as a second detector for fluorescent compounds. Preparative chromatography was used to separate the product from the reactant mixtures by replacing the 20 μL injector loop and ODS analytical column with a 5 mL Teflon coil 1/16 inch diameter and an Altex 25 cm × 2.54 cm glass column packed with E. Merck Silica gel 60. Later preparations were purified by flash chromatography using a 75 cm × 2.54 cm glass column packed with the same material. Fractions of the eluted material were concentrated through removal of the volatile solvents by Buchi rotary evaporators, and further purification of one of the components was obtained from sublimation at 130-140 °C and 0.03 Torr from a Kugelrohr distillation apparatus. Thin layer chromatography was performed on the product and reactant mixtures using E. Merck silica gel 60-F 20 × 20 cm glass plates, Eastman Kodak #13179 No. 6061 or Alltech Associates silica gel 60 F-254 EM #5775 plastic plates. The UV-absorbing and fluorescent spots were detected with an ultraviolet hand-lamp with maximum emission at 340 nm.

Syntheses

Tetraethyleneglycol-di-(toluene-p-sulfonate, (TEG-di-tosylate), was prepared according to the procedure of Brewster and Ciotti from tetraethylene glycol and p-toluenesulfonyl chloride (83).

Monoaza-18-crown-6, (monoaza-4,7,10,13,16-pentaoxa-cyclooctadecane), was prepared according to the 1981 published method of Okahara et al., (84) by reacting the above product with diethanolamine in potassium t-butoxide mixture and p-dioxane under nitrogen. The resulting mixture was a light-yellow sludge that was filtered over dry filtering aid with occasional rinses with p-dioxane. Excess dioxane was removed from the dark, yellow viscous product by rotary evaporation leaving 125 mL of an even more viscous product. Water was added to the mixture which was extracted first with hexane to remove hexane soluble materials, and then dichloromethane. The dichloromethane extracts were combined and reduced by rotary evaporation leaving about 45 mL of brown viscous residue. The residue was transferred to a Kugelrohr distillation apparatus and moist yellowish-white crystals were collected when the sublimation temperature was raised 130-140 °C. The crystals were washed from the collection flask with warm hexane. The hexane was removed from the product first by

gentle heating; the crystals were then put under strong vacuum for two days. Four recrystallizations from pentane (HPLC grade) produced large white crystals with a mp of 49-51 °C which agrees with the literature values for the product. (84, 85). The yield from this synthesis was 1.1226 g of monoaza-18-crown-6 (MW 263.3). $^{1}H_{nmr}$ ($CDCl_3$) ppm, 3.67 (m, 16 H), 2.8 (t, 4 H), 2.25 (s, 1H). IR (KBr) NH 3330 cm^{-1}, CH_2 2889,2817 cm^{-1}, 1477, 1460 cm^{-1}, 1350 cm^{-1}, C-N-C 1111 cm^{-1}, C-O-C 999 cm^{-1}. This synthesis was performed twice over the course of the project.

When more monoaza-18-crown-6 was required a year later, 1.7 g was synthesized in two batches by R. Glowinski following the 1982 published method by Okahara et al., (86) for the first synthesis and the earlier method of Okahara et al., (84) that was described here for the second batch.

N-(4-nitrobenzofurazan)-monoaza-18-crown-6, (MA-NBD). Two methods were used to synthesize this reagent; the synthetic route is presented in Figure 3. The first method following the procedure used by Ahnoff et al., requires more time and more controlled conditions (87). The second method is faster. It only requires heating on a hot plate under a stream of nitrogen, and the only components present are the reactants and the organic solvent in which the reaction occurs. Either method requires extensive

SYNTHETIC ROUTE FOR FLUORESCENT REAGENT

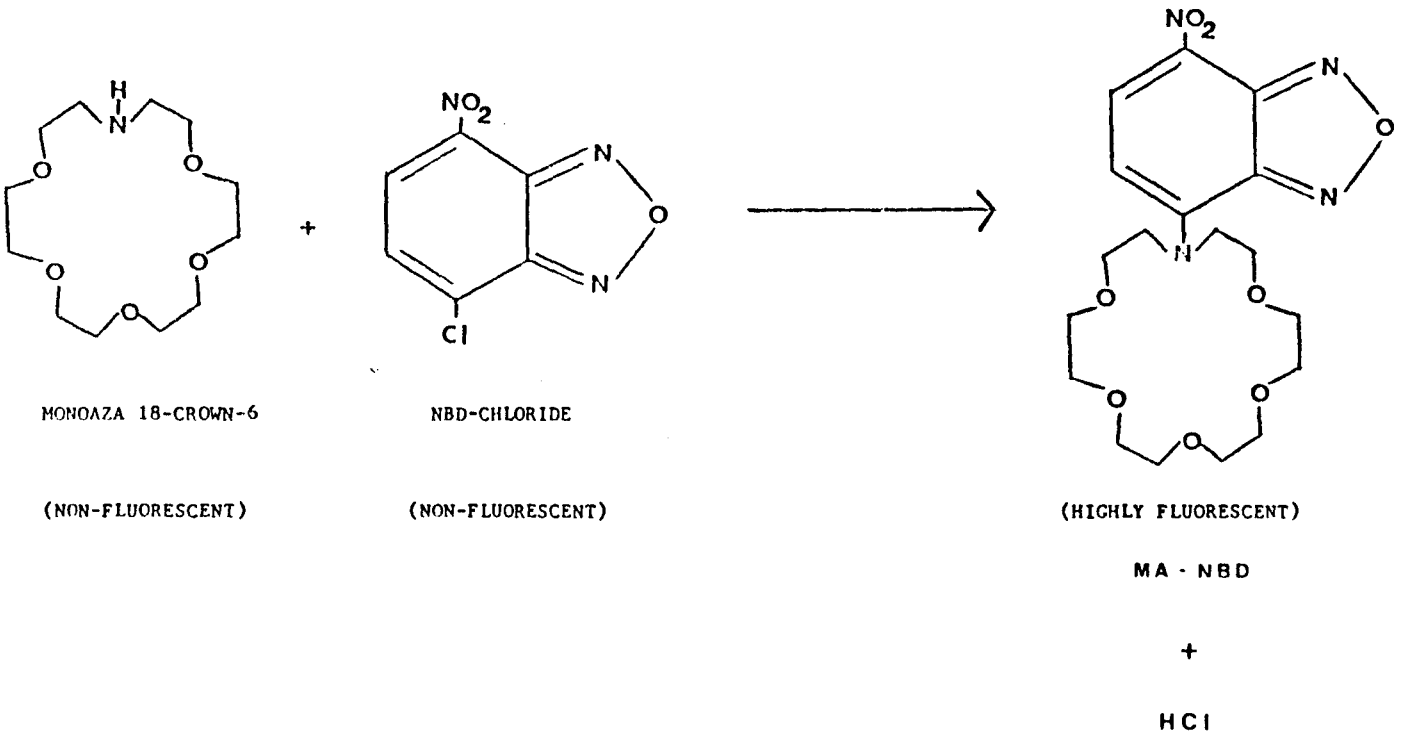

FIGURE 3. SYNTHETIC ROUTE FOR MA-NBD.

purification via preparative column chromatography and results in rather low yields. One modification of the Ahnoff et al. method (87) was the substitution of lithium for potassium in the recommended $K_2B_4O_7 \cdot H_2O$ buffer. The buffer of pH 9.5 and 0.4 mol/L concentration. was prepared from aqueous solutions of boric acid and lithium hydroxide A second modification of the method used a higher concentration of methanol to inhibit decomposition observed in more the aqueous solution (87). Monoaza-18-crown-6, 0.514 g (2.0 mmol), was weighed into a 250-mL erlenmeyer flask and dissolved in 20 mL of methanol (MeOH). Fifteen milliliters of the lithium borate buffer were added, and the solution was stirred using a magnetic stirrer and stir bar while suspended in a 55°C water bath. Four tenths of a gram (2.0 mmol) of 4-chloro-7-nitrobenzofurazan (NBD-Cl) was dissolved in 40 mL of MeOH and slowly added to the buffered amine solution with a pasteur pipet. The reaction mixture was stirred for one half hour at 55°C in a darkened room as Ahnoff had warned that the reaction can be light sensitive. The flask was then chilled in an ice-bath inside a Dewar flask and acidified with 2.0 M HCl to a pH of 1.5, in order to stop the reaction from proceeding further and decomposing. A blank reaction mixture was also prepared for NBD-Cl containing all the components except for the monoaza-18-crown-6. This blank was later used to determine spectral characteristics of any NBD-Cl by-products that

might have developed during the preparation of the MA-NBD. The flask containing the MA-NBD reaction mixture was heated on a hot plate between 70-80 °C under a stream of nitrogen leaving an oily residue around the sides of the flask and about 4 mL of liquid. Of the solvents tested, chloroform was the most successful in dissolving the orange residue. The $CHCl_3$ solution was found to contain several absorbing and fluorescent products. The $CHCl_3$ was removed from the product mixture under reduced pressure, the residue dissolved in HPLC grade MeOH, and the solution then concentrated to less than 10 mL by further rotary evaporation. This solution was passed through a 0.5 μL Nylon-66 filter membrane (using a Rainin microfiltration-syringe kit) and injected onto a prep-column packed with E. Merck silica gel 60 and eluted with HPLC grade MeOH. Five fractions of unequal volumes were collected as products were detected by the UV absorbance detector and the Perkin-Elmer LS-5 spectrofluorometer set at 475 nm ex and 540 nm em as fluorescence detector. The fifth fraction contained the most highly absorbing and fluorescent band, and thin layer chromatography (TLC) plates developed with MeOH showed that only one product was present with an R_f of 0.42. This fraction was reduced to 4 mL of an intense red-orange syrup by rotary evaporation. Five mL of MeOH was added to the flask which was sealed and stored in a freezer overnight. The following day, the flask was

accidentally bumped as it was removed from the freezer, and when a few mL of MeOH were used to rinse down the walls of the flask, the product immediately started to crystallize into deep orange shiny flakes. The flakes were filtered with a Hirsch funnel and the mp of this MA-NBD product determined to be 76 °C. Analysis, calculated for $C_{18}H_{26}N_4O_8$, (MW 426.43): C, 50.70%; H, 6.14%; N, 13.14%. Found: C, 50.29%; H, 6.20%; N, 13.18%. (Micro-tech Laboratories, Inc., Skokie, IL 60626). $^1H_{nmr}$ ($CDCl_3$) ppm, 8.5 (d, 1 H), 6.4 (d, 1 H), 4.3 (t, 4 H), 3.7 (m, 10 H). IR (KBr), 3439 cm^{-1}, 2872 cm^{-1}, 1610 cm^{-1}, 1558 cm^{-1}, 1493 cm^{-1}, 1335 cm^{-1}, 1296 cm^{-1}, 1178 cm^{-1}, 1097 cm^{-1}, 1001 cm^{-1}, 945 cm^{-1}, 801 cm^{-1}, 741 cm^{-1}, 600 cm^{-1}.

The second method of synthesizing MA-NBD used 0.672 g (2.6 mmol) of monoaza-18-crown-6 dissolved in 15 mL spectral grade chloroform ($CHCl_3$) and 0.499 g (2.5 mmol) of NBD-Cl also dissolved in 15 mL $CHCl_3$ mixed together in a 200-mL tall beaker. A blank was also run on the NBD-Cl dissolved in the $CHCl_3$ without the crown amine in order to determine what side products form from the NBD-Cl under the same conditions. The reaction mixtures were heated to dryness on a low hot plate while under a N_2 stream. The original monoaza-18-crown-6 in $CHCl_3$ was colorless and the NBD-Cl in $CHCl_3$ was originally pale yellow before combining the two. Once the two solutions were mixed the resulting solution immediately turned light orange and developed a

darker orange as the heating continued. After reaching dryness, the solutions were twice reconstituted with 20 mL of $CHCl_3$ and reevaporated to dryness on the hot plate. By the end of the second evaporation to dryness the product mixture became a dark red-brown and oily solid. The blank containing the NBD-Cl alone merely developed a more concentrated yellow color. A TLC plate used to test the reaction mixtures showed four spots for the MA-NBD preparation with the predominant component being the desired bright orange fluorescent MA-NBD with an R_f of 0.42. The blank NBD-Cl showed only two spots also present in the other preparation. These are the two fastest eluting components, a dark yellow fluorescent spot with an R_f of 0.87 and an absorbent yellow spot with an R_f of 0.76. Later development in an iodine vapor chamber showed the presence of some unreacted monoaza-18-crown-6 in the MA-NBD reaction mixture that did not move up the plate with the methanol. The MA-NBD reaction mixture was then redissolved in about 5 mL MeOH and applied to a flash chromatography column packed with 6 inches of E. Merck silica gel 60 and eluted with HPLC grade MeOH. Five fractions were collected as different orange and brown bands could be seen eluting down the column. Thin layer chromatography showed the first two fractions contained the two fastest eluting components, the third and fourth fractions contained the third component and the desired product, and the last

fraction contained a low concentration of the desired product with a trace of contamination from the previous fraction. These last three fractions were combined, reconcentrated by rotary evaporation, and reapplied to the flash column. The process was repeated until the desired MA-NBD could be collected without contamination. Several recrystallizations from MeOH were required before the red-orange shiny crystals (mp of 74-75 °C) could be isolated. Analysis, calculated for $C_{18}H_{26}N_4O_8$: C, 50.70%; H, 6.14%; N, 13.14%. Found: C, 50.23%; H, 6.13%; N, 13.30%.

Reaction of Kryptofix 22 (1,10-diaza-4,7,13,16-tetraoxacyclooctadecane) with NBD-Cl: Kryptofix 22 is an 18-membered heterocyclic crown amine with a structure like monoaza-18-crown-6, except that it has nitrogen in the ring at both the 1- and 10-positions. Kryptofix 22 was reacted with NBD-Cl in exactly the same fashion and with the same two synthetic methods as for the synthesis of MA-NBD. Because of the two possible secondary amine sites available for derivatization with NBD-Cl, 1:1 and 2:1 mole ratios of NBD-Cl to Kryptofix 22 were prepared. Prep-column chromatography with both normal phase and reversed-phase packing were used to separate the desired fluorescent compounds form the reaction mixtures. Some of the separations produced fractions that were very close to yielding a pure product, but when final purifications were attempted, fur-

ther contamination with decomposition products were always evident. Eventually all attempts to isolate a Kryptofix-NBD compound were abandoned and all research efforts were directed towards the isolation and studies of MA-NBD.

Spectral Studies of MA-NBD

UV-Visible Absorption Characteristics of MA-NBD: The absorbance spectrum of MA-NBD in MeOH, $CHCl_3$, CH_3CN, and water was determined using the Perkin-Elmer 330 or the Perkin-Elmer Coleman 575 UV-Vis spectrophotometers. Experiments using both spectrophotometers at the same time showed no difference in wavelength maxima, or in absorbance readings beyond the third decimal place. Molar absorptivities were determined for the two absorbance maxima around 470 nm and 340 nm of MA-NBD in each of these solvents. The experiments used standard solutions whose concentrations ranged from 1×10^{-6} to 1×10^{-4} mol/L and adhered to the limitations of Beers Law by not exceeding 1.5 absorbance units. The standards were measured against the appropriate solvent blanks either by using matched 1 cm quartz cuvettes with the solvent blank inserted in the reference chamber, or by using the background correction capability of the Perkin-Elmer 330 spectrophotometer. The absorbance data was obtained and the results appear in Tables 2-5. Calibration curves were plotted for absorbance vs. concentration of MA-NBD at both wavelength maxima.

Molar absorptivities were determined by linear regression analysis for the slope of the curve using a Texas Instrument-55 scientific calculator. The spectra were scanned from 250-600 nm on the P.E. 330 at 50 nm/min scan speed; 1 nm slit width; and response of 2. Instrumental settings for the P.E. 575 were 60 nm/min scan speed; 1 nm slit width; response: medium; scan range from 250-600 nm.

Fluorescence Emission Characteristics of MA-NBD:

The excitation and emission spectra of MA-NBD were determined in MeOH, $CHCl_3$, CH_3CN, and water. Fluorescence measurements used dilute concentrations of the MA-NBD standards prepared earlier for the determination of molar absorptivities. To avoid inner filtering, the extent of the dilution was such that the absorbance of MA-NBD in any of the solvents did not exceed 0.05 A. The two excitation wavelength maxima and the maximum emission wavelength were determined for MA-NBD in all four solvents. The results appear in Tables 6-9. Calibration curves were plotted for fluorescence intensity vs. the concentration of MA-NBD for each of the solvents at both excitation maxima. Constants were derived for fluorescence intensity/molar concentration of MA-NBD (F/C) in each solvent. These measurements were compared to a solution of quinine bisulfate under the same instrumental conditions and parameters for a correction to relative fluorescence. The fluorescence spectra and results as reported here are uncorrected spectra. This

procedure and the set of calculations were repeated on several occasions: primarily when the source or other electronic components were replaced and on other occasions when the sensitivity of the LS-5 spectrofluorometer appeared to change. On each of these occasions the fluorescence intensity of standard concentrations of MA-NBD in the solvents used for experimental work was measured and compared to a standard solution of quinine bisulfate, and the molar absorptivities were revalidated. Spectrofluorometer settings used 5 × 5 nm ex/em slits; response of 2; 120 nm/min scan speed. Emission spectra were scanned from 500-600 nm, with the excitation wavelength fixed at 474 nm for MeOH, 475 nm for $CHCl_3$, 475 nm for CH_3CN, and 485 nm for water. All excitation spectra were scanned from 320-520 nm with the emission wavelength fixed at 540 nm. (Slit settings other than these were used on certain occasions. They are indicated for those specific results.) All fluorescence intensities have been reported after scale correction to the LS-5 Fixed Scale sensitivity setting of 1.00.

The Effect of pH on the Absorbance Spectra of MA-NBD in Aqueous Media: Buffer solutions were prepared according to tables from Kolthoff (88) that covered a pH range from 2.15 to 11.50 using combinations of HCl, H_3PO_4, Na_2CO_3 and NaOH. Because the monoaza-18-crown-6 part of the reagent is known to complex with sodium to some extent, lithium

hydroxide and lithium carbonate were substituted for the sodium salts. When pH higher than 12.00 was required, a solution of LiOH/LiCl with weak buffering capacity was prepared, producing a solution with a pH of 12.10. The ionic strength of the buffer solutions was kept near 0.01. Solutions were prepared containing 1.13×10^{-4} mol/L MA-NBD in buffered solution at pH values of 2.15, 2.87, 7.80, 8.60, 9.53, 10.02, 11.05, 11.45, and 12.10. Each solution was scanned using the Perkin-Elmer 330 spectrophotometer. The change of maximum wavelength and absorbance of MA-NBD with pH was determined and an isosbestic point was found.

The Effect of pH on the Fluorescence Spectra of MA-NBD in Aqueous Media: The same buffer solutions were used to prepare MA-NBD at different pH values for fluorescence measurements. The concentration of MA-NBD had to be diluted to 2.3×10^{-5} mol/L in order to prevent inner filtering due to intense absorbance of the solution. Excitation scans were done for all solutions from 320-520 nm with the emission held constant at 540 nm. Emission scans were run from 500-600 nm with the excitation wavelength held constant at 480 nm.

The Effect of pH on the Distribution of MA-NBD Between Chloroform and Aqueous Phases: Three and one half milliliters of 2.1×10^{-5} mol/L MA-NBD in water were added to six small test tubes. These preparations were adjusted to a pH of 3.0, 5.5, 7.5, 10.0, 11.0, and 12.0.

Three and one half milliliters of spectral grade $CHCl_3$ were pipetted into each test tube which was then capped and inverted several times to assure complete mixing of the two phases. The phases were carefully removed separately from each test tube by a pasteur pipet and transferred to a 1 cm cuvette. The UV-visible spectrum for each solution was scanned against the appropriate solvent blank of either water or $CHCl_3$.

MA-NBD as a Reagent for the Extraction of KSCN from Aqueous Phase to Chloroform with a Change in pH: A set of six aqueous solutions were prepared with exactly the same concentration of MA-NBD, 2.1×10^{-5} mol/L, and the same set of pH values from 3.0 to 12.0, as were described in the previous section. The only difference was that about 0.01 mol/L potassium thiocyanate (KSCN) was added to each preparation before extraction with $CHCl_3$. Aqueous and organic phases were separated, as before, and their UV-visible spectra measured to discover if the KSCN complexes with the MA-NBD and affects its distribution and absorbance in either phase. Other aqueous solutions containing the MA-NBD with KNO_3 and KCl were also prepared and treated in the same manner in order to observe whether different anions combined with potassium would have any affect on the absorbance.

Effects of the Presence of Metal Cations on the Fluorescence Emission of MA-NBD in Chloroform:Methanol; Concentration of Metal Salts vs. Fluorescence Intensity:

Titration curves were plotted showing the relationship between the concentration of metal salts present and the enhancement of the fluorescence emission of MA-NBD as it complexes with the metal cation in a 1:1 $CHCl_3$:MeOH solvent system. All of the titration studies used three 10.00-mL Class B microburets to prepare the solutions. The individual burets contained; 1) a standard concentration of the metal salt in HPLC grade MeOH, 2) HPLC grade MeOH alone, and 3) 7.0×10^{-7} mol/L MA-NBD in spectral grade $CHCl_3$. Solutions were prepared in small 125 × 10 mm test tubes by adding 1.50 mL of the MA-NBD in $CHCl_3$ plus some combination of added volumes of the metal salt in MeOH and the MeOH from the other two burets that always added up to 1.50 mL. In this way, the resulting volume of the sample solution was always 3.00 mL and the solvent medium was always 1:1 $CHCL_3$:MeOH. The solutions were quickly stirred for 20 sec using either a small glass rod, or a small cuvette-size magnetic stir bar, and then transferred to a 1 cm quartz fluorescence cuvette. The solution in the cuvette was measured by exciting at 475 nm and scanning emission wavelengths from 515-555 nm at a scan speed 120 nm/min, response of 3, and widths set at 5 × 10 nm for excitation and emission slits. The final concentration of

MA-NBD in all of the solutions was 3.5×10^{-7} mol/L, and the initial fluorescence of the MA-NBD - before any metal salt was added - was 85 to 87 Fluorescence units when corrected to a Fixed Scale of 1.00. The cuvette was cleaned between solutions by rinsing first with acetone, then deionized H_2O, and finally HPLC grade MeOH. It was wiped with a lint free tissue and then dried by placing over a 1/4 " diameter Teflon tube attached to a water aspirator. The metal salts tested in this 1:1 $CHCl_3$:MeOH solvent system were silver perchlorate, silver nitrate, sodium chloride, sodium thiocyanate, potassium chloride, potassium thiocyanate, and ammonium thiocyanate. They were used in concentrations ranging from 1×10^{-3} mol/L up to 5×10^{-2} mol/L. A number of other alkali, alkaline earth, and transition metal salts were tested but these produced little or no change in fluorescence emission when mixed with MA-NBD in 1:1 $CHCl_3$:MeOH.

Effect of the Presence of Metal Cations on the Fluorescence Emission of MA-NBD in Acetonitrile; Concentration of Metal Salts vs. Fluorescence Intensity:

Using the same procedure as described in the previous section, three 10.00-mL Class B microburets were used to prepare the solutions to be measured by fluorescence. In this case, however, the chloroform:methanol solvent system was replaced by spectral grade acetonitrile. Several different concentrations of MA-NBD lying between 1×10^{-8}

and 2×10^{-6} mol/L in CH_3CN were examined, and the optimum concentration for each study was chosen depending upon the maximum fluorescence intensity of the complexes of the individual metal salts with MA-NBD. Because the fluorescence emission of MA-NBD is stronger in CH_3CN than in $CHCl_3$:MeOH, both the excitation and emission slits were adjusted to 5 × 5 nm. Excitation was again set at 475 nm and the emission wavelengths scanned from 515-555 nm. Other instrumental parameters were the same as described in the previous section. The metal salts used for the titration studies were calcium nitrate tetrahydrate, calcium perchlorate tetrahydrate, cadmium nitrate tetrahydrate, magnesium nitrate hexahydrate, anhydrous magnesium perchlorate and magnesium perchlorate hexahydrate, potassium perchlorate and sodium perchlorate. These were used in concentrations ranging from 1×10^{-8} mol/L to 9×10^{-2} mol/L. Several other alkali, alkaline earth, and transition metal salts were also tested but produced little or no change in fluorescence emission when mixed with MA-NBD in acetonitrile.

Determination of the Formation Constant of MA-NBD Complexes: Most of the curves of fluorescence intensity of the MA-NBD solution versus the log of the molar concentration of metal salt added are S-curves very much like those obtained for pH titrations. A formation constant (K_f) for 1:1 metal complexes with MA-NBD was easily derived

by 1) finding the midpoint of the tangent equal to the point of the greatest change of slope for the curve (this point also corresponds to 50% of the maximum complexation), 2) finding the concentration of the metal salt added at that point, and 3) inserting this value into the equilibrium constant expression after determining the remaining concentration of the metal salt at equilibrium.

$$K_f = [M^{n+} \cdot MA\text{-}NBD] \; / \; ([M^{n+}] \; [MA\text{-}NBD]) \qquad \text{(Eq. 3)}$$

Because the concentration of the complex, $[M^{n+} \cdot MA\text{-}NBD]$, is equal to [MA-NBD], the remaining concentration of uncomplexed MA-NBD at 50% complexation, the expression simplifies to:

$$K_f = 1 \; / \; [M^{n+}] \qquad \text{(Eq. 4)}$$

The formation constant is the reciprocal of the equilibrium molar concentration of the metal salt at that point. The equilibrium concentration of metal salt is equal to the total concentration of metal salt added, minus 1/2 the total concentration of MA-NBD added to the solution.

An alternative way of determining the formation constant uses a somewhat more strenuous set of calculations.

There is only a small change in the maximum emission wavelength of the complexed and uncomplexed forms of MA-NBD,

so that when both species are present only one peak is observed, but a greater difference exists between the maximum fluorescence intensities of these two forms of MA-NBD at a given concentration. The largest difference between the fluorescence intensity of uncomplexed and complexed MA-NBD has been seen with calcium nitrate tetrahydrate in acetonitrile, and this system will used for demonstrating the determination of K_f.

The uncomplexed form of MA-NBD has its maximum emission at 538-540 nm. For a given concentration of MA-NBD (represented here by the symbol for ligand, L) a constant relationship exists with fluorescence intensity: $F_L/[L]$, because the pathlength in all cases is 1 cm. The complexed form of MA-NBD with Ca^{2+} in calcium nitrate tetrahydrate has its maximum emission at 527 nm, and there is also a constant relationship between fluorescence intensity and a given concentration of the complex: $F_{Ca \cdot L^{2+}}/[Ca \cdot L^{2+}]$. The following equations show the contributions of both species to the total fluorescence intensity, where C_L and $C_{Ca \cdot L^{2+}}$ represent the equilibrium molar concentrations of L (MA-NBD) and the complex of calcium nitrate tetrahydrate with MA-NBD, respectively:

$$F_L + F_{Ca \cdot L^{2+}} \longrightarrow F_{Total} \qquad \text{(Eq. 5)}$$

$$C_L \times F_L/[L] + C_{Ca\cdot L^{2+}} \times F_{Ca\cdot L^{2+}}/[Ca\cdot L^{2+}] \longrightarrow F_{Total} \quad \text{(Eq. 6)}$$

The total fluorescence intensity, F_{Total}, is obtained from some point corresponding to a certain percent of the complex formed along the curve of fluorescence intensity vs. log molar concentration of $Ca(NO_3)_2\cdot 4H_2O$. Extrapolation to the abscissa and antilog conversion gives the total molar concentration of $Ca(NO_3)_2\cdot 4H_2O$ added to the solution. The equilibrium molar concentration of $Ca(NO_3)_2\cdot 4H_2O$ is obtained by subtracting the amount of $Ca(NO_3)_2\cdot 4H_2O$ complexed (which is equal to the original concentration of MA-NBD added to the solution, multiplied by the percent complexation) from the total molar concentration $Ca(NO_3)_2\cdot 4H_2O$ added. Several points were chosen along the curve corresponding to a different percent of maximum complexation, with particular weight given to those points surrounding 50% complexation. Once the equilibrium concentrations of 1) the complex, 2) the remaining MA-NBD and 3) $Ca(NO_3)_2\cdot 4H_2O$ were calculated, they were inserted in the equilibrium constant expression and the value of the formation constant was obtained. All of the K_f values for the different concentrations of MA-NBD used were averaged to obtain the final reported value for K_f.

Purification of Acetonitrile to Produce Optically Pure and Dry Solvent: The method of Walter and Ramaley (89)

was used to prepare optically pure and dry acetonitrile from the better grade commercial acetonitriles manufactured by the Sohio process. In this process the CH_3CN is produced as a byproduct from the manufacture of acrylonitrile from propylene and ammonia. The preparation of the purified and dried CH_3CN was performed twice, once using Burdick and Jackson distilled in glass UV grade CH_3CN and later using Fisher Scientific HPLC grade CH_3CN. The purification involved four steps: 1) reflux over anhydrous aluminum chloride (15 g/L) for 1 hour prior to rapid distillation; 2) reflux over alkaline potassium permanganate (10 g $KMnO_4$/L and 10 g Li_2CO_3/L) for 15 min prior to rapid distillation; 3) reflux over potassium bisulfate (15 g/L) for 1 hour prior to rapid distillation; and finally, 4) reflux over calcium hydride (2 g/L) for 1 hour prior to careful distillation from a fractionating column at high reflux ratio. The middle 80% distillate is retained. The entire distillation set-up was kept under dry nitrogen and the distillations were from a Vigreaux column. The acetonitrile distillate was transferred to clean and dried 1-L or 1-gal brown glass bottles capped with rubber septa using the recommended procedure for transferring air-sensitive and moisture-sensitive reagents (90). The bottles were first purged with dry nitrogen and the solvent was then transferred from distillation flask to the bottles through a flexible double-tipped stainless steel needle by

nitrogen pressurization. Those bottles of CH_3CN to be used in the H_2O/CH_3CN analysis remained sealed until the time of the study. If some solvent had to removed before the entire bottle was opened for the actual experiment, it was removed by the same method described above for the transfer of air and moisture sensitive reagents.

The Determination of the Water Content of Various Sources of Acetonitrile Based on the Change in Fluorescence Intensity of the MA-NBD Complex with Calcium nitrate tetrahydrate: This particular study was performed twice over the course of one year with little change in equipment used or methods of sample preparation and fluorescence analysis. The modifications in procedure used for the second study will appear at the end of these next few sections that describe experimental procedure used for the initial study.

Equipment Used: The entire preparation of all standard and unknown sample solutions to be measured by fluorescence spectroscopy was performed in a glove box purged for three days with dry nitrogen. The equipment and materials to be used were moved into the glove box after it had been purged two days.

All glassware to be used in the experiment was first soaked in the following solutions: 1) alcoholic KOH; 2) a commercial detergent designed specifically for the removal of metal cations; 3) a 7 M nitric acid solution; and 4) basic EDTA solution. Deionized water was used to rinse

glassware before transferring to each subsequent soaking solution as well as for the final rinse. The glassware was thoroughly dried in an oven set at 110 °C and then transferred to the drying oven set at 65 °C which was located close to the glove box. All plastic materials, such as test tube racks, stoppers, or powder funnels, or special equipment with plastic or Teflon (polytetrafluoroethylene) parts such as a 2-mL microburet and a 3-mL automatic pipet, were also dried and stored in the 65 °C-drying oven. All items remained stored in the 65 °C-drying oven for a time interval of several days to several weeks before being transferred to the nitrogen purged glove box. Flasks, test tubes and other glassware were capped or sealed before being moved from the drying oven to the glove box chamber. After cooling to room temperature inside the chamber, caps and seals were removed from the glassware which was then allowed to equilibrate with the dry nitrogen atmosphere for 24 hours before the preparation of the samples. Two wide-mouth jars filled with phosphorous pentoxide with some indicating drierite were opened during this period of time, as was a small vial containing the blue anhydrous form of cobalt chloride. The phosphorous pentoxide and the cobalt chloride did not change color or consistency until after the solutions were prepared and removed from the chamber indicating that no detectable moisture was present in the atmosphere of the glove box. All standard and sample

solutions to be measured by fluorescence spectroscopy were prepared in 150 × 15 mm (25-mL vol) borosilicate glass test tubes capped with polyethylene stoppers. The preparation of the solutions required several volumetric pipets ranging from 1-mL to 15-mL sizes (used with 3-way valved automatic pipet bulbs), a 2-mL microburet (with 0.002-mL divisions), a 3-mL Oxford automatic pipet (able to deliver 0.800-3.000 mL aliquots in 0.020-mL increments), and Eppendorf pipets with adjustable volumes from 7-100 μL and 100-1000 μL sizes with disposable polyethylene tips.

Reagents and Chemicals Used: About 3.5 liters of Fisher Scientific HPLC grade CH_3CN was dried and purified using the procedure (89) described in the previous section on purification of solvents. This particular preparation of CH_3CN was completed 10 days before the experiment was performed. A 0.91 mg portion of MA-NBD was quickly weighed into a dry 50-mL volumetric flask, sealed with a polyethylene stopper, and transferred to the purged glove box. The night before the experiment was to be performed, the MA-NBD was dissolved and the flask brought to volume with the dried CH_3CN producing a solution 4.22×10^{-5} mol/L MA-NBD. Crystals of calcium nitrate tetrahydrate were taken from a tared weigh vial containing about 0.07 gram of the salt and transferred to a dry 100 ml volumetric flask. Later weighing of the vial indicated that 0.0622 g of the $Ca(NO_3)_2 \cdot 4H_2O$ had been added. Ten milliliters of the MA-

NBD solution was added to the flask using a volumetric pipet, the salt and MA-NBD were shaken and brought to volume with the dried CH_3CN in the 100-mL flask producing a standard solution containing 4.22×10^{-6} M MA-NBD and 2.63×10^{-3} M $Ca(NO_3)_2 \cdot 4H_2O$. Repeated shaking over an hour's time was necessary to dissolve all the salt in the solution. A 10% (v/v%) H_2O in CH_3CN standard was prepared by pipetting 10 mL of HPLC grade water into a 100 mL volumetric flask and bringing to volume with the dry acetonitrile. Pure HPLC grade H_2O was stored in a small 25-ml stoppered flask to be used for the preparation of standard solutions where higher concentrations of water were required.

Unknown H_2O/Acetonitrile Samples: Six acetonitrile samples whose water content was to be determined by this fluorescence method included: the remaining volume from an earlier batch of dried and purified CH_3CN; Aldrich Gold Label acetonitrile 99+%, (two bottles from the same lot, but opened on different occasions); Fisher HPLC grade CH_3CN; Burdick and Jackson distilled in glass UV grade CH_3CN, and Eastman 488 CH_3CN. Other details such as lot numbers, opening date and usage, and storage conditions of each of these samples will appear in Tables 38 and 39 in the Results and Discussion section of the dissertation. Each of these samples to be tested was transferred from its original container to a dry 60-cc borosilicate glass bottle

sealed with a polyethylene lined screw-cap. These bottles were filled to the neck, capped tightly, and were then transferred to the glove box one day before the sample preparations.

Preparation of the Standard and Unknown Solutions:

All standard solutions contained 20.00 mL of solution and were prepared in the 25-mL test tubes by adding 1) 3.00 mL of the 4.22×10^{-6} M MA-NBD/2.63×10^{-3} M $Ca(NO_3)_2 \cdot 4H_2O$ solution; 2) 2.000 mL of different concentrations of H_2O in CH_3CN; and finally 3) 15.00 mL of the dried acetonitrile. The addition of the reagent and the dried acetonitrile was accomplished by using 3.00-mL and 15.00-mL volumetric pipets respectively. The lowest concentrations of H_2O in CH_3CN standards (from 0.01% to 0.50%) were prepared by adding some volume of 10.0% H_2O/CH_3CN from a 2-mL microburet (0.002-mL divisions) and some volume of the dried acetonitrile from the 3-mL automatic pipet (0.020-mL divisions) so that the two volumes together always made up a total of 2.000 mL. The higher standards, (from 0.80% to 6.00% H_2O in CH_3CN) were prepared in the same manner but used adjustable eppendorf pipets to add some volume of pure H_2O, plus some volume of the dried CH_3CN again from the 3-mL automatic pipet so that the two together contributed 2.000 mL out of the 20.00 mL total volume. The unknown solutions were prepared, in triplicate, by adding 1) 3.00 mL of MA-NBD/$Ca(NO_3)_2 \cdot 4H_2O$ solution; 2) 2.00 mL of the

dried CH_3CN from the automatic pipet; and 3) 15.00 mL of the unknown CH_3CN sample using a 15-mL volumetric pipet. In this way both standard and unknown solutions always contained 20.00 mL of solution and constant concentrations of 6.33×10^{-7} M MA-NBD and 3.94×10^{-4} M $Ca(NO_3)_2 \cdot 4H_2O$. Once the standard or unknown solutions were prepared, the test tubes were tightly sealed with the polyethylene stoppers. When the solutions were removed from the glove box just prior to their measurement by fluorescence spectroscopy, the test tubes were also tightly wrapped with parafilm about the mouth and stoppers to further protect the samples from moisture in the air.

Fluorescence Intensity of the Standard and Unknown Solutions: The LS-5 spectrofluorometer was set at 475 nm excitation by 527 nm emission for automatic integration of fluorescence intensity. As the solutions reached $\geq$ 1.00% H_2O in CH_3CN concentrations, the fixed emission wavelength for integration was gradually increased towards 540 nm as the maximum emission shifted to slightly longer wavelengths. The settings were 475 nm excitation and 515-555 nm for emission scans; slits were 10 × 5 nm; fixed scale of 1.00; response 3; scan speed 120 nm/min. The standard solutions with the lowest concentration of water, from 0.00% to 0.50%, were measured first. The unknown sample solutions were measured next, and the standards with the highest water concentrations, from 0.80% to 6.00%, were

measured last. The following sequence of events was performed as quickly as possible for each solution in order to limit the time of contact between the solution and the moist atmosphere. The solution was mixed on a vortex-mixer for 15 sec while still stoppered, the fluorescence cuvette was rinsed twice with the solution, refilled and inserted in the LS-5 cuvette chamber. The fluorescence of the solution was integrated at a fixed emission of 527 nm which was immediately repeated until 5 back-to-back integrations were completed. The solution was then scanned twice followed by a final integration. The cuvette was cleaned by rinsing three times with deionized water, then rinsing twice with HPLC grade or UV grade acetonitrile. The cuvette was then wiped with a lint-free tissue and placed over a 1/4 inch diameter Teflon tube attached to a water aspirator while using air flow from a heat gun for 30 sec to assist in evaporation of the CH_3CN. Once the cuvette returned to room temperature, it was removed from the tube/aspirator and the next solution was measured.

Determination of H_2O in Acetonitrile Samples by Gas Chromatography: The remaining volume (about 10 mL) of the six H_2O/CH_3CN unknowns contained in their sample bottles were capped tightly and wrapped with parafilm on removal from the glove box. At the same time these bottles had originally been filled with the unknown samples, 4-5 mL of each CH_3CN sample was also poured into a small 15-mL vial

made from soft glass tubing and stoppered with a thin polyethylene cap. These six samples in their two different containers, and a sample of the dried and purified CH_3CN used to prepare the standards for the study, were analyzed for H_2O concentration by C. Patel of Witco Chemical Co. (6200 W. 51st St., Stickney, IL) by gas chromatography using a Poropak Q, 4' × 1/4" diameter-stainless steel column (125 °C) and thermal conductivity detector (TCD) - 250 °C, 3 μL sample injections, injection port 200 °C, Helium flow 69 mL/min. Chromatograms were recorded and the percent H_2O and CH_3CN calculated using a Hewlett Packard HP3392A Integrator. The chromatography on these samples was not able to be done until one month after the fluorescence determination.

Changes in the Experimental Procedure Used For the Second Water Study: There was no change in the equipment used for the second study. Most of the modifications concerned greater effort in preventing the contamination of the sample with water from the atmosphere or retained on the surface of the containers that would hold the unknown H_2O/CH_3CN samples. An additional change was planned where the H_2O/CH_3CN samples were to be tested immediately following the fluorescence analysis by gas chromatography. Rather than sending the samples away for outside analysis, preparations were made to perform the analysis at Loyola. A Perkin-Elmer Sigma 3 B Gas Chromatograph with TCD was set

up with a 5' × 1/4" stainless-steel 80/100 mesh Poropak Q column. The injector temperature was 225 °C, the column 115 °C, the TCD 250 °C. Helium flow was 30 mL/min. Sample chromatograms were recorded and the percent H_2O and CH_3CN were calculated using a Hewlett Packard HP3392A Integrator.

Two of the prospective CH_3CN samples for this second study and two standard solutions of 0.182% and 0.695% H_2O/CH_3CN were tested by this G.C. and also sent to Witco for Karl Fischer titration as a comparison. The results from the Karl Fischer analysis were in close agreement to those obtained by gas chromatography showing that this would be a valid method. In addition, this preliminary analysis of water content by both methods showed that the fresh gallon of Burdick and Jackson distilled in glass UV grade acetonitrile, Lot AP438, was the driest CH_3CN obtainable for the standard and unknown preparations. The B & J CH_3CN was therefore used for the preparations of all the standard solutions for the second water study. When some of this solvent was needed before the actual study it was always removed by the dry-solvent transfer method under nitrogen pressurization.

Eight unknown H_2O/acetonitrile samples were chosen for the second water study. Those selected included fresh Burdick and Jackson distilled in glass UV grade CH_3CN (this was the dry solvent used for the standard solution preparations), fresh Aldrich Sure Seal CH_3CN, the remaining

volume of the dried and purified CH_3CN from the first water study, Fisher HPLC grade CH_3CN, Aldrich Gold Label CH_3CN (two bottles opened on two separate occasions), Eastman 488 CH_3CN, and the remainder of an earlier lot of Burdick and Jackson distilled in glass UV grade CH_3CN. Other details such as lot numbers and opening dates of each of these samples will appear in the Results and Discussion section.

Because the H_2O/CH_3CN samples were to be tested by gas chromatography after the analysis by fluorescence, two identical containers were filled with about 60 mL of the sample at the same time. One container was moved into the glove box for the preparation of the samples for fluorescence analysis, the other container was stored in a desiccator charged with drierite where it was to remain unopened until the time of the G.C. analysis. The sample containers used for the identical pairs were the same 60 cc borosilicate glass bottles used in the first study, or 100-mL borosilicate round bottom flasks with 24/40 ground glass stoppers. (The only exception was the remaining 80 mL out of an older gallon of Burdick and Jackson CH_3CN which was kept in a 125-mL erlenmeyer flask with 24/40 ground glass joint and stopper.) All of these sample containers were first soaked in alcoholic KOH, then cleaned in the same manner as the glassware used in the first study. The containers were allowed to dry for several days in the 110 °C oven. They were taken from the

oven and immediately put in desiccators while still hot, where they remained until needed.

The two unopened acetonitrile samples which were assumed to have very low water content according to manufacturing specifications, Burdick and Jackson, Aldrich Sure Seal, and a bottle containing some of the previously dried and purified CH_3CN, were transferred to these containers by the dry solvent transfer method under nitrogen pressurization (90). The standard MA-NBD/ $Ca(NO_3)_2 \cdot 4H_2O$ reagent was prepared in the same manner as for the earlier study. On this occasion, 0.00200 g of the MA-NBD was quickly weighed into a 50-mL volumetric flask which was stoppered and transferred to the nitrogen-purged glove box. On the same morning that the study was to be performed, the MA-NBD was dissolved and the flask brought to volume with dry CH_3CN producing a 9.38×10^{-5} M MA-NBD solution. Crystals of $Ca(NO_3)_2 \cdot 4H_2O$ were transferred from a tared weigh vial into a dry 200-mL volumetric flask and later found to weigh 0.2424 grams. Ten milliliters of the MA-NBD solution were pipetted into the flask containing the salt which was dissolved and brought to volume with the dry CH_3CN. Considerable shaking over an hour's time was again required to make all of the salt dissolve. The resulting concentration of the standard solution was 4.69×10^{-6} M MA-NBD and 5.15×10^{-3} M $Ca(NO_3)_2 \cdot 4H_2O$. Because 3.00 mL of this solution was again used to prepare all of the

standard and unknown solutions consisting of 20.00 mL total volume, the final concentration of all the solutions to be measured by fluorescence was 7.04×10^{-7} M MA-NBD and 7.72×10^{-4} M $Ca(NO_3)_2 \cdot 4H_2O$. Fluorescence measurements were taken immediately after the preparation of the standard and unknown solutions was completed. The LS-5 spectrofluorometer was programmed with the same instrumental settings as described for the first study, except the response setting was changed to 2. The fluorescence intensity of each solution was measured by automatic integration of the signal repeated every 15 sec for the first two minutes, emission was scanned once, then integration once more at 3 min. The solution was vortexed once more, the cuvette refilled, and the process repeated. The large number of intensity readings were taken to monitor a drop in fluorescence signal that occurred over time. Three quartz fluorescence cuvettes were used on this occasion that had previously been tested and found to have the same background. The cuvettes were cleaned in the same manner as described for the first study, but were used in sequence so that they could be stored in a desiccator to cool until needed again for every third solution, (about every 15 min). In this way it was hoped that each solution would be measured in cuvettes that were as free of moisture as possible.

Determination of H_2O in Acetonitrile Samples by Karl Fischer Titration. When the thermal conductivity detector failed, the samples were sent to an outside facility: Phoenix Chemical Laboratory, Inc. (3953 Shakespeare Avenue, Chicago, IL 60647), to have their water content determined by a modified Karl Fischer titration. Their analysis used a 633 Karl Fischer Automat apparatus with 655 Dosimat by Metrohm (Brinkman), the commercial titrant used was # 34806 Hydranal-Composite 2 from Reidel-de Haen. Because of the cost per sample it was not possible to send more than ten samples to be analyzed. Therefore all eight samples were sent but only two duplicates were allowed: the Burdick and Jackson CH_3CN that had been used as the driest acetonitrile, and a second sample of the Aldrich Sure Seal CH_3CN. The results were reported in ppm H_2O.

Calculation of H_2O in Acetonitrile Samples by Fluorescence Method: The maximum fluorescence intensity of each standard solution was plotted against the mol/L concentration of water in the standard. Once the residual amount of water in the "dry" acetonitrile was determined by the back-up methods, this correction factor was added to the standard solutions. The maximum fluorescence intensity for each sample solution prepared was extrapolated from the curve down to the abscissa and the concentration of water in each 20.00 mL sample was determined. Because each sample solution consisted of 3.00 mL of reagent in dry

acetonitrile, 2.00 mL of the dry acetonitrile, and then 15.00 mL of the unknown sample, the following calculations were used to determine the concentration of H_2O in each original sample:

$$\text{Total mmol } H_2O \text{ in 20.00 mL sample solution} = \begin{array}{c}\text{mmol } H_2O \text{ in 5 mL dried } CH_3CN \\ + \\ \text{mmol } H_2O \text{ in 15 mL } CH_3CN \text{ sample}\end{array} \qquad \text{(Eq. 7)}$$

M_1 = mol/L residual H_2O in the dry CH_3CN
M_2 = mol/L H_2O in 20.00 mL sample solution obtained from curve

$$20.00 \text{ mL} \times M_2 = (5.00 \text{ mL} \times M_1) + (15.00 \text{ mL} \times \text{mol/L } H_2O \text{ in unknown sample}) \qquad \text{(Eq. 8)}$$

The molar concentration of water in the original unknown sample can be obtained by rearranging the second equation. A conversion factor of 5.56×10^{-3} mol/L equal to 0.010% H_2O was used to derive the percent H_2O present in each CH_3CN sample. Results were reported in terms of percent H_2O per sample.

UV-Visible Absorbance Spectra: MA-NBD was found to be very soluble in chloroform, and soluble to only a slightly lesser extent in acetonitrile and methanol. Original concentrations of greater than 3×10^{-4} mol/L in these three solvents were easily prepared. The solubility in water was much lower and ultra-sonication was required to produce concentrations in aqueous solution of 1.4×10^{-4} mol/L. The solutions of MA-NBD in $CHCl_3$ were bright yellow with a greenish-fluorescent cast to them, the solutions of MA-NBD in CH_3CN and MeOH were bright orange and in water a dull orange color. In each solvent the major absorbance band occurs at 480 nm, and has about 2.8 times greater absorptivity than the second absorbance band that lies between 340 and 355 nm. A very small absorbance band only about one-tenth of the maximum absorbance appears at 270 nm and is not useful for analytical measurements. Results and the calculation of the molar absorptivity of MA-NBD in the four solvents appear in Tables 2 through 5. Absorbance spectra of MA-NBD in the four solvents appear in the supplementary section labelled Spectra. The summarized results for MA-NBD in these four solvents for the first and second wavelength maxima and the corresponding molar absorptivities are: for MeOH λ 484 nm, ϵ = 28,800 and λ 343 nm, ϵ = 10,200; for H_2O λ 500 nm, ϵ = 34,100 and λ 354 nm,

ϵ = 7,640; for CH_3CN λ 484 nm, ϵ = 26,200 and λ 343 nm, ϵ = 9,270; and for $CHCl_3$ λ 480 nm, ϵ = 26,600 and λ 340 nm, ϵ = 9,560; Where ϵ represents the molar absorptivity with units of $L \cdot mol^{-1} \cdot cm^{-1}$. The spectrum for MA-NBD in H_2O is the most unusual of the four, not only because the λ_{max} is shifted furthest toward the red in comparison to the others - being the most polar of the solvents - but it also deviates slightly from the typical gaussian peak as its apex inclines from 480 nm to a slightly higher maximum at the indicated wavelength of 500 nm.

Fluorescence Spectra of MA-NBD: Solutions of MA-NBD in MeOH, H_2O, CH_3CN and $CHCl_3$ were scanned on the Perkin-Elmer LS-5 spectrofluorometer, and like most NBD-derivatives of secondary amines their maximum emission occurs near 540 nm when excited at 475 nm. The fluorescence spectra of MA-NBD in all four solvents produced excitation spectra that parallel their absorption spectra, with the primary excitation maxima occurring near 475 nm, but having more than 3 times the intensity than the second excitation band centered near 340 nm. The fluorescence excitation spectrum of MA-NBD in H_2O is again unusual at the maximum wavelength. The deformation of the apex of the peak is slightly different than the deformation of the absorption spectrum: the maximum intensity occurs at 476 nm, and a shoulder apex that is lower in intensity occurs at 500 nm. This is not a surprising phenomenon considering the

absorption spectrum, but it is also possible that the source intensity correction is incomplete. The individual results for the fluorescence intensity vs. the concentration of MA-NBD in the four solvents appear in Tables 6 through 9. All excitation spectra where taken with 540 nm fixed emission wavelength, 5 × 5 nm slit widths, and Fixed Scale of 1.00. The summarized results for the first and second excitation bands for different concentrations of MA-NBD in the four solvents are presented as follows: for MeOH λ 474 nm, F/C = 2.51×10^7 and λ 340 nm, F/C = 7.53×10^6; for H_2O λ 485 nm, F/C = 1.70×10^7 and λ 350 nm, F/C = 3.97×10^6; for CH_3CN λ 475 nm, F/C = 2.42×10^7 and λ 343 nm, F/C = 6.86×10^6; and for $CHCl_3$ λ 475 nm, F/C = 1.58×10^8 and λ 340 nm, F/C = 4.68×10^7. The values following the term, F/C, represent the ratio of maximum fluorescence intensity/molar concentration of MA-NBD at the indicated excitation wavelength, when the cell pathlength is fixed at 1 cm. The F/C value for MA-NBD in a given solvent and at fixed parameters is a constant quantity as long as the solutions involved include concentrations whose absorbances do not exceed 0.05 A. These F/C values are useful for comparing the intensities of the two bands to each other for MA-NBD in the same solvent, as well as comparing the intensity of MA-NBD in one solvent to its fluorescence intensity in other solvents. All of these values are directly related to the

ABSORBANCE CHARACTERISTICS

Table 2: Absorbance vs. Concentration of MA-NBD in MeOH. Calculation of Molar Absorptivity.

Concentration MA-NBD (mol/L)	Absorbance P.E. 330 (484 nm)	Molar Absorptivity (ϵ)
4.93×10^{-6}	0.140	2.84×10^{4}
1.97×10^{-5}	0.576	2.92×10^{4}
2.96×10^{-5}	0.856	2.89×10^{4}
4.94×10^{-5}	1.410	2.86×10^{4}
	Avg:	2.88×10^{4}

Concentration MA-NBD (mol/L)	Absorbance P.E. 330 (343 nm)	Molar Absorptivity (ϵ)
1.97×10^{-5}	0.208	1.06×10^{4}
2.96×10^{-5}	0.300	1.01×10^{4}
4.94×10^{-5}	0.490	9.94×10^{3}
	Avg:	1.02×10^{4}

Table 3: Absorbance vs. Concentration of MA-NBD in H_2O. Calculation of Molar Absorptivity.

Concentration MA-NBD (mol/L)	Absorbance P.E. 330 (500 nm)	Molar Absorptivity (ϵ)
1.18×10^{-5}	0.401	3.45×10^4
1.48×10^{-5}	0.503	3.40×10^4
2.96×10^{-5}	1.020	3.40×10^4
	Avg:	3.41×10^4

Concentration MA-NBD (mol/L)	Absorbance P.E. 330 (354 nm)	Molar Absorptivity (ϵ)
1.18×10^{-5}	0.090	7.63×10^3
1.48×10^{-5}	0.115	7.77×10^3
2.96×10^{-5}	0.250	8.45×10^3
	Avg:	7.95×10^3

Table 4: Absorbance vs. Concentration of MA-NBD in CH_3CN. Calculation of Molar Absorptivity.

Concentration MA-NBD (mol/L)	Absorbance P.E. 330 (484 nm)	Absorbance P.E. 575 (484 nm)	Molar Absorptivity (ϵ)
1.88×10^{-5}	0.490	0.488	2.61×10^4
2.34×10^{-5}	0.611	0.613	2.62×10^4
4.69×10^{-5}	1.228	1.221	2.61×10^4
		Avg:	2.61×10^4

Concentration MA-NBD (mol/L)	Absorbance P.E. 330 (343 nm)	Absorbance P.E. 575 (343 nm)	Molar Absorptivity (ϵ)
1.88×10^{-5}	0.170	0.177	9.23×10^3
2.34×10^{-5}	0.218	0.221	9.38×10^3
4.69×10^{-5}	0.426	0.436	9.19×10^3
		Avg:	9.27×10^3

Table 5: Absorbance vs. Concentration of MA-NBD in $CHCl_3$. Calculation of Molar Absorptivity.

Concentration MA-NBD (mol/L)	Absorbance P.E. 330 (480 nm)	Molar Absorptivity (ϵ)
1.48×10^{-5}	0.412	2.75×10^{4}
2.46×10^{-5}	0.686	2.79×10^{4}
4.93×10^{-5}	1.345	2.78×10^{4}
	Avg:	2.77×10^{4}

Concentration MA-NBD (mol/L)	Absorbance P.E. 330 (340 nm)	Molar Absorptivity (ϵ)
1.48×10^{-5}	0.142	9.49×10^{3}
2.46×10^{-5}	0.236	9.59×10^{3}
4.93×10^{-5}	0.468	9.60×10^{3}
	Avg:	9.56×10^{3}

FLUORESCENCE CHARACTERISTICS

Table 6: Fluorescence Intensity vs. Concentration of MA-NBD in MeOH - (540 nm emission).

Concentration (mol/L)	F Int (474 nm ex)	F/C *
9.86×10^{-7}	25.5	2.59×10^{7}
1.48×10^{-6}	36.7	2.48×10^{7}
2.46×10^{-6}	60.5	2.46×10^{7}
	Avg:	2.51×10^{7}

Concentration (mol/L)	F Int (340 nm ex)	F/C
9.86×10^{-7}	7.7	7.81×10^{6}
1.48×10^{-6}	10.9	7.36×10^{6}
2.46×10^{-6}	18.3	7.44×10^{6}
	Avg:	7.53×10^{6}

---

* F/C: Fluorescence intensity/Concentration MA-NBD

Table 7: Fluorescence Intensity vs. Concentration of MA-NBD in H_2O - (540 nm emission).

Concentration (mol/L)	F Int (485 nm ex)	F/C
4.72×10^{-7}	8.6	1.82×10^{7}
1.18×10^{-6}	20.4	1.73×10^{7}
2.36×10^{-6}	36.7	1.56×10^{7}
	Avg:	1.70×10^{7}

Concentration (mol/L)	F Int (350 nm ex)	F/C
4.72×10^{-7}	1.9	4.02×10^{6}
1.18×10^{-6}	4.8	4.07×10^{6}
2.36×10^{-6}	9.0	3.81×10^{6}
	Avg:	3.97×10^{6}

Table 8: Fluorescence Intensity vs. Concentration of MA-NBD in CH_3CN - (540 nm emission).

Concentration (mol/L)	F Int (475 nm ex)	F/C
1.88×10^{-7}	5.1	2.71×10^{7}
7.52×10^{-7}	18.8	2.50×10^{7}
1.17×10^{-6}	25.6	2.19×10^{7}
1.88×10^{-6}	43.0	2.29×10^{7}
	Avg:	2.42×10^{7}

Concentration (mol/L)	F Int (343 nm ex)	F/C
1.88×10^{-7}	1.4	7.44×10^{6}
7.52×10^{-7}	5.4	7.18×10^{6}
1.17×10^{-6}	7.1	6.10×10^{6}
1.88×10^{-6}	12.6	6.70×10^{6}
	Avg:	6.86×10^{6}

Table 9: Fluorescence Intensity vs. Concentration of MA-NBD in $CHCl_3$ - (540 nm emission).

Concentration (mol/L)	F Int (475 nm ex)	F/C
5.92×10^{-7}	97.0	1.64×10^{8}
9.86×10^{-7}	157.0	1.59×10^{8}
1.18×10^{-6}	187.0	1.58×10^{8}
1.97×10^{-6}	297.0	1.51×10^{8}
	Avg:	1.58×10^{8}

Concentration (mol/L)	F Int (340 nm ex)	F/C
5.92×10^{-7}	28.0	4.73×10^{7}
9.86×10^{-7}	47.0	4.77×10^{7}
1.18×10^{-6}	55.0	4.66×10^{7}
1.97×10^{-6}	90.0	4.57×10^{7}
	Avg:	4.68×10^{7}

quantum efficiency of fluorescence, ϕ_f, but are not the actual ϕ_f value which would require corrected fluorescence intensities. Over the course of this research, this ratio of F/C was subject to variation due to changes in the sensitivity of the LS-5 spectrofluorometer. Obvious reasons for such variations in sensitivity include repairs to the instrument. The first noticeable change in intensity appeared after the xenon source had to be replaced along with both the detector and reference RP-28 photomultiplier tubes. A plug and chip from a component to the power supply later burned out and were replaced. The instrument response to MA-NBD in CH_3CN was retested to so that the results would be optimized for the water in CH_3CN study by adjusting the concentrations of the standards accordingly. In each of these instances, 1) the fluorescence intensity of MA-NBD in the solvents of current interest was reassessed, 2) its molar absorptivity in the same solvents was retested and confirmed, and 3) both sets of data were compared to standard reference solutions of quinine bisulfate in 0.1 N H_2SO_4. The fluorescence of MA-NBD in $CHCl_3$ and CH_3CN increased about 1.9 times, almost twice the original intensity for the same instrumental settings, (fixed scale sensitivity, slit widths, wavelengths, etc.) after the source and PMTs were first replaced. The intensities increased about another 1.24 times when the plug and chip to the power supply were

replaced. The intensities later decreased to 0.9 times the previous measurements for no discernable reasons other than a decrease in the intensity of the LS-5 xenon source, due simply, perhaps, to the inevitable aging of the source.

The Effect of pH on the Absorption Spectra of MA-NBD in Aqueous Media: The absorbance spectra of aqueous solutions containing 3.0×10^{-5} mol/L MA-NBD at pH values ranging from 2.15 to 12.10 are presented in the section containing spectra. The spectra of the solutions with pH 2.15 to 8.60 are identical. For these solutions, the maximum intensity, as described earlier, is a distorted peak with maximum intensity at 500 nm (0.860 A) and shoulder at 480 nm (0.800 A). The solutions at pH of 9.53 and 10.02 show only a slight decrease in absorbance, and no significant change occurs until pH 10.60 where absorbance dropped almost 11 % with a shift in maximum to 495 nm. Successively more basic solutions continued to shift the absorbance maximum ending with 465-467 nm at the pH of 12.10, with an ever decreasing shoulder peak at 510 nm almost entirely disappearing. An isosbestic point occurs at 470 nm. The weaker absorbance band at 354 nm showed virtually no change at any pH. The same changes in the wavelength of maximum absorbance with pH are visually apparent. Acidic, neutral, and basic solutions of MA-NBD up to pH 10 all appear to be a dull orange color. At pH 11 or higher, the solution immediately develops an

intense pale yellow tint. Enough 1.0 mol/L HCl was added to the bright yellow basic MA-NBD solution at pH 12.10 in order to regenerate the original acid form of MA-NBD. Not only did the orange color fail to reappear, but the yellow disappeared and the solution became essentially colorless. The absorbance spectrum of this new solution also proved to be entirely different from that of any typical NBD-derivative. The original bands at 480-500 nm and 350 nm had disappeared and a very broad new band appeared with its maximum wavelength at 390-400 nm. When the strong base 0.2 M LiOH was added to this new species the bright yellow basic form of the MA-NBD was regenerated. These two species and their spectra were found to be reversible with the alternate addition of strong acid, then strong base, but the original MA-NBD spectra could never be regenerated. A possible explanation for this behavior was later found in the same paper by Ahnoff et.al., (87) where the first of the synthetic procedures used for making NBD-derivatives had been obtained. Ahnoff described base-catalyzed hydrolysis of secondary amine NBD derivatives like that of hydroxyproline (NBD-Hyp) as a typical and rapidly occurring phenomenon first observed by Aboderin et. al. (91) for NBD derivatives of morpholine at a pH of 10.3. The secondary amine is a weak leaving group in nucleophilic substitution reactions, yet substitution by a hydroxy group occurs since the formed NBD-OH is acidic and is stabilized as a

phenolate ion. Their NBD-Hyp was also susceptible to light-induced decomposition which occurred rapidly on exposure to light when in water or MeOH/H_2O solution unless acidified to a pH of 1.5. Long exposure of such solutions to light resulted in almost colorless solutions. Our aqueous MA-NBD stock solutions were kept in the dark when not in use, but remained stable in solution as long as the pH was 6 or less. Periodic spectra and TLC plates were run for our MA-NBD product which continued to produce the same spectra and only one fluorescent TLC spot (R_f around 0.41; normal phase plate developed in HPLC grade MeOH) over time. Solutions of MA-NBD in the other solvents; MeOH, CH_3CN and $CHCl_3$, remained stable over the course of the research. Ahnoff's NBD-Hyp in MeOH was more resistant to light only if acidified slightly with HCl. Ahnoff's paper lead to our conclusion that the MA-NBD at pH 12.10 was undergoing base-catalyzed hydrolysis to the bright yellow phenolate ion of NBD releasing free monoaza-18-crown-6. In reacidified solution, the ion was likely protonated to form NBD-OH, the nearly colorless solution, and the NBD-OH could be easily deprotonated and protonated repeatedly by changing the pH. The orange color did not appear again in the reacidified solution because the derivative of NBD and the MA-18-C-6 had not reformed.

Before the conclusion was formed that exposure to basic pH caused the decomposition of the MA-NBD product to

the NBD-phenolate ion, which removed the possibility of using MA-NBD to extract metal cations from basic aqueous solution and the subsequent determination of the metal cation concentration using fluorescence spectroscopy, attempts had been made to extract aqueous solutions of acidic to basic pH of 12 containing potassium ion present in KSCN, KNO_3 and KCl salts. In each case, absorbance results for the aqueous and $CHCl_3$ phases were no different than the blanks. After discovery of the base-catalyzed hydrolysis phenomenon, the negative results obtained for the attempted extraction of K^+ were understandable. Even if monoaza-18-crown-6 ring was complexing with the added potassium, the crown was no longer part of the NBD structure. Subsequent use of MA-NBD as a reagent for the determination of metal cations must be limited to only acidic or neutral aqueous solutions or nonaqueous media.

The Effect of pH on the Fluorescence Spectra of MA-NBD in Aqueous Solution: The same individual preparations of MA-NBD used for the absorbance study were diluted. This produced aqueous solutions that contained a constant concentration of 1.9×10^{-6} mol/L MA-NBD - with the same set of pH values used for the absorbance study. The emission spectra of each solution was scanned from 500-600 nm with fixed excitation of 480 nm, and the excitation spectra of each solution was scanned from 320-520 nm with fixed emission of 540 nm monitoring both the maximum

fluorescence excitation band at 480-500 nm and the band of lesser intensity at 350 nm. From pH of 2 through 7.8 there is virtually no drop in fluorescence intensity which can be observed from the spectra. As the pH of the MA-NBD solutions became more alkaline, the fluorescence intensity dropped more rapidly. The resulting fluorescence excitation spectra with variation in pH does not resemble the absorbance spectra which shows a shift in maximum wavelength and what appears to be an isosbestic point. There is little noticeable change in wavelength as the pH increases, but the major feature is the continuous drop in fluorescence intensity associated with the basic decomposition of the MA-NBD described in the previous section.

The Effect of Metal Salts on the Fluorescence Intensity of MA-NBD: MA-NBD in aqueous solution or methanol alone exhibited no change in fluorescence intensity on the addition of several metal salts. Compounds tested included the salts of several alkali metals, alkaline earth metals, and some transition metals that were reported to complex to some extent with 18-crown-6, monoaza-18-crown-6, and diaza-18-crown-6 (Kryptofix 22) ligands in the literature. Chloroform was the first solvent used in which a slight change in fluorescence intensity was observed when a few crystals of the metal salts were added to the fluorescence cuvette containing a dilute solution of MA-NBD in $CHCl_3$. The solvent system was

modified by adding MeOH because of its miscibility with $CHCl_3$, and because it improved the solubility of the metal salts. As reported in the previous section, MA-NBD in $CHCl_3$ has the largest quantum efficiency of the four solvents discussed - it has 6.3 times the intensity of MA-NBD in methanol - and the addition of MeOH to the system causes the fluorescence intensity to drop in a near logarithmic fashion. The solvent combination used for this portion of the study, 50% chloroform:50% methanol, or 1:1 $CHCl_3$:MeOH, decreased the fluorescence intensity 3.6 times that of MA-NBD in pure $CHCl_3$, but the increased solubility of the metal salts in the modified solvent medium justified the sacrifice. The best results were obtained with MA-NBD in UV grade acetonitrile both in terms of the solubility factor and a greater enhancement of fluorescence intensity with the addition of certain metal salts, and generally surpassed results seen in the $CHCl_3$:MeOH system for any of the salts. The results for the acetonitrile system will be presented first.

The Effect of Metal salts on the Fluorescence Intensity of MA-NBD in Acetonitrile: The fluorescence intensity of MA-NBD with certain calcium, magnesium, cadmium, sodium and potassium salts is enhanced to a great extent when all are dissolved in acetonitrile. The intensity of the MA-NBD solution increases with higher concentrations of the added metal salt in nonlinear

fashion, and the extent of the change in intensity depends upon which metal salt is added. Accompanying the change in intensity is a shift in the maximum emission wavelength from 539 nm for MA-NBD alone to as much as 527 nm after addition of the metals. The use of CH_3CN as the solvent medium provides greater solubility of the metal salts than was possible with the chloroform:methanol system. Aside from the exception of cadmium nitrate, all the salts remained soluble long enough to provide titration curves of fluorescence intensity with increased concentration of the metal salts. The determined ratios of $F_{comp}/F_{MA\text{-}NBD}$ (the fluorescence intensity at maximum complexation of the metals over the fluorescence intensity of the MA-NBD alone), were large enough to reduce the emission slit of the LS-5 and set both slits at 5 × 5 nm for the acetonitrile studies. This is significant when compared to the $CHCl_3$:MeOH work that required 5 × 10 nm slits for the same sensitivity scale. In order to attain this maximum change attributed to the maximum complexation of MA-NBD with any of these metal salts, a very large concentration ratio of $[M^{n+}]/[MA\text{-}NBD]$ was required, often greater than several thousand times the concentration of the ligand alone. This has been attributed to what appear to be low K_f, formation constants, so that we essentially forced the maximum complexation between the metal cation and the MA-NBD to occur by adding a large excess of metal salt.

The concentration of MA-NBD held constant for titration with the metal salts was varied from 1.8×10^{-8} to 2.6×10^{-6} mol/L depending on the effect of the metal salt involved.

The studies of metal salts added to MA-NBD in acetonitrile were more interesting and pursued in much more detail than the earlier $CHCl_3$:MeOH studies for several reasons in addition to the greater changes in fluorescence intensity on complexation. The data produced much steeper nonlinear curves for the plot of fluorescence intensity vs. concentration of the added metal salts. Generally, the data produced an "S"-curve, or some modification of an S-curve, very much like a typical pH titration, when fluorescence intensity vs. the log of the molar concentration of the metal salt was plotted. The useful concentration ranges of the curves often covered more than one order of magnitude [M^{n+}] concentration for some of the added metal salts. The estimated limits of detection were often quite low, a few in the ppb range, and formation constants were often larger than those for the chloroform:methanol system.

The metal salts that gave best results and highest ratios of $F_{comp}/F_{MA\text{-}NBD}$ are listed as follows: $Ca(NO_3)_2 \cdot 4H_2O = 21.3 > Cd(NO_3)_2 \cdot 4H_2O = 17.6 > Ca(ClO_4)_2 \cdot 4H_2O = 13.4 >$ anhydrous $Mg(ClO_4)_2 = 11.0 >> NaClO_4 = 3.7$, $Mg(ClO_4)_2 \cdot 6H_2O = 3.1 > KClO_4 = 1.6$, and

$Mg(NO_3)_2 \cdot 6H_2O$ only 1.3 times. The fluorescence data results of the individual studies for each metal salt tested appear in Tables 10 through 22. The important data features and determined values such as formation constants and estimated detection limits for all the metal salts tested in CH_3CN are summarized for comparison in Table 27. The resulting titration curves of the plots for fluorescence intensity vs. the molar concentration of metal salts and plots for fluorescence intensity vs. the log of the molar concentration of the metal salts appear in Figures 4 through 17.

MA-NBD with $Ca(NO_3)_2 \cdot 4H_2O$ in CH_3CN: The metal salt producing the best results for the greatest enhancement of fluorescence, largest K_f determined and lowest estimated detection limits was $Ca(NO_3)_2 \cdot 4H_2O$, calcium nitrate tetrahydrate. The titration study was repeated four times with a different concentration of MA-NBD in CH_3CN held constant on each occasion. These were 1) 1.88×10^{-8} mol/L, 2) 7.52×10^{-8} mol/L, 3) 3.13×10^{-7} mol/L and finally 4) 1.50×10^{-6} mol/L. The results of the four titrations are presented in Tables 10 through 13, and a summary of the important values and data features appear in Table 27. For all four studies, the average ratio for $F_{comp}/F_{MA\text{-}NBD}$ = 21 times, and the plots of fluorescence intensity vs. log $[Ca^{2+}]$ were typical S-curves from which the calculated formation constants (K_f) produced an average value

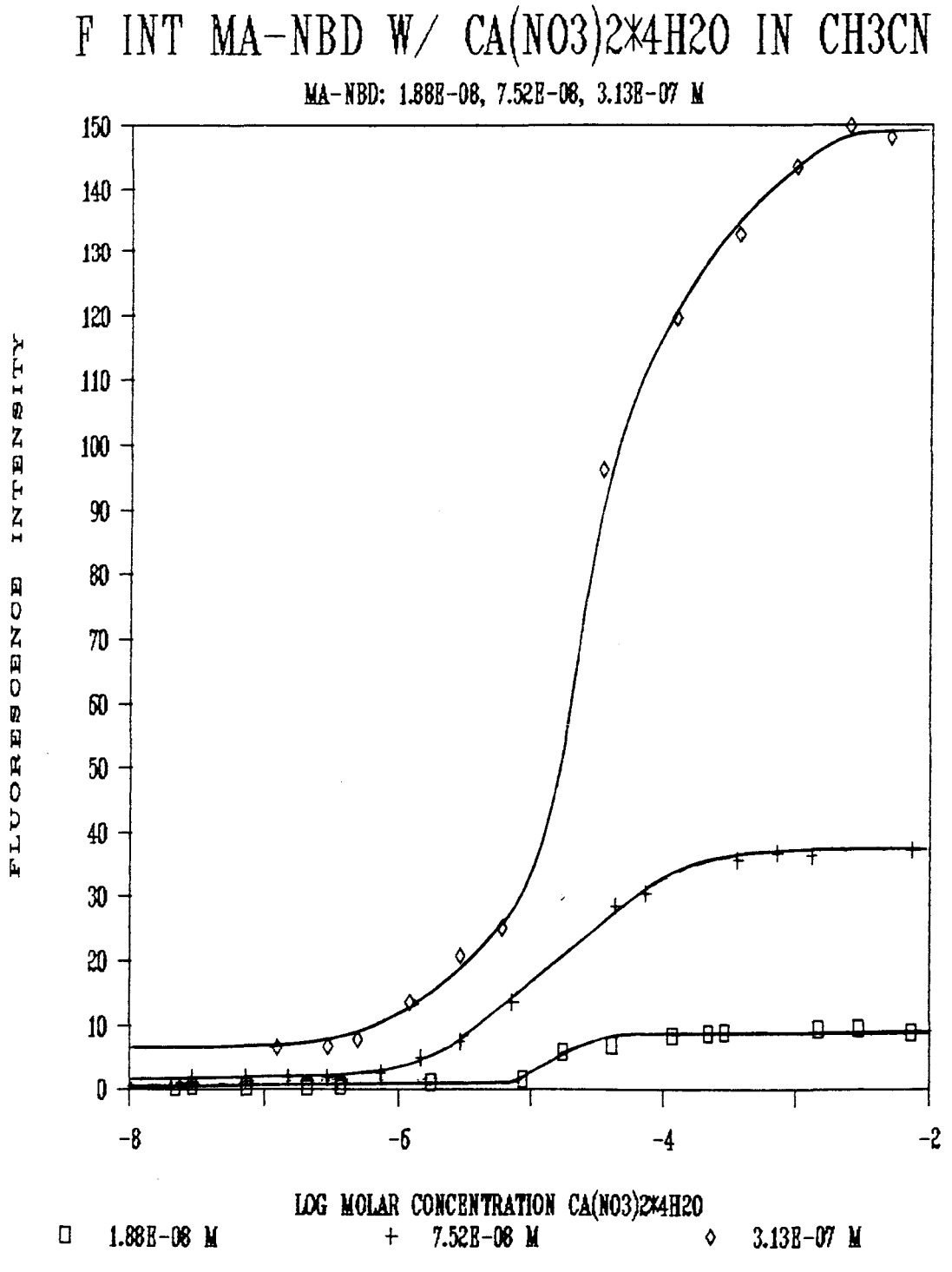

FIGURE 4. Fluorescence Intensity of MA-NBD with $Ca(NO_3)_2 \cdot 4H_2O$ in CH_3CN.

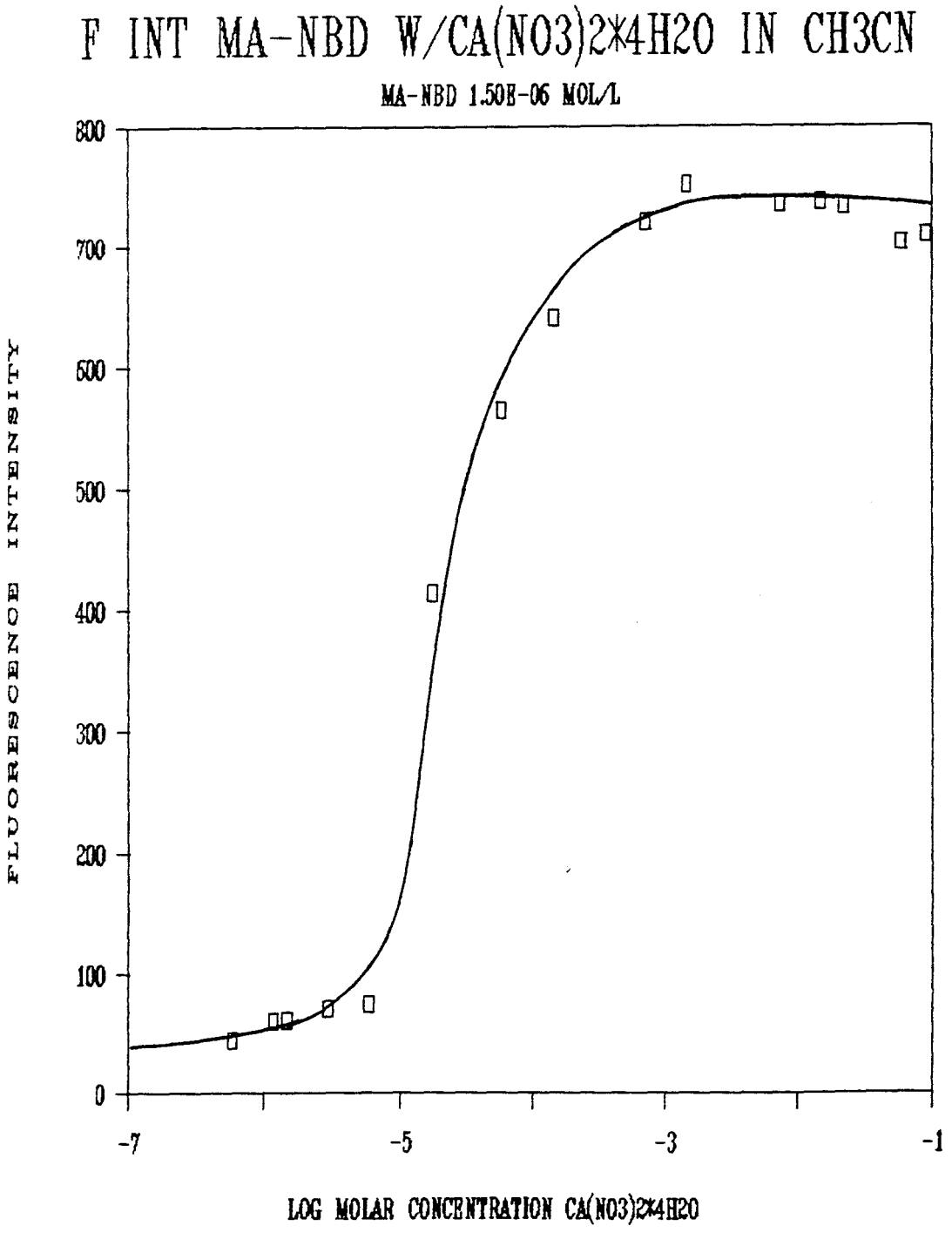

FIGURE 5. Fluorescence Intensity of MA-NBD with $Ca(NO_3)_2 \cdot 4H_2O$ in CH_3CN.

Table 10: Fluorescence Intensity of MA-NBD w/$Ca(NO_3)_2 \cdot 4H_2O$ in CH_3CN.

Conc $Ca(NO_3)_2 \cdot 4H_2O$ (Moles/L)	Log Conc $Ca(NO_3)_2 \cdot 4H_2O$	F Int Soln	Ratio Conc Ca^{2+}/MA-NBD
0.00E+00	----	0.5	0
2.19E-08	-7.66	0.5	1
2.92E-08	-7.53	0.6	2
7.30E-08	-7.14	0.5	4
2.04E-07	-6.69	0.5	11
3.65E-07	-6.44	0.6	19
1.75E-06	-5.76	1.1	93
8.76E-06	-5.06	1.6	470
1.75E-05	-4.76	5.9	930
4.09E-05	-4.39	6.8	2170
1.17E-04	-3.93	8.3	6210
2.19E-04	-3.66	8.8	11600
2.92E-04	-3.53	8.9	15500
1.46E-03	-2.84	9.4	77700
2.92E-03	-2.53	9.5	155000
7.30E-03	-2.14	8.9	388000

Concentration MA-NBD: 1.88E-08 M.

Table 11: Fluorescence Intensity of MA-NBD w/$Ca(NO_3)_2 \cdot 4H_2O$ in CH_3CN.

Conc $Ca(NO_3)_2 \cdot 4H_2O$ (Moles/L)	Log Conc $Ca(NO_3)_2 \cdot 4H_2O$	F Int Soln	Ratio Conc Ca^{2+}/MA-NBD
0.00E+00	----	1.7	0
2.92E-08	-7.53	1.8	0
7.30E-08	-7.14	1.8	1
1.46E-07	-6.84	1.9	2
2.92E-07	-6.53	1.9	4
7.30E-07	-6.14	2.5	10
1.46E-06	-5.84	4.9	19
2.92E-06	-5.53	7.4	39
7.30E-06	-5.14	13.5	97
4.38E-05	-4.36	28.5	580
7.30E-05	-4.14	30.5	970
3.65E-04	-3.44	35.7	4850
7.30E-04	-3.14	36.7	9700
1.31E-03	-2.88	36.3	17500
7.27E-03	-2.14	37.3	93300

Concentration MA-NBD: 7.52E-08 M.

Table 12: Fluorescence Intensity of MA-NBD w/$Ca(NO_3)_2 \cdot 4H_2O$ in CH_3CN.

Conc $Ca(NO_3)_2 \cdot 4H_2O$ (Moles/L)	Log Conc $Ca(NO_3)_2 \cdot 4H_2O$	F Int Soln	Ratio Conc Ca^{2+}/MA-NBD
0.00E+00	----	6.4	0
1.22E-07	-6.91	6.5	0
2.92E-07	-6.53	6.7	1
4.87E-07	-6.31	7.8	2
1.22E-06	-5.91	13.5	4
2.92E-06	-5.53	20.7	9
6.08E-06	-5.22	25.0	19
3.41E-05	-4.47	96.2	110
1.22E-04	-3.91	119.6	390
3.65E-04	-3.44	133.0	1170
9.73E-04	-3.01	143.6	3110
2.43E-03	-2.61	149.8	7770
4.87E-03	-2.31	148.0	15600

Concentration MA-NBD: 3.13E-07 M.

Table 13: Fluorescence Intensity of MA-NBD w/$Ca(NO_3)_2 \cdot 4H_2O$ in CH_3CN.

Conc $Ca(NO_3)_2 \cdot 4H_2O$ (Moles/L)	Log Conc $Ca(NO_3)_2 \cdot 4H_2O$	F Int Soln	Ratio Conc Ca^{2+}/MA-NBD
0.00E+00	----	34.3	0
5.84E-07	-6.23	44.0	0
1.17E-06	-5.93	59.7	1
1.46E-06	-5.84	61.0	1
2.92E-06	-5.53	70.7	2
5.84E-06	-5.23	74.7	4
1.75E-05	-4.76	413.3	12
5.84E-05	-4.23	564.0	39
1.46E-04	-3.84	640.0	97
7.30E-04	-3.14	722.0	485
1.46E-03	-2.84	752.0	970
7.30E-03	-2.14	736.0	4850
1.46E-02	-1.84	738.0	9710
2.19E-02	-1.66	734.0	14600
5.84E-02	-1.23	702.0	38800
9.00E-02	-1.05	710.0	59800

Concentration MA-NBD: 1.50E-06 M.

of 5.68×10^4 for formation of a 1:1 [Ca^{2+}:MA-NBD] complex. The maximum emission wavelength of the complex shifts to 527 nm, which is the largest shift observed for MA-NBD with any of the metal salts.

Figure 4 shows the first three plots together (fluorescence intensity vs. log molar concentration calcium nitrate) for the three lowest concentrations of MA-NBD and the consistent behavior of the calcium nitrate:MA-NBD system is evident. The resulting curve for the addition of calcium nitrate to the highest concentration of MA-NBD (1.50×10^{-6} mol/L) had to be plotted separately in Figure 5 since the fluorescence intensities were significantly larger and would dwarf the other three curves, but the similarity to the others is obvious. Certain trends are suggested by these four curves and the summarized data in Table 27: 1) the higher the MA-NBD concentration, the larger the analytically useful concentration range for the [Ca^{2+}]. The steepest slope for 1.88×10^{-8} mol/L MA-NBD covers less than one order of magnitude for the calcium nitrate concentration and stretches to somewhat better than 2 orders of magnitude when the highest concentration of 1.50×10^{-6} M MA-NBD was used. 2) The estimated minimum detection limit for Ca^{2+} (the first concentration of Ca^{2+} when a significant change in fluorescence intensity was seen,) decreases from 70 ppb seen with the lowest MA-NBD concentration (1.88×10^{-8} mol/L) down to 23 ppb with the

highest MA-NBD concentration (1.50×10^{-6} mol/L). 3) In order to encourage complexation, lower concentration ratios of $[Ca^{2+}]/[MA\text{-}NBD]$ are necessary in order to see the first change in fluorescence intensity - as well as to observe the final maximum fluorescence intensity associated with the point of maximum formation of the complex - when the concentration of the MA-NBD is increased.

Theoretically, if still higher concentrations of MA-NBD were used, steeper curves with a larger $[Ca^{2+}]$ concentration ranges and lower detection limits would be obtained. However, the maximum possible concentration of MA-NBD in CH_3CN cannot exceed 1.50×10^{-6} mol/L by much, because it would then exceed the 0.05 absorbance limit by approaching the point where inner filtering of the fluorescence is likely to occur. In addition, a concentration of MA-NBD equal to 2.0×10^{-6} mol/L would provide an initial fluorescence intensity of 50, and the maximum ratio for $F_{comp}/F_{MA\text{-}NBD}$ = 21 times would result in a fluorescence intensity reading (for 5 × 5 nm slits) of greater than 1000. The LS-5 spectrofluorometer would only show readings > 1000 as a blinking display signifying the detector is overloaded and such data cannot be accurately interpreted.

MA-NBD with $Ca(ClO_4)_2 \cdot 4H_2O$ in CH_3CN: The other calcium salt studied, $Ca(ClO_4)_2 \cdot 4H_2O$, was tested with an optimum concentration of 1.53×10^{-6} mol/L MA-NBD in CH_3CN. The ratio of $F_{comp}/F_{MA\text{-}NBD}$ for $Ca(ClO_4)_2 \cdot 4H_2O$ at maximum

complexation with MA-NBD is 13.4, which is lower than the calcium nitrate system but still quite large compared to any metal salt in the chloroform/methanol system. The maximum emission wavelength shifts to 528 nm on complexation. The first evidence of a change in fluorescence intensity of MA-NBD with addition of this Ca salt occurred with the lowest prepared standard concentration of calcium added - (see Figures 6 and 7, and Table 14) the estimated detection limit is 56 ppb ; almost as low as the detection limit for calcium nitrate in 1.50×10^{-6} mol/L MA-NBD. The concentration ratio of $[Ca^{2+}]/[MA\text{-}NBD]$ needed to observe the first change in fluorescence intensity is less than 1; that needed for the final maximum fluorescence intensity is also very low, at only 3600! Even though these fluorescence changes occur at very low $[Ca^{2+}]$ concentrations, the resulting fluorescence intensity vs. log molar concentration of $Ca(ClO_4)_2 \cdot 4H_2O$ curve produced is not sharp. The plot is a smooth, gradually ascending S-curve, and although the curve for fluorescence intensity vs. molar concentration (non-log plot, Figure 6) appears to level out for the last nine most concentrated standards (between 2×10^{-3} and 6×10^{-3} mol/L $[Ca^{2+}]$), on observation of the log-plot (Figure 7) the S-curve does not appear complete with a true symmetric plateau - it looks cutoff.

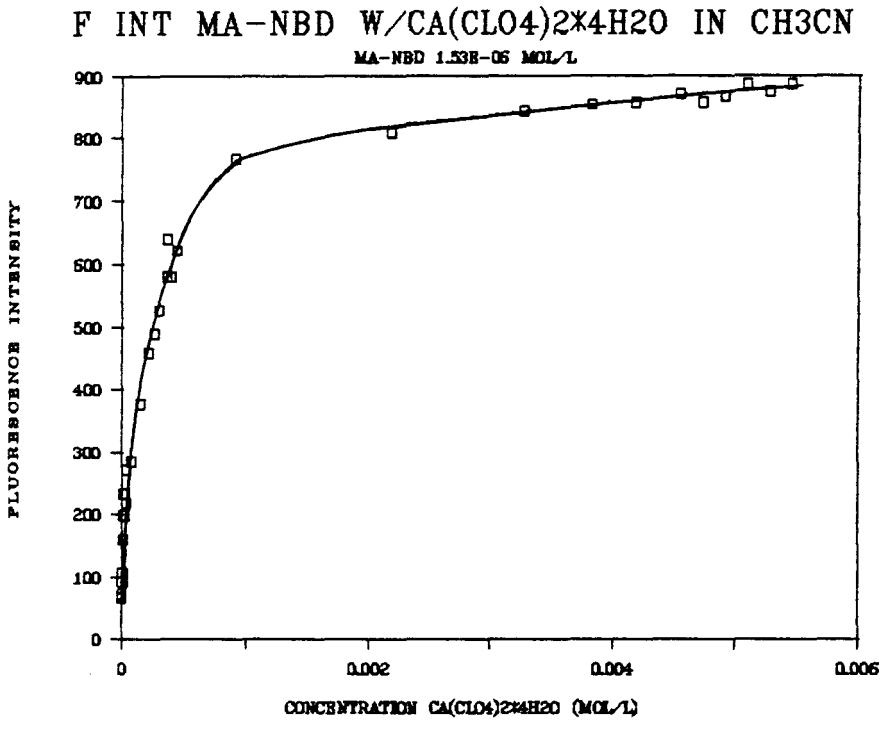

FIGURE 6. Fluorescence Intensity of MA-NBD with $Ca(ClO_4)_2 \cdot 4H_2O$ - (Molar Concentration).

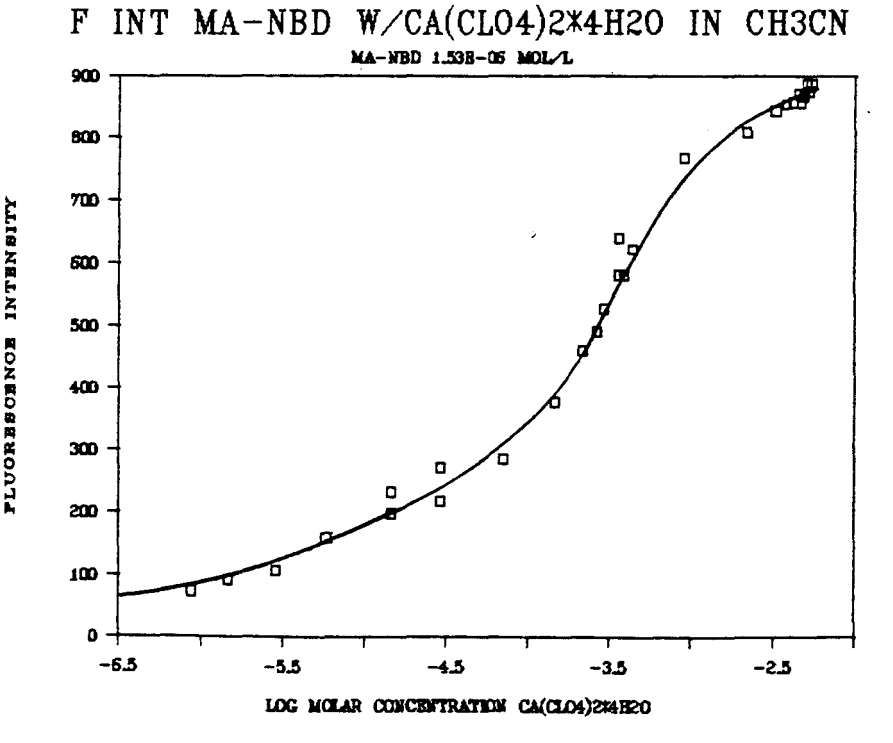

FIGURE 7. Fluorescence Intensity of MA-NBD with $Ca(ClO_4)_2 \cdot 4H_2O$ - (Log Molar Concentration).

Table 14: Fluorescence Intensity of MA-NBD w/$Ca(ClO_4)_2 \cdot 4H_2O$ in CH_3CN.

Conc $Ca(ClO_4)_2 \cdot 4H_2O$ (Moles/L)	Log Conc $Ca(ClO_4)_2 \cdot 4H_2O$	F Int Soln	Ratio Conc Ca^{2+}/MA-NBD
0.00E+00	----	66	0
8.70E-07	-6.06	72	1
1.45E-06	-5.84	92	1
2.81E-06	-5.55	106	2
5.80E-06	-5.24	160	4
1.45E-05	-4.84	232	9
1.45E-05	-4.84	198	9
2.90E-05	-4.54	272	19
2.91E-05	-4.54	218	19
7.27E-05	-4.14	284	47
1.45E-04	-3.84	378	95
2.18E-04	-3.66	458	140
2.62E-04	-3.58	490	170
2.91E-04	-3.54	526	190
3.63E-04	-3.44	580	240
3.63E-04	-3.44	640	240
3.92E-04	-3.41	580	256
4.36E-04	-3.36	622	285

(Table continued on following page.)

Table 14: Fluorescence Intensity of MA-NBD w/$Ca(ClO_4)_2 \cdot 4H_2O$ in CH_3CN. (Continued.)

Conc $Ca(ClO_4)_2 \cdot 4H_2O$ (Moles/L)	Log Conc $Ca(ClO_4)_2 \cdot 4H_2O$	F Int Soln	Ratio Conc Ca^{2+}/MA-NBD
9.08E-04	-3.04	768	590
2.18E-03	-2.66	808	1420
3.27E-03	-2.49	844	2140
3.82E-03	-2.42	854	2490
4.18E-03	-2.38	856	2730
4.54E-03	-2.34	870	2970
4.72E-03	-2.33	856	3090
4.91E-03	-2.31	866	3200
5.09E-03	-2.29	886	3320
5.27E-03	-2.28	874	3440
5.45E-03	-2.26	886	3560

Concentration MA-NBD: 1.53E-06 M.

The K_f determined at the point of 50 % complexation for the 1:1 complex with MA-NBD approaches 1×10^4, which is almost as large as the K_f determined for calcium nitrate. Extrapolating a symmetrical extension of the log curve for higher concentrations of calcium also shifts the 50 % complexation point to a higher calcium concentration and changes the K_f to a slightly lower value of 3.4×10^3. The projected ratio of $[Ca^{2+}]/[MA\text{-}NBD]$ at maximum complexation then approaches 10,000 - a ratio much closer to the concentration ratio obtained in the same region for the calcium nitrate with 1.50×10^{-6} mol/L MA-NBD.

MA-NBD with $Cd(NO_3)_2 \cdot 4H_2O$ in CH_3CN: The metal salt inducing the second greatest change in the fluorescence intensity of MA-NBD in CH_3CN upon complexation in comparison to $Ca(NO_3)_2 \cdot 4H_2O$ was cadmium nitrate tetrahydrate, $Cd(NO_3)_2 \cdot 4H_2O$. At the maximum possible complexation - the ratio, $F_{comp}/F_{MA\text{-}NBD}$ was 17.6, and the maximum emission wavelength shifted to 530 nm. Three studies were done in which the concentrations of MA-NBD were held constant at 1.88×10^{-7} mol/L, 6.67×10^{-7} mol/L and 1.00×10^{-6} mol/L in CH_3CN with the $Cd(NO_3)_2 \cdot 4H_2O$ concentrations ranging from 2×10^{-5} mol/L to 2×10^{-2} mol/L. The results appear in Tables 15 - 17, and the plots of fluorescence intensity vs. molar concentration and fluorescence intensity vs. the log of molar concentration of $Cd(NO_3)_2 \cdot 4H_2O$ appear in Figures 8 and 9, respectively.

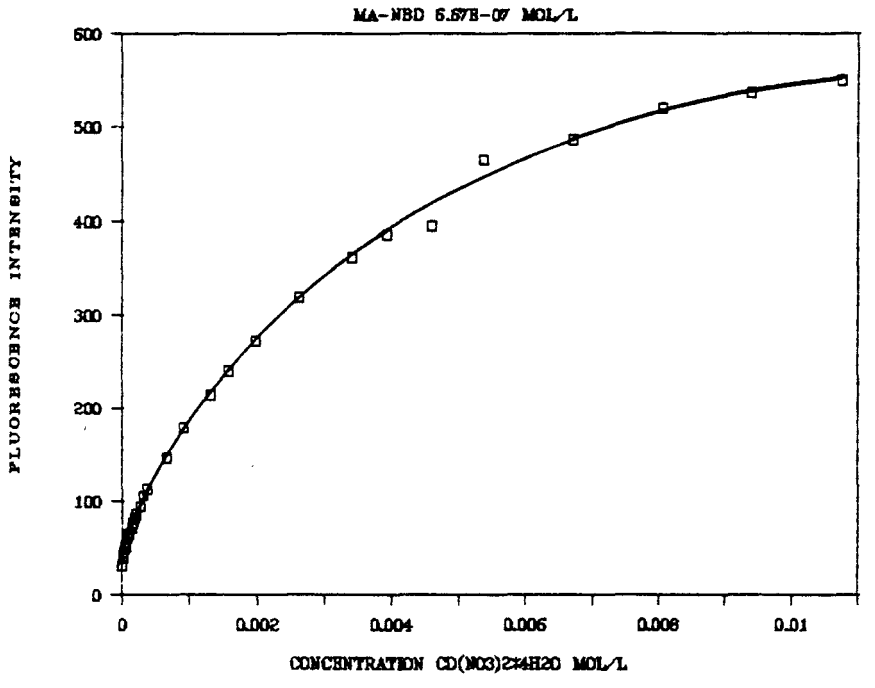

FIGURE 8. Fluorescence Intensity of MA-NBD with $Cd(NO_3)_2 \cdot 4H_2O$ - (Molar Concentration).

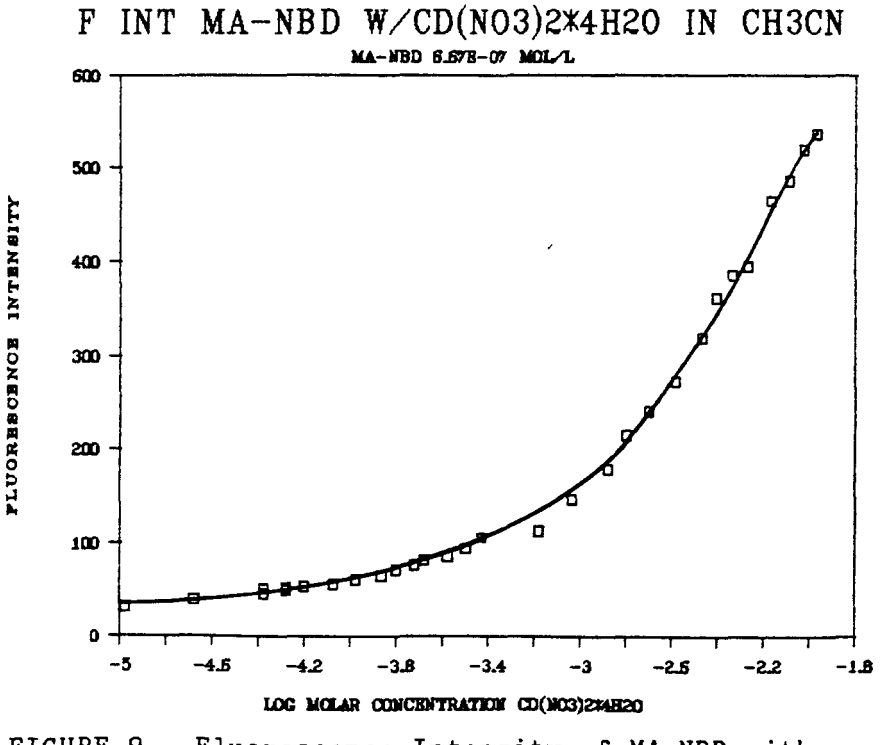

FIGURE 9. Fluorescence Intensity of MA-NBD with $Cd(NO_3)_2 \cdot 4H_2O$ - (Log Molar Concentration).

Table 15: Fluorescence Intensity of MA-NBD w/$Cd(NO_3)_2 \cdot 4H_2O$ in CH_3CN.

Conc $Cd(NO_3)_2 \cdot 4H_2O$ (Moles/L)	Log Conc $Cd(NO_3)_2 \cdot 4H_2O$	F Int Soln	Ratio Conc Cd^{2+}/MA-NBD
0.00E+00	----	45.5	0
2.10E-05	-4.68	72.0	21
4.20E-05	-4.38	73.1	42
6.30E-05	-4.20	101.8	63
8.40E-05	-4.08	101.7	84
1.05E-04	-3.98	94.4	105
1.58E-04	-3.80	108.8	160
2.10E-04	-3.68	125.4	210
2.62E-04	-3.58	126.0	260
2.63E-04	-3.58	138.2	260
3.15E-04	-3.50	151.0	315
6.56E-04	-3.18	206.4	656
1.05E-03	-2.98	266.0	1050
1.31E-03	-2.88	302.8	1310
1.57E-03	-2.80	348.0	1570
1.97E-03	-2.71	369.3	1970

(Table continued on following page.)

Table 15: Fluorescence Intensity of MA-NBD w/$Cd(NO_3)_2 \cdot 4H_2O$ in CH_3CN. (Continued.)

Conc $Cd(NO_3)_2 \cdot 4H_2O$ (Moles/L)	Log Conc $Cd(NO_3)_2 \cdot 4H_2O$	F Int Soln	Ratio Conc Cd^{2+}/MA-NBD
2.36E-03	-2.63	428.7	2360
2.62E-03	-2.58	452.0	2620
2.89E-03	-2.54	457.0	2890
3.28E-03	-2.48	504.0	3280
3.94E-03	-2.41	550.0	3940
4.29E-03	-2.37	588.0	4290
5.37E-03	-2.27	630.0	5370
6.44E-03	-2.19	683.0	6440
8.05E-03	-2.09	715.0	8050
8.06E-03	-2.09	785.0	8060
1.30E-02	-1.89	ppt	13000
1.63E-02	-1.79	ppt	16200
1.95E-02	-1.71	ppt	19500

Concentration MA-NBD: 1.00E-06 M.

Table 16: Fluorescence Intensity of MA-NBD w/$Cd(NO_3)_2 \cdot 4H_2O$ in CH_3CN.

Conc $Cd(NO_3)_2 \cdot 4H_2O$ (Moles/L)	Log Conc $Cd(NO_3)_2 \cdot 4H_2O$	F Int Soln	Ratio Conc Cd^{2+}/MA-NBD
0.00E+00	----	31.1	0
1.05E-05	-4.98	39.6	16
2.10E-05	-4.68	45.9	31
4.20E-05	-4.38	51.7	63
4.20E-05	-4.38	49.9	63
5.25E-05	-4.28	52.7	79
5.25E-05	-4.28	53.2	79
6.30E-05	-4.20	56.2	94
8.40E-05	-4.08	61.6	126
1.05E-04	-3.98	65.5	157
1.37E-04	-3.86	71.9	205
1.58E-04	-3.80	76.8	236
1.89E-04	-3.72	82.0	283
2.10E-04	-3.68	86.0	315
2.63E-04	-3.58	94.0	394

(Table continued on following page.)

Table 16: Fluorescence Intensity of MA-NBD w/$Cd(NO_3)\cdot 4H_2O$ in CH3CN. (Continued.)

Conc $Cd(NO_3)_2\cdot 4H_2O$ (Moles/L)	Log Conc $Cd(NO_3)_2\cdot 4H_2O$	F Int Soln	Ratio Conc Cd^{2+}/MA-NBD
3.15E-04	-3.50	105.4	472
3.68E-04	-3.43	112.9	551
6.56E-04	-3.18	146.3	983
9.18E-04	-3.04	178.2	1380
1.31E-03	-2.88	214.0	1970
1.57E-03	-2.80	240.1	2360
1.97E-03	-2.71	272.1	2950
2.62E-03	-2.58	318.5	3930
3.41E-03	-2.47	361.2	5110
3.94E-03	-2.41	385.4	5900
4.59E-03	-2.34	394.6	6880
5.37E-03	-2.27	464.7	8050
6.71E-03	-2.17	485.9	10100
8.05E-03	-2.09	520.0	12100
9.39E-03	-2.03	536.3	14100
1.07E-02	-1.97	548.6	16100
1.30E-02	-1.89	ppt	19500

Concentration MA-NBD: 6.67E-07 M.

Table 17: Fluorescence Intensity MA-NBD w/$Cd(NO_3)_2 \cdot 4H_2O$ In CH_3CN

Conc $Cd(NO_3)_2 \cdot 4H_2O$ (Moles/L)	Log Conc $Cd(NO_3)_2 \cdot 4H_2O$	F Int Soln	Ratio Conc Cd^{2+}/MA-NBD
0.00E+00	----	10.7	0
3.28E-05	-4.48	13.9	175
1.31E-04	-3.88	20.4	700
2.30E-04	-3.64	27.1	1220
2.63E-04	-3.58	29.5	1400
3.28E-04	-3.48	30.2	1750
6.57E-04	-3.18	43.5	3500
9.85E-04	-3.01	55.1	5250
1.31E-03	-2.88	66.5	7000
1.64E-03	-2.78	78.6	8750
3.28E-03	-2.48	113.8	17500
4.93E-03	-2.31	136.2	26200
6.57E-03	-2.18	149.0	35000
8.21E-03	-2.09	165.1	43700
9.85E-03	-2.01	173.9	52500
1.15E-02	-1.94	182.0	61200
1.25E-02	-1.90	187.6	66500
1.28E-02	-1.89	187.0	68200
1.31E-02	-1.88	185.7	70000
1.31E-02	-1.88	194.6	70000

Concentration MA-NBD: 1.88E-07 M.

There is only half an order of magnitude difference between the lowest MA-NBD concentration and the highest used for the three studies with cadmium. This is less than the range covering nearly two orders of magnitude for the concentrations of MA-NBD used for all the calcium nitrate curves. The curves for all three concentrations of cadmium nitrate are strikingly similar and therefore only one concentration is shown. Comparison of the three sets of results for $Cd(NO_3)_2 \cdot 4H_2O$ included in Table 27, which summarizes all the important data features for the metal salts with MA-NBD in CH_3CN, show them to agree closely. The average of the results for ratios of the maximum $F_{comp}/F_{MA\text{-}NBD} = 17.6$; the estimated limits of detection = 2.4 ppm Cd^{2+}, and the value determined for $K_f = 4.39 \times 10^2$ for $Cd(NO_3)_2 \cdot 4H_2O$ with MA-NBD. Unlike the more sharply rising curves for the addition of calcium salts with CH_3CN, all three curves with cadmium show a gradually ascending curve for the fluorescence vs. mólar concentration $[Cd^{2+}]$ plots. The fluorescence vs. the log molar concentration plots are characterized by a gradually rising base for the S-curve, and a gentle change in slope for the sharpest rise in the curve, followed by a abrupt stop. No symmetrical plateau appears at the top of any of the three log concentration curves. Three studies were performed with slightly different concentrations of MA-NBD in an attempt to extend the curves. These curves stopped

abruptly because the cadmium nitrate with MA-NBD solutions developed a finely suspended precipitate at concentrations above 8 to 9 mmol/L, indicating the solution of $Cd(NO_3)_2 \cdot 4H_2O$ in CH_3CN was saturated. On completion of the other two cadmium nitrate titrations, whose data is presented in Tables 16 and 17, the maximum solubility of $Cd(NO_3)_2 \cdot 4H_2O$ was determined to be less than 1.4×10^{-2} mol/L in a solution of MA-NBD in CH_3CN.

Because the curves were incomplete, the estimated K_f values of about 4×10^2 were obtained using the estimated 50 % complexation point from the existing data. The value of K_f could be somewhat smaller if the 50 % complexation point was shifted to higher concentrations of $Cd(NO_3)_2 \cdot 4H_2O$. It is somewhat unusual that the estimated detection limit of 1.2 to 3.7 ppm Cd^{2+} is quite high when the $F_{comp}/F_{MA\text{-}NBD}$ ratio is as large as 17.6. For the calcium salts, a large ratio for $F_{comp}/F_{MA\text{-}NBD}$ was correlated with better detection limits and earlier changes in the fluorescence intensity at lower concentrations of added metal salt.

Cadmium nitrate was the only transition metal tested with MA-NBD in acetonitrile that produced a significant change in fluorescence intensity. Lead, copper, zinc and cadmium were cited in the early crown literature as metals observed to complex with 18-crown-6, monoaza-18-crown-6 and other aza-crown structures. The nitrates of these three

metals were tested but produced no change in fluorescence intensity with MA-NBD in CH_3CN except for a slight decrease in fluorescence for lead nitrate ($F_{comp}/F_{MA\text{-}NBD}$ = 0.95). Silver salts could not be used, or did not work, although they produced the best results in $CHCl_3$:MeOH, probably due to the complexing ability of the -CN group in acetonitrile.

MA-NBD with Alkali Metal Salts in CH_3CN: The two alkali metals, sodium and potassium, were tested with MA-NBD in CH_3CN in the form of several of their salts, and preliminary data for these appears in Table 28. The sodium salts produced ratios of maximum $F_{comp}/F_{MA\text{-}NBD}$ in the following order: $NaClO_4$ = 3.7; $NaNO_3$ = 1.4; and NaCl = 1.1. (No value for NaSCN is available.) The potassium salts produced ratios of maximum $F_{comp}/F_{MA\text{-}NBD}$ in the following order: $KClO_4$ = 1.6; KSCN = 1.4; KNO_3 = 1.1; and KCl = 0.95. Only the $NaClO_4$ and $KClO_4$ were chosen for further study as they produced the highest change in fluorescence when added to MA-NBD in CH_3CN. Both perchlorate salts were run with the concentration of MA-NBD in CH_3CN held constant at 6.60×10^{-7} mol/L. The results for $KClO_4$ appear in Table 18 and the curves for fluorescence intensity vs. molar concentration and fluorescence intensity vs. log of molar concentration in Figures 10 and 11. The results for $NaClO_4$ appear in Table 19 and Figures 12 and 13.

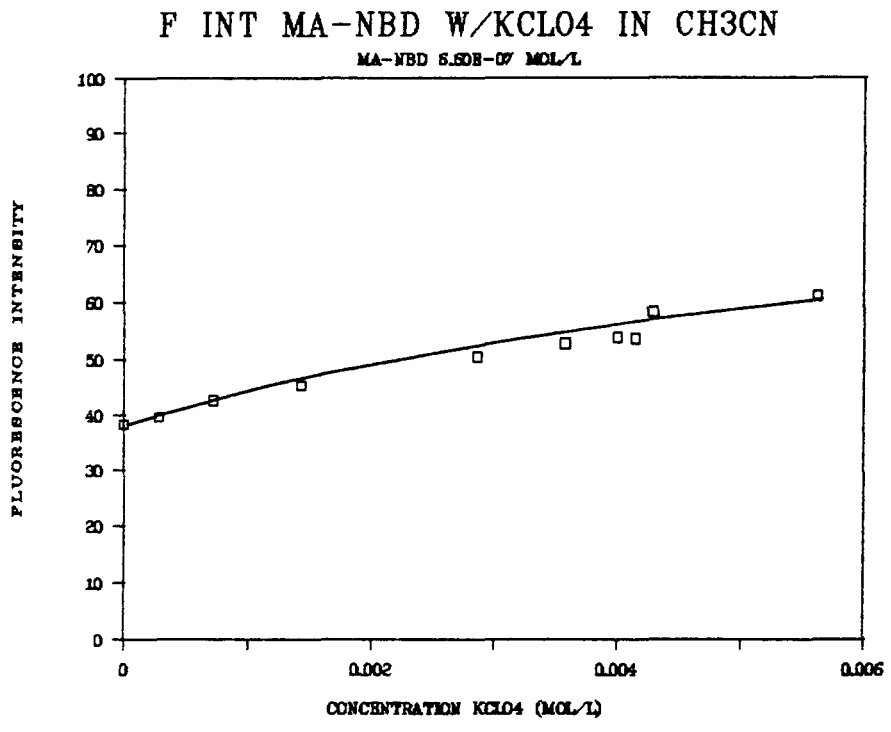

FIGURE 10. Fluorescence Intensity of MA-NBD with $KClO_4$ - (Molar Concentration).

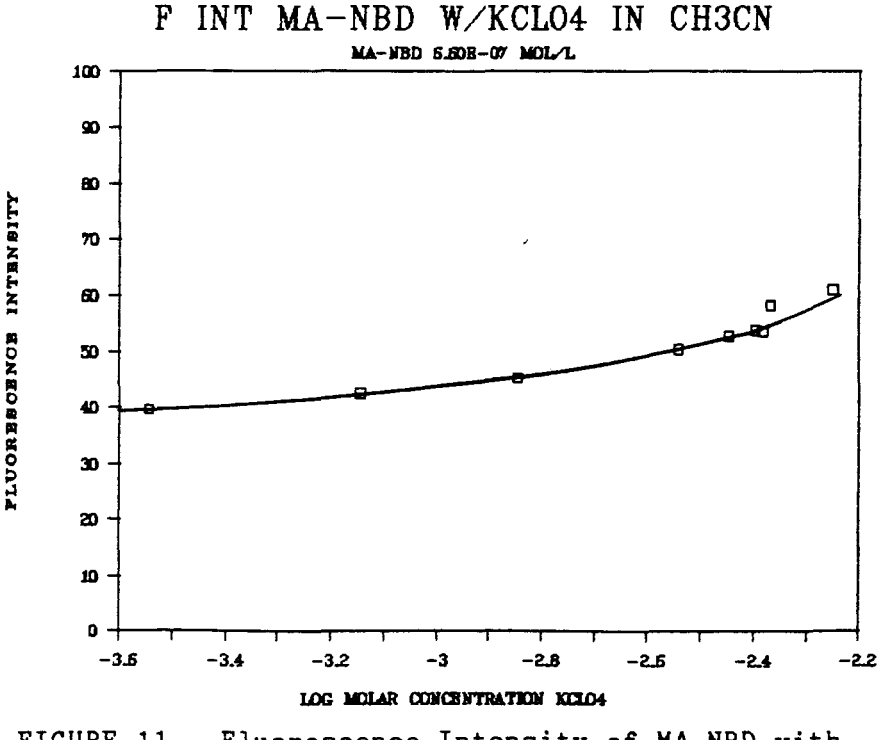

FIGURE 11. Fluorescence Intensity of MA-NBD with $KClO_4$ - (Log Molar Concentration).

Table 18: Fluorescence Intensity of MA-NBD w/$KClO_4$ in CH_3CN.

Conc $KClO_4$ (Moles/L)	Log Conc $KClO_4$	F Int Soln	Ratio Conc K^+/MA-NBD
0.00E+00	----	38.4	0
2.86E-04	-3.54	39.7	430
7.14E-04	-3.15	42.6	1080
1.43E-03	-2.85	45.3	2160
2.86E-03	-2.54	50.4	4330
3.57E-03	-2.45	52.7	5410
4.00E-03	-2.40	53.7	6060
4.14E-03	-2.38	53.6	6280
4.29E-03	-2.37	58.3	6490
5.62E-03	-2.25	61.0	8520

Concentration MA-NBD: 6.60E-07 M.

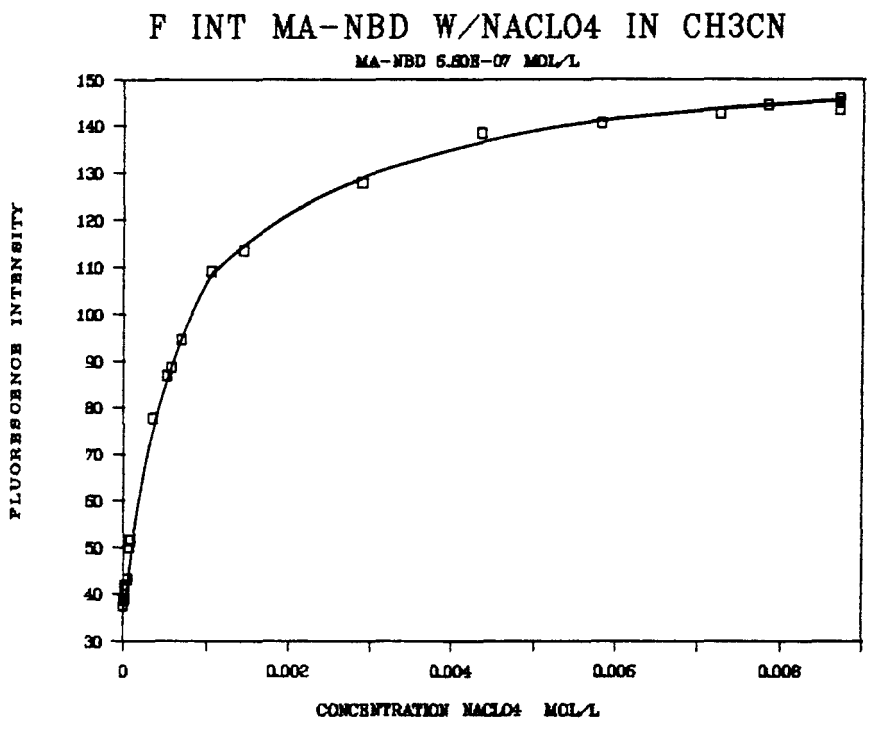

FIGURE 12. Fluorescence Intensity of MA-NBD with $NaClO_4$ - (Molar Concentration).

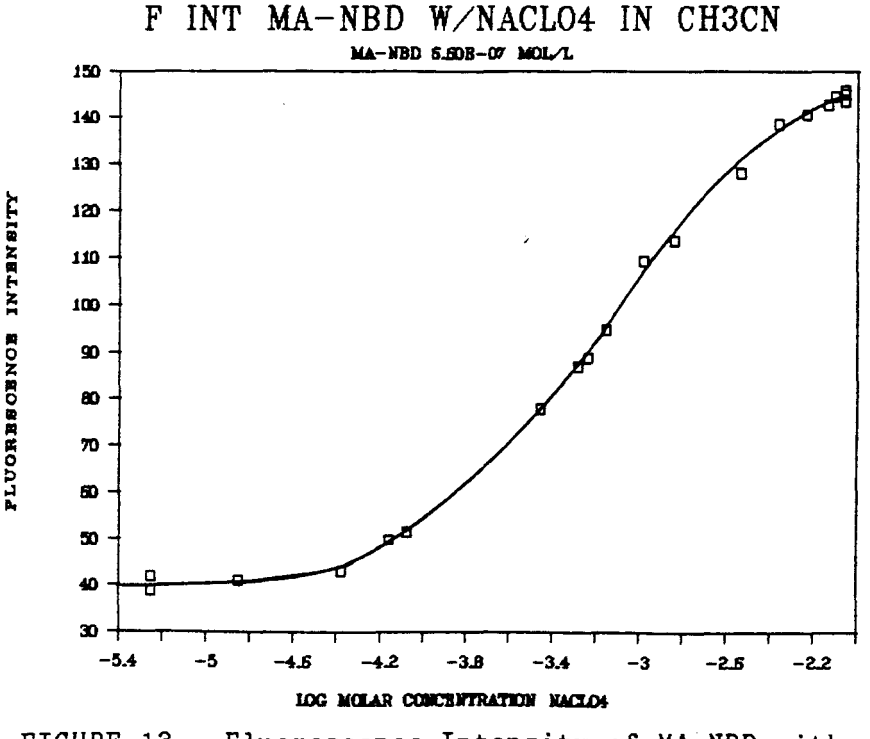

FIGURE 13. Fluorescence Intensity of MA-NBD with $NaClO_4$ - (Log Molar Concentration).

Table 19: Fluorescence Intensity of MA-NBD w/$NaClO_4$ in CH_3CN.

Conc $NaClO_4$ (Moles/L)	Log Conc $NaClO_4$	F Int Soln	Ratio Conc Na^+/MA-NBD
0.00E+00	----	37.7	0
0.00E+00	----	39.0	0
5.57E-06	-5.25	39.0	8
5.57E-06	-5.25	42.0	8
1.39E-05	-4.86	41.1	21
4.18E-05	-4.38	43.3	63
6.97E-05	-4.16	49.8	110
8.35E-05	-4.08	51.5	130
3.48E-04	-3.46	77.8	530
5.23E-04	-3.28	86.8	790
5.80E-04	-3.24	88.6	880
6.97E-04	-3.16	94.6	1060
1.05E-03	-2.98	109.2	1580
1.45E-03	-2.84	113.5	2200
2.90E-03	-2.54	128.0	4390
4.35E-03	-2.36	138.6	6590
5.80E-03	-2.24	140.6	8790
7.25E-03	-2.14	142.6	10990
7.83E-03	-2.11	144.4	11860
8.70E-03	-2.06	143.5	13180
8.70E-03	-2.06	145.0	13180
8.70E-03	-2.06	145.8	13180

Concentration MA-NBD: 6.60E-07 M.

The two curves for $KClO_4$ do not end because the solubility was limited - as was the case for cadmium nitrate - but because there was no further increase in fluorescence. The slight change in slope was not useful for further calculations. In order to produce any observable change in fluorescence intensity, the potassium perchlorate also required a concentration ratio of $[K^+]/[MA\text{-}NBD]$ larger than 1000. In comparison, the $NaClO_4$ curves do produce the expected S-curve format with the plot of fluorescence intensity vs. log molar concentration of $NaClO_4$, but the curve stops before the expected plateau was well defined. A much lower concentration ratio of $[Na^+]/[MA\text{-}NBD]$ of 20 was required to produce the first change in fluorescence intensity. Subsequent to the collection of data presented in Table 19 for the $NaClO_4$ system, it was noted that the ratio of maximum $F_{comp}/F_{MA\text{-}NBD}$ was only 3.3, which was not as large as the 3.6 and 3.7 obtained previously and reported in Table 28. The last standard prepared - containing 8.70×10^{-3} mol/L $NaClO_4$ with 6.60×10^{-7} mol/L MA-NBD in CH_3CN - was remeasured and a few crystals of solid $NaClO_4$ were added, which dissolved completely. The remeasured fluorescence had increased to a new high of 151. This provided a new ratio for maximum $F_{comp}/F_{MA\text{-}NBD}$ = 3.9, somewhat higher than - but closer to - the original preliminary test results of 3.7.

MA-NBD with Magnesium Salts in CH_3CN: The last set of metal salts studied with MA-NBD in CH_3CN were the magnesium salts $Mg(ClO_4)_2$, anhydrous magnesium perchlorate, $Mg(ClO_4)_2 \cdot 6H_2O$, magnesium perchlorate hexahydrate, and $Mg(NO_3)_2 \cdot 6H_2O$, magnesium nitrate hexahydrate. The magnesium salts produced maximum $F_{comp}/F_{MA\text{-}NBD}$ ratios in CH_3CN in the following order: anhydrous $Mg(ClO_4)_2$ = 11.0; $Mg(ClO_4)_2 \cdot 6H_2O$ = 3.1; and $Mg(NO_3)_2 \cdot 6H_2O$ = 1.3. The concentration of 1.91×10^{-6} mol/L MA-NBD was held constant for these studies in CH_3CN, and the results for each study appear in Tables 20 - 22. The fluorescence intensity vs. molar concentration and fluorescence intensity vs. the log of molar concentration curves for the anhydrous magnesium perchlorate, (this study was duplicated over a two day period), and for the magnesium perchlorate hexahydrate appear in Figures 14-17. The magnesium nitrate hexahydrate data is not presented because the change in fluorescence intensity was too small to be analytically useful. Concentrations from 10^{-4} mol/L to 10^{-2} mol/L of $Mg(NO_3)_2 \cdot 6H_2O$ were added to a solution of MA-NBD in CH_3CN but the maximum ratio of $F_{comp}/F_{MA\text{-}NBD}$ never exceeded 1.3. These low results for $Mg(NO_3)_2 \cdot 6H_2O$ were consistently observed on several occasions. This slight change in fluorescence is even smaller than the previously discussed ratio for $KClO_4$, $F_{comp}/F_{MA\text{-}NBD}$ = 1.6, which was considered insignificant. Results for the complexation of magnesium nitrate with

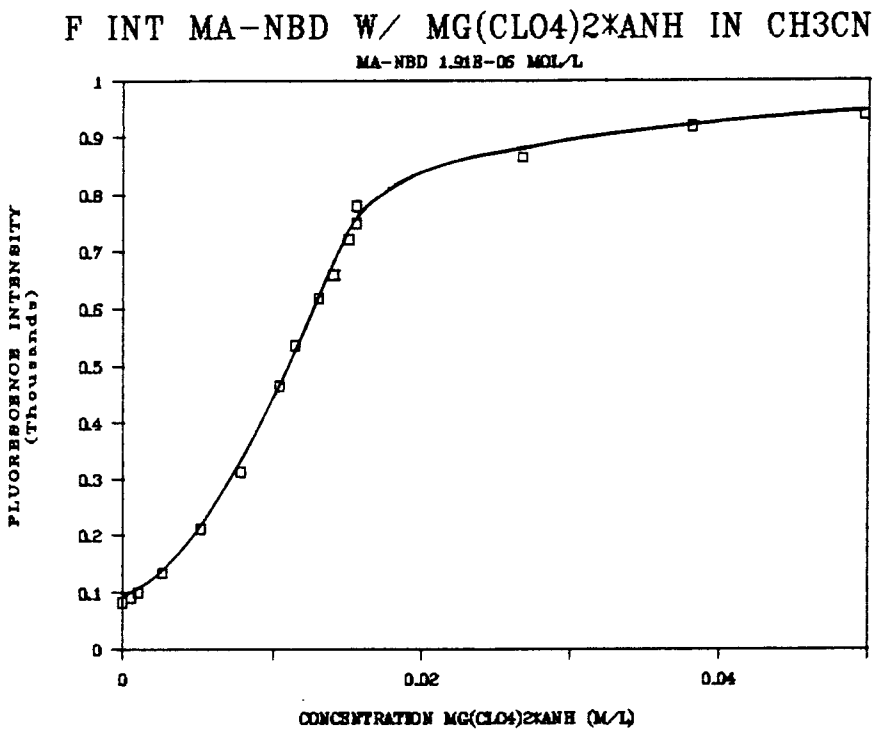

FIGURE 14. Fluorescence Intensity of MA-NBD with Anhydrous $Mg(ClO_4)_2$ - (Molar Concentration).

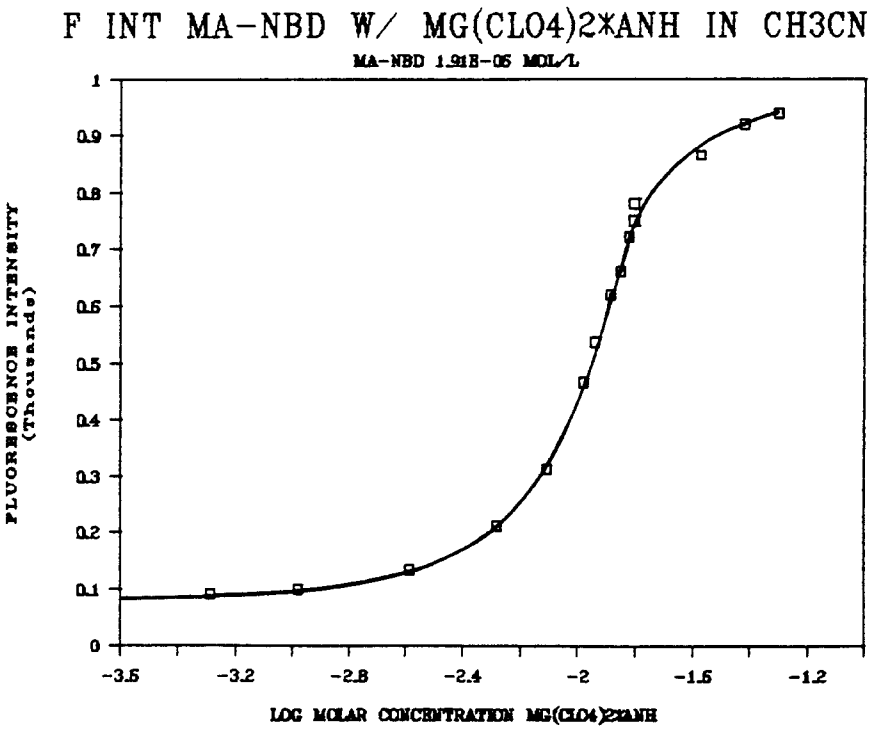

FIGURE 15. Fluorescence Intensity of MA-NBD with Anhydrous $Mg(ClO_4)_2$ - (Log Molar Concentration).

Table 20: Fluorescence Intensity of MA-NBD w/Anhydrous $Mg(ClO_4)_2$ in CH_3CN.

Conc $Mg(ClO_4)_2$ (Moles/L)	Log Conc $Mg(ClO_4)_2$	F Int Soln	Ratio Conc Mg^{2+}/MA-NBD
0.00E+00	----	82	0
5.20E-04	-3.28	91	270
1.04E-03	-2.98	100	545
2.60E-03	-2.58	134	1360
5.20E-03	-2.28	211	2720
7.80E-03	-2.11	313	4080
1.04E-02	-1.98	465	5450
1.14E-02	-1.94	536	5990
1.30E-02	-1.89	619	6800
1.40E-02	-1.85	660	7350
1.51E-02	-1.82	723	7900
1.56E-02	-1.81	781	8170
1.56E-02	-1.81	750	8170
2.68E-02	-1.57	865	14030
3.81E-02	-1.42	919	19970
4.96E-02	-1.30	940	25990

Concentration MA-NBD: 1.91E-06 M.

Table 21: Fluorescence Intensity of MA-NBD w/Anhydrous $Mg(ClO_4)_2$ in CH_3CN. (Conc MA-NBD - 1.91E-06 M)

Conc $Mg(ClO_4)_2$ (Moles/L)	Log Conc $Mg(ClO_4)_2$	F Int Soln	Ratio Conc Mg^{2+}/MA-NBD
0.00E+00	----	90	0
8.33E-05	-4.08	90	44
2.08E-04	-3.68	93	110
4.17E-04	-3.38	98	220
6.25E-04	-3.20	100	330
8.33E-04	-3.08	113	440
8.33E-04	-3.08	106	440
1.04E-03	-2.98	110	550
1.04E-03	-2.98	108	550
1.25E-03	-2.90	120	650
2.60E-03	-2.59	176	1360
2.64E-03	-2.58	296	1380
4.72E-03	-2.33	324	2470
6.61E-03	-2.18	570	3460
9.43E-03	-2.03	454	4940
1.04E-02	-1.98	520	5450
1.30E-02	-1.89	621	6810
1.32E-02	-1.88	828	6920
1.98E-02	-1.70	920	10400
2.64E-02	-1.58	946	13840
3.30E-02	-1.48	914	17300
3.97E-02	-1.40	890	20760

[a] This is a repeat study of data from Table 20 on previous page, performed 3 days later.

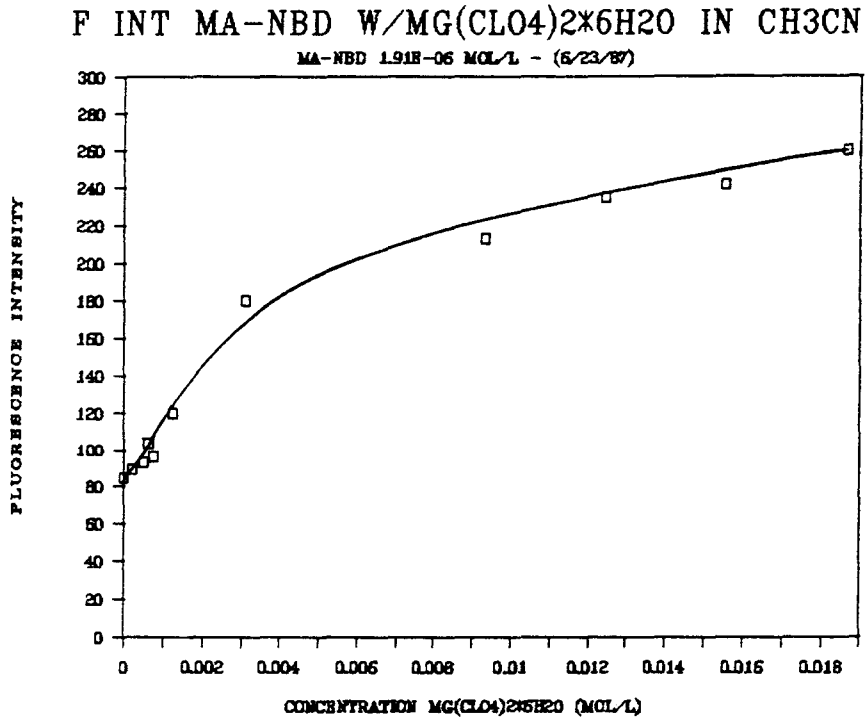

FIGURE 16. Fluorescence Intensity of MA-NBD with $Mg(ClO_4)_2 \cdot 6H_2O$ - (Molar Concentration).

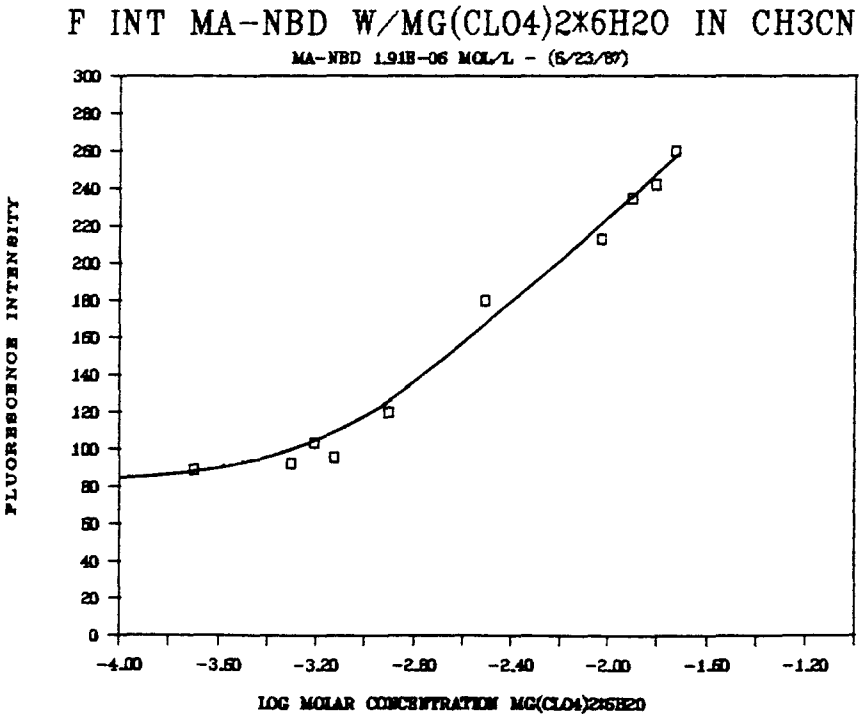

FIGURE 17. Fluorescence Intensity of MA-NBD with $Mg(ClO_4)_2 \cdot 6H_2O$ - (Log Molar Concentration).

Table 22: Fluorescence Intensity of MA-NBD w/$Mg(ClO_4)_2 \cdot 6H_2O$ In CH_3CN.

Conc $Mg(ClO_4)_2 \cdot 6H_2O$ (Moles/L)	Log Conc $Mg(ClO_4)_2 \cdot 6H_2O$	F Int Soln	Ratio Conc Mg^{2+}/MA-NBD
0.00E+00	----	85	0
1.99E-04	-3.70	89	104
4.97E-04	-3.30	93	260
7.45E-04	-3.13	96	390
6.22E-04	-3.21	104	325
1.24E-03	-2.90	120	650
3.11E-03	-2.51	180	1630
9.33E-03	-2.03	213	4880
1.24E-02	-1.90	235	6510
1.55E-02	-1.81	242	8140
1.87E-02	-1.73	260	9760

Concentration MA-NBD: 1.91E-06 M.

MA-NBD in CH_3CN are stressed here in light of the results to be presented in subsequent sections.

Tables 20 and 21, and curves in Figures 14 and 15, present the results of the addition of anhydrous $Mg(ClO_4)_2$ to 1.91×10^{-6} mol/L MA-NBD in CH_3CN. Examination of both sets of data allow calculation of an average ratio of the maximum $F_{comp}/F_{MA\text{-}NBD} = 11.0$, an estimated limit of detection of 11.4 ppm Mg^{2+}, and $K_f = 1.02 \times 10^2$. The concentration ratio of $[Mg^{+2}]/[MA\text{-}NBD]$ required to reach maximum fluorescence intensity for the anhydrous $Mg(ClO_4)_2$ complex must be at least 15,000 times the concentration of 2×10^{-6} mol/L MA-NBD.

Standard solutions of the hydrated magnesium perchlorate salt, $Mg(ClO_4)_2 \cdot 6H_2O$, were also added to a solution containing 1.91×10^{-6} mol/L MA-NBD in CH_3CN. The results for this study are presented in Table 22 and the curves in Figures 16 and 17. The curves are not as steep as those obtained for the anhydrous magnesium perchlorate. The plot of fluorescence intensity vs. the log of molar concentration $Mg(ClO_4)_2 \cdot 6H_2O$ appears to terminate rather abruptly at log = -1.73 (1.87×10^{-2} mol/L salt), however, the same concentration of MA-NBD with more concentrated $Mg(ClO_4)_2 \cdot 6H_2O$ solution, 4.72×10^{-2} mol/L (log -1.33) later produced negligibly higher fluorescence intensity. Although the hydrated salt produces a considerably more shallow curve (the ratio of maximum $F_{comp}/F_{MA\text{-}NBD}$ was

only 3.1) in comparison to the curve for anhydrous $Mg(ClO_4)_2$, the estimated detection limit of 12 ppm Mg^{2+} is close to the limit obtained for the anhydrous salt, and the calculated formation constant for the hydrate, $K_f = 2.5 \times 10^2$, is slightly larger than the value for the anhydrous salt. In order to produce the maximum ratio of $F_{comp}/F_{MA\text{-}NBD} = 3.1$ for the $Mg(ClO_4)_2 \cdot 6H_2O$, the concentration ratio of $[Mg^{2+}]/[MA\text{-}NBD]$ must be almost 10,000.

The Effect of Added $Mg(NO_3)_2 \cdot 6H_2O$ to Solutions of MA-NBD and the $Mg(ClO_4)_2$ Salts in CH_3CN: Magnesium nitrate hexahydrate, $Mg(NO_3)_2 \cdot 6H_2O$, was added to a solution of MA-NBD and anhydrous $Mg(ClO_4)_2$ in CH_3CN where the concentration of magnesium perchlorate was high enough to produce about 85 % the maximum complexation. This procedure resulted in an unusual response in fluorescence intensity and the results appear in Table 23. (Because the MA-NBD concentration is slightly higher than the optimum amount, the fluorescence of the complex with anhydrous magnesium perchlorate was too intense and the emission slit width was reduced. Slit settings of 5 × 3 nm were therefore used only for this study; the reported fluorescence intensities are greater than 1000 units because they have been corrected to provide intensities observed with the usual 5 × 5 nm slits widths for the same concentrations of the complex.)

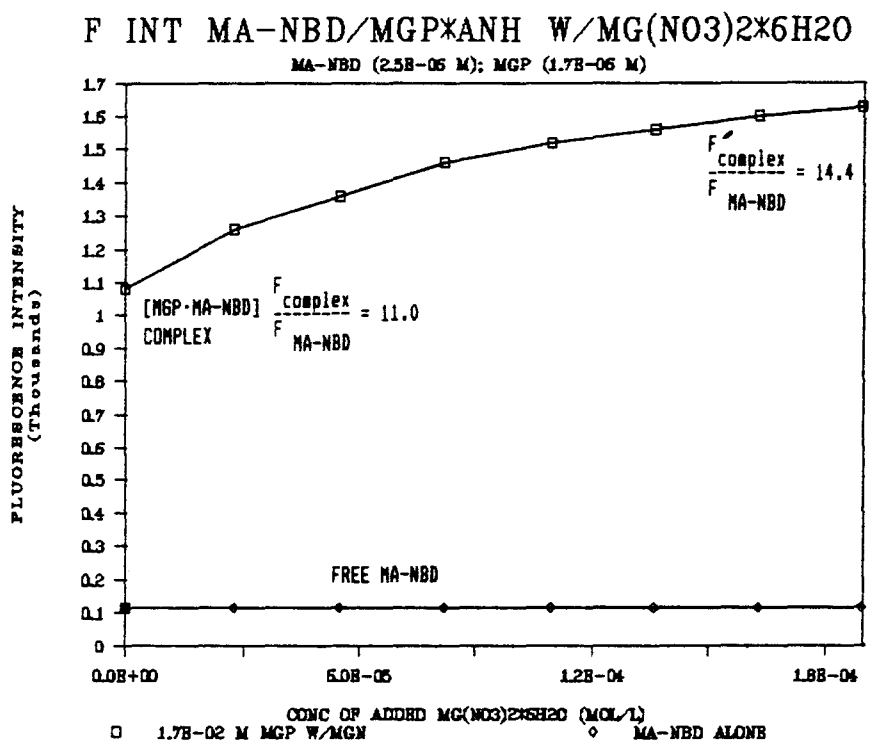

FIGURE 18. Fluorescence Intensity of MA-NBD and Anhydrous $Mg(ClO_4)_2$ with Addition of $Mg(NO_3)_2 \cdot 6H_2O$.

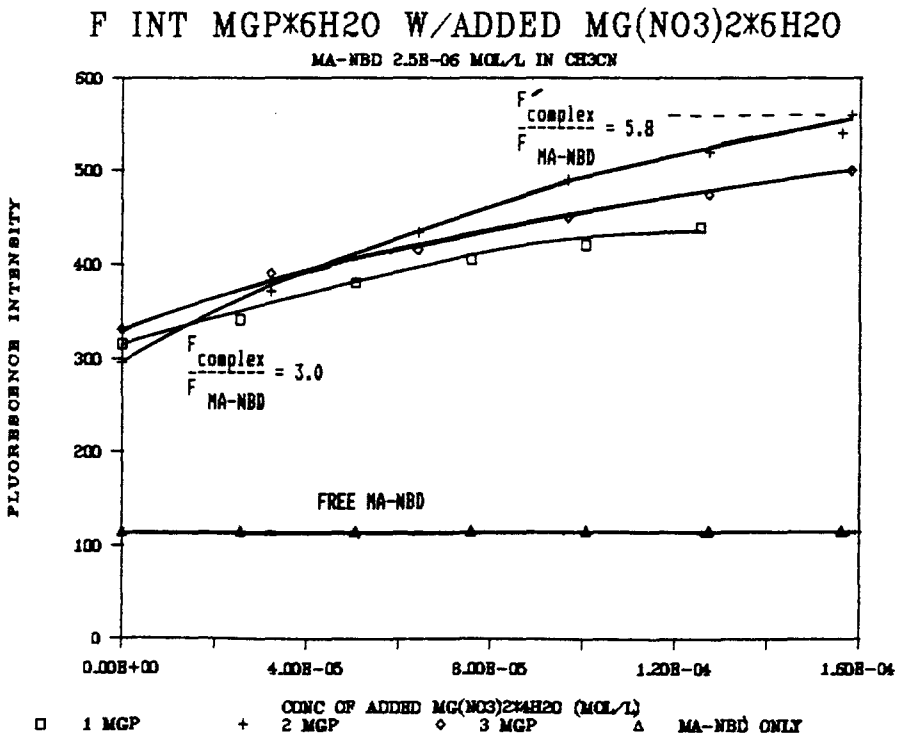

FIGURE 19. Fluorescence Intensity of MA-NBD and $Mg(ClO_4)_2 \cdot 6H_2O$ with Addition of $Mg(NO_3)_2 \cdot 6H_2O$.

Table 23: Fluorescence Enhancement of MA-NBD and Anhydrous $Mg(ClO_4)_2$ in CH_3CN with Increasing Added Concentration of $Mg(NO_3)_2 \cdot 6H_2O$.

Conc Added $Mg(NO_3)_2 \cdot 6H_2O$ (Moles/L)	Conc $Mg(ClO_4)_2$ (Moles/L)	Total Conc Mg^{2+} (Moles/L)	F Int Soln (Corr[a])	Ratio Total Conc Mg^{2+}/MA-NBD	Ratio F Comp/ F MA-NBD
0.000E+00	0.000E+00	0.000E+00	115 [b]	0	---
0.000E+00	1.702E-02	1.702E-02	1080	6657	9.4
2.752E-05	1.697E-02	1.700E-02	1260	6668	11.0
5.489E-05	1.693E-02	1.698E-02	1360	6679	11.8
8.210E-05	1.688E-02	1.696E-02	1460	6689	12.7
1.092E-04	1.683E-02	1.694E-02	1520	6700	13.2
1.361E-04	1.678E-02	1.692E-02	1560	6711	13.6
1.628E-04	1.674E-02	1.690E-02	1600	6722	13.9
1.894E-04	1.669E-02	1.688E-02	1625	6733	14.1

(Original Concentration MA-NBD = 2.6E-06 M and $Mg(ClO_4)_2$ = 1.7E-02 M)

[a] There is a correction for the slight dilution in the concentration of the anhydrous $Mg(ClO_4)_2$ for each subsequent entry in the table because 10 uL of 9.66E-03 M $Mg(NO_3)_2 \cdot 6H_2O$ in CH_3CN was added each time to the same sample solution being measured. The MA-NBD was also diluted accordingly during the same process. Original volume of solution was 3.50 mL; final volume after additions was 3.57 mL.

[b] Fluorescence intensity was also corrected for a Fixed Scale sensitivity of 1.00 and typical 5 X 5 nm slit settings used in all the reported fluorescence data for work in CH_3CN. Slits were set at 5 x 3 nm for this study only to keep the results of this study on scale - no fluorescence readings far over 1000 would have been possible otherwise using the Perkin-Elmer LS-5.

Two solutions containing 2.6×10^{-6} mol/L MA-NBD in CH_3CN were prepared, one with additional anhydrous $Mg(ClO_4)_2$ at 1.72×10^{-2} mol/L and one without any Mg-salt added. The initial volumes of both solutions was 3.50 mL. The MA-NBD blank solution measured 115, the second solution with added magnesium perchlorate measured 1080 - which produced a ratio for $F_{comp}/F_{MA\text{-}NBD} = 9.4$ for this solution. This ratio is somewhat below (about 85 %) the maximum complexation ratio of 11.0, but this observation could be expected, since the molar concentration ratio of $[Mg^{+2}]/[MA\text{-}NBD]$ is only 6660 in this preparation. This is less than one-half the concentration ratio $[Mg^{2+}]/[MA\text{-}NBD]$ required to attain the maximum fluorescence intensity for the complex based on the earlier standard curve results, shown in Tables 20 and 21. To the cuvette containing the 3.50 mL solution of 1.72×10^{-2} mol/L anhydrous $Mg(ClO_4)_2$ and 2.6×10^{-6} mol/L MA-NBD with a fluorescence intensity = 1080, a 10 μL aliquot of 9.66×10^{-3} mol/L $Mg(NO_3)_2 \cdot 6H_2O$ in CH_3CN solution was added using an Eppendorf pipet. After stirring with a small magnetic stir-bar, the solution was remeasured and the fluorescence had increased to 1264! The new ratio of $F_{comp}/F_{MA\text{-}NBD}$ was now 11.0, which is equal to the maximum ratio of $F_{comp}/F_{MA\text{-}NBD}$ normally observed when the maximum complexation intensity is attained at considerably higher concentrations of anhydrous magnesium perchlorate. The new concentration ratio of

$[Mg^{+2}]/[MA\text{-}NBD]$ was only 6670 after this small addition of $Mg(NO_3)_2 \cdot 6H_2O$. Six more 10 μL aliquots of the $Mg(NO_3)_2 \cdot 6H_2O$ solution were added until the final volume was 3.57 mL. Overall dilution of MA-NBD and original anhydrous $Mg(ClO_4)_2$ was less than 2 %. The results show a surprising enhancement of fluorescence for the addition of a very small amount of magnesium nitrate to a solution of $Mg(ClO_4)_2$ and MA-NBD already near maximum complexation. Examination of the results in Table 23 show that each successive addition of the $Mg(NO_3)_2 \cdot 6H_2O$ solution increases the fluorescence beyond the maximum ratio for $F_{comp}/F_{MA\text{-}NBD}$ = 11.0, for the MA-NBD complex with anhydrous magnesium perchlorate. The final fluorescence intensity was 1658 - producing an enhanced maximum ratio with $F_{comp}/F_{MA\text{-}NBD}$ = 14.4. After the initial jump in fluorescence of 184 units, each successive addition produced a smaller increase in fluorescence intensity. A plot of the data obtained for fluorescence intensity of the $Mg(ClO_4)2$:MA-NBD complex vs. molar concentration of added $Mg(NO_3)_2 \cdot 6H_2O$ is presented in Figure 18.

For purposes of comparison, Table 20 data for the standard titration of MA-NBD with anhydrous $Mg(ClO_4)_2$ shows a fluorescence of 619 corresponding to the concentration ratio $[Mg^{+2}]/[MA\text{-}NBD]$ of 6800. The MA-NBD blank was 82 and 619/82 produces a $F_{comp}/F_{MA\text{-}NBD}$ ratio = 7.5. Farther down the table, an average fluorescence of 765 corresponds

to a concentration ratio for $[Mg^{+2}]/[MA\text{-}NBD]$ of 8170, which produces a ratio of 9.3 for $F_{comp}/F_{MA\text{-}NBD}$. The MA-NBD concentration was 1.91×10^{-6} mol/L for the Table 20 study, slightly lower than 2.6×10^{-6} mol/L concentration used here for Table 23 - 26 study results. In the early calcium nitrate and cadmium nitrate titrations of MA-NBD in CH_3CN, one observed phenomenon - and a consequence of the K_f - was that the higher the MA-NBD concentration used for the study, the lower the concentration ratio $[M^{n+}]/[MA\text{-}NBD]$ required to reach the maximum fluorescence intensity. Examination of the summarized results in Table 27 for the Ca- and Cd-nitrate salts with MA-NBD in CH_3CN quickly supports this statement. This behavior also seems consistent for other $F_{comp}/F_{MA\text{-}NBD}$ fluorescence intensity ratios below maximum complexation. Therefore, it is not surprising that for the anhydrous magnesium perchlorate plus magnesium nitrate study, where 2.6×10^{-6} mol/L MA-NBD and 1.7×10^{-2} mol/L $Mg(ClO_4)_2$ produced an initial $F_{comp}/F_{MA\text{-}NBD}$ ratio of 9.4, the accompanying concentration ratio of $[Mg^{2+}]/[MA\text{-}NBD] = 6660$, was lower by using a higher concentration of MA-NBD. Even when the anhydrous $Mg(ClO_4)_2$ standard titration of MA-NBD was repeated in Table 21- where the data shows less precision than the first data presented in Table 20 - the concentration ratio of $[Mg^{2+}]/[MA\text{-}NBD]$ had to be at least 6900 to reach a ratio for $F_{comp}/F_{MA\text{-}NBD} = 9.4$, and at least 13,900 to reach the

maximum ratio $F_{comp}/F_{MA\text{-}NBD}$ of 11.0. Table 20 data shows that a concentration ratio of $[Mg^{2+}]/[MA\text{-}NBD]$ greater than 20,000 is required for the maximum ratio $F_{comp}/F_{MA\text{-}NBD}$ of 11.0. Here, the total concentration ratio $[Mg^{2+}]/[MA\text{-}NBD]$ for the perchlorate and the nitrate together is only 6730, and the enhanced maximum ratio for $F_{comp}/F_{MA\text{-}NBD}$ is 14.4.

A similar study was also done for the hydrated magnesium perchlorate. In this study - though less dramatic - the same type of response was observed for a system containing a fixed amount of MA-NBD and $Mg(ClO_4)_2 \cdot 6H_2O$ in CH_3CN to which small amounts of magnesium nitrate hexahydrate, $Mg(NO_3)_2 \cdot 6H_2O$, were added. In order to be sure the observed phenomenon was actually occurring, the experiment was repeated in triplicate. The results appear in Tables 24 - 26, with plots of the data from these tables presented in the same Figure 19.

For each study, a "blank" solution of 2.6×10^{-6} mol/L MA-NBD in CH_3CN was prepared without any magnesium salts. A second 2.6×10^{-6} mol/L MA-NBD solution was prepared with added magnesium perchlorate hexahydrate, $Mg(ClO_4)_2 \cdot 6H_2O$, at 1.87×10^{-2} mol/L, 2.01×10^{-2} mol/L, and 4.7×10^{-2} mol/L concentrations. In each case the original MA-NBD blank measured 115 fluorescence units and the original solutions with magnesium perchlorate hexahydrate measured 315, 295, and 330 respectively. When comparing these preparations of MA-NBD with $Mg(ClO_4)_2 \cdot 6H_2O$ to the results

Table 24 : Fluorescence Intensity of MA-NBD and $Mg(ClO_4)_2 \cdot 6H_2O$ in CH_3CN with Increasing Added Concentration of $Mg(NO_3)_2 \cdot 6H_2O$.

Conc Added $Mg(NO_3)_2 \cdot 6H_2O$ (Moles/L)	Conc $Mg(ClO_4)_2 \cdot 6H_2O$ (Moles/L)	Total Conc $[Mg^{2+}]$ (Moles/L)	F Int Corr for Dilution	Ratio Total Conc Mg^{2+}/MA-NBD	Ratio of F Comp/ F MA-NBD
0.00E+00	0.00E+00	0.000E+00	115	0	
0.00E+00	1.87E-02	1.870E-02	315	7313	2.74
2.54E-05	1.87E-02	1.873E-02	341	7343	2.97
5.06E-05	1.87E-02	1.870E-02	382	7354	3.32
7.57E-05	1.86E-02	1.868E-02	408	7361	3.55
1.01E-04	1.86E-02	1.865E-02	424	7372	3.69
1.26E-04	1.85E-02	1.863E-02	446	7380	3.88

(Original Concentration MA-NBD = 2.55 X 10^{-6} M and $Mg(ClO_4)_2 \cdot 6H_2O$ = 1.87 X 10^{-2} M.[a])

[a] There is a slight dilution in the molar concentration of the $Mg(ClO_4)_2 \cdot 6H_2O$ for each subsequent entry in the table because 10 uL of 9.66E-03 M $Mg(NO_3)_2 \cdot 6H_2O$ in CH_3CN was added each time to the same sample solution being measured. The MA-NBD was also diluted accordingly during the same process. Original volume of solution was 3.80 mL; final volume after additions was 3.85 mL.

Table 25: Fluorescence Enhancement of MA-NBD and $Mg(ClO_4)_2 \cdot 6H_2O$ in CH_3CN with Increasing Added Concentration of $Mg(NO_3)_2 \cdot 6H_2O$.

Conc Added $Mg(NO_3)_2 \cdot 6H_2O$ (Moles/L)	Conc $Mg(ClO_4)_2 \cdot 6H_2O$ (Moles/L)	Total Conc $[Mg^{2+}]$ (Moles/L)	F Int Corr for Dilution	Ratio Total Conc Mg^{2+}/MA-NBD	Ratio of F Comp/ F MA-NBD
0.00E+00	0.00E+00	0.000E+00	115	0	
0.00E+00	2.01E-02	2.010E-02	295	7882	2.57
3.20E-05	2.01E-02	2.008E-02	371	7900	3.23
6.40E-05	2.00E-02	2.005E-02	438	7917	3.81
9.56E-05	1.99E-02	2.002E-02	495	7927	4.30
1.27E-04	1.99E-02	1.999E-02	527	7944	4.58
1.58E-04	1.98E-02	1.995E-02	569	7954	4.95
1.41E-03	1.95E-02	2.088E-02	672	8461	5.84

(Original Concentration of MA-NBD = 2.55 X 10^{-6} M and $Mg(ClO_4)_2 \cdot 6H_2O$ = 2.01 X 10^{-2} M.[a])

[a] There is a slight dilution in the molar concentration of the $Mg(ClO_4)_2 \cdot 6H_2O$ for each subsequent entry in the table because 10 uL of 9.66E-03 M $Mg(NO_3)_2 \cdot 6H_2O$ in CH_3CN was added each time to the same sample solution being measured. The MA-NBD was also diluted accordingly during the same process. Original volume of solution was 3.00 mL; final volume after additions was 3.10 mL.

Table 26: Fluorescence Enhancement of MA-NBD and $Mg(ClO_4)_2 \cdot 6H_2O$ in CH_3CN with Increasing Added Concentration of $Mg(NO_3)_2 \cdot 6H_2O$.

Conc Added $Mg(NO_3)_2 \cdot 6H_2O$ (Moles/L)	Conc $Mg(ClO_4)_2 \cdot 6H_2O$ (Moles/L)	Total Conc $[Mg^{2+}]$ (Moles/L)	F Int Corr for Dilution	Ratio Total Conc Mg^{2+}/MA-NBD	Ratio of F Comp/ F MA-NBD
0.00E+00	0.00E+00	0.000E+00	115	0	
0.00E+00	4.73E-02	4.727E-02	330	18537	2.87
3.20E-05	4.71E-02	4.714E-02	391	18545	3.40
6.40E-05	4.70E-02	4.701E-02	418	18561	3.63
9.56E-05	4.68E-02	4.690E-02	454	18573	3.95
1.27E-04	4.66E-02	4.677E-02	481	18588	4.18
1.58E-04	4.65E-02	4.665E-02	508	18600	4.42
1.44E-03	4.65E-02	4.793E-02	671	19110	5.83

(Original Concentration of MA-NBD = 2.55×10^{-6} M and $Mg(ClO_4)_2 \cdot 6H_2O$ = 4.72×10^{-2} M.[a])

[a] There is a slight dilution in the molar concentration of the $Mg(ClO_4)_2 \cdot 6H_2O$ for each subsequent entry in the table because 10 uL of 9.66E-03 M $Mg(NO_3)_2 \cdot 6H_2O$ in CH_3CN was added each time to the same sample solution being measured. The MA-NBD was also diluted accordingly during the same process. Original volume of solution was 3.00 mL; final volume after additions was 3.05 mL.

for the standard curve presented in Table 22, it can be seen that the first two preparations contain close to the amount [Mg^{2+}] required to provide the maximum fluorescence at maximum complexation of hydrated magnesium perchlorate with MA-NBD. The third solution contains about twice the necessary magnesium concentration. The maximum $F_{comp}/F_{MA\text{-}NBD}$ reported for the earlier results in Table 22 was 3.1 and the corresponding concentration ratio of [Mg^{2+}]/[MA-NBD] required to produce that fluorescence intensity was 9760. In comparison, it can be seen from the second entries in Tables 24, 25, and 26 - that the resulting fluorescence intensity ratio of $F_{comp}/F_{MA\text{-}NBD}$ for these three preparations are 2.7, 2.6, and 2.9, and the corresponding initial concentration ratios of [Mg^{2+}]/[MA-NBD] are 7330, 7890, and 18540 respectively. (The [Mg^{2+}]/[MA-NBD] concentration ratios reported in Table 22 of 6510 and 8140 correspond to $F_{comp}/F_{MA\text{-}NBD}$ ratios of 2.8 and 2.9, so that the initial results in these studies are in line with those of earlier $Mg(ClO_4)_2 \cdot 6H_2O$ studies.)

To these original solutions containing the mixtures of the MA-NBD and $Mg(ClO_4)_2 \cdot 6H_2O$, successive 10 μL increments of 9.66×10^{-3} mol/L magnesium nitrate hexahydrate, $Mg(NO_3)_2 \cdot 6H_2O$, in CH_3CN were added. Following each new addition of the magnesium nitrate the resulting fluorescence intensity was measured after thorough mixing. There is a surprising increase in fluorescence intensity with the

very small increase in concentration of $Mg(NO_3)_2 \cdot 6H_2O$, a salt that caused no more than a 1.3-fold increase in the fluorescence of MA-NBD for any amount added (even when solid crystals of the salt are used directly). On examination of the data in Tables 24, 25 and 26, the fluorescence can be seen to increase dramatically with only insignificant increases in the overall $[Mg^{2+}]/[MA\text{-}NBD]$ ratio. The fluorescence intensity was enhanced up to 5.8 times- almost 100 % higher than the maximum $F_{comp}/F_{MA\text{-}NBD}$ previously observed at much higher $Mg(ClO_4)_2 \cdot 6H_2O$/MA-NBD concentration ratios. After five 10 μL additions of the 9.33×10^{-3} mol/L magnesium nitrate solution and 0.001 g of solid $Mg(NO_3)_2 \cdot 6H_2O$, the increase in fluorescence intensity leveled off. Near the bottom of Figure 19 is a straight line marking the initial fluorescence intensity of 115 units for the MA-NBD blank.

These studies demonstrate an extremely interesting synergistic effect in which adding a salt, $Mg(NO_3)_2 \cdot 6H_2O$, which normally has such a weak effect when combined alone with MA-NBD in acetonitrile, appears to enhance the fluorescence intensity of complexes of the hydrated or anhydrous magnesium perchlorate salts with MA-NBD and which cannot be explained at this time. It is hoped that future work on these combined magnesium perchlorate/magnesium nitrate with MA-NBD systems will elucidate this unusual synergistic fluorescence enhancement effect.

Table 27: Summary of Fluorescence Intensity Data for Metal Salt Complexes with MA-NBD in CH_3CN.

Metal Salt Tested	Conc MA-NBD (Mol/L)	F Int MA-NBD	Max F Int Complex	Ratio F Int (Complex/ MA-NBD)	Complex Max (nm)
$Ca(NO_3)_2 \cdot 4H_2O$					
	1.88E-08	0.5	9.5	19.0	527
	7.52E-08	1.7	37.3	21.9	527
	3.13E-07	6.5	149.6	23.0	527
	1.50E-06	34.3	738.0	21.5	527
			Avg:	21.4	
$Cd(NO_3)_2 \cdot 4H_2O$					
	1.00E-06	45.5	785.0	17.2	530
	6.67E-07	31.1	548.6	17.6	530
	1.88E-07	10.7	190.2	17.8	530
			Avg:	17.6	
$Ca(ClO_4)_2 \cdot 4H_2O$					
	1.53E-06	66.0	886.0	13.4	528
$NaClO_4$	6.67E-07	37.7	124.8	3.3	535
$NaClO_4$	6.67E-07	37.4	145.0	3.8	535
$KClO_4$	6.67E-07	38.4	61.0	3.6	535
$Mg(ClO_4)_2 \cdot ANH$					
	1.91E-06	82.0	940.0	11.5	530
	1.91E-06	90.0	946.0	10.5	530
$Mg(ClO_4)_2 \cdot 6H_2O$					
	1.91E-06	85.0	260.0	3.1	532
$Mg(NO_3)_2 \cdot 6H_2O$					
	2.50E-06	115.0	140.0	1.3	539

Initial maximum emission wavelength of MA-NBD in CH_3CN before addition of metal salts: 538 - 540 nm.

(Table continued on following page.)

Table 27: Summary of Fluorescence Intensity Data for Metal Salt (Cont'd) Complexes with MA-NBD in CH_3CN.

Metal Salt Tested	Conc MA-NBD (Mol/L)	Ratio F Int (Complex/ MA-NBD)	Ratio Conc. $[M^{n+}]/[MA\text{-}NBD]$ 1st[a]	Final[b]	Est. Detection Limits	K_f Formation Constant
$Ca(NO_3)_2 \cdot 4H_2O$						
	1.88E-08	19.00	93	155000	70.1 ppb	5.89E+04
	7.52E-08	21.94	10	93300	29.3 ppb	5.88E+04
	3.13E-07	23.02	4	7770	48.9 ppb	4.50E+04
	1.50E-06	21.52	< 1	9710	23.4 ppb	6.46E+04
					Avg:	5.68E+04
$Cd(NO_3)_2 \cdot 4H_2O$						
	1.88E-07	17.78	175	70000	3.7 ppm	4.47E+02
	6.67E-07	17.64	16	10700	1.2 ppm	4.20E+02
	1.00E-06	17.25	21	8060	2.4 ppm	4.50E+02
					Avg:	4.39E+02
$Ca(ClO_4)_2 \cdot 4H_2O$						
	1.53E-06	13.42	1	3560	56.1 ppb	3.98E+03
$NaClO_4$	6.67E-07	3.31	21	13400	0.32 ppm	1.60E+03
$NaClO_4$	6.67E-07	3.88				
$KClO_4$	6.67E-07	1.59	1080	8520	27.9 ppm	----
$Mg(ClO_4)_2 \cdot ANH$						
	1.91E-06	11.46	272	25600	12.6 ppm	9.10E+01
	1.91E-06	10.51	218	20800	10.1 ppm	1.12E+02
					Avg:	1.02E+02
$Mg(ClO_4)_2 \cdot 6H_2O$						
	1.91E-06	3.06	260	9760	12.1 ppm	2.51E+02

$Mg(NO_3)_2 \cdot 6H_2O$ (No data; curve to short to make valid calculations.)

a Ratio of the molar concentrations of [metal cation]/[MA-NBD] resulting in 1st change in fluorescence intensity from that of the same concentration of MA-NBD alone.

b Ratio of the $[M^{n+}]/[MA\text{-}NBD]$ when the curve levels off and/or maximum fluorescence intensity was attained.

Table 28: Preliminary Tests for the Fluorescence Intensity of Metal Salt Crystals Added Directly to a Solution of MA-NBD in CH_3CN in Fluorescence Cuvette.

Metal Salt Added	Conc MA-NBD (Mol/L)	F Int MA-NBD	Max F Int Complex	Ratio F Int (Complex/ MA-NBD)	Complex Max (nm)
$Mg(NO_3)_2 \cdot 6H_2O$	7.52E-07	16.5	21.5	1.30	539
KCl	"	16.5	15.6	0.95	539
KSCN	"	16.5	23.8	1.44	539
$KClO_4$	"	16.5	30.2	1.83	536
KNO_3	"	16.5	18.5	1.12	539
$Ba(NO_3)_2$	"	16.5	15.6	0.95	539
$Cs(NO_3)_2$	"	16.5	16.0	0.97	539
NaCl	"	18.3	19.8	1.08	539
NaCl	"	18.3	20.9	1.14	539
$NaClO_4$	"	16.5	60.2	3.65	535
$NaClO_4$	"	18.3	67.5	3.69	535
$NaNO_3$	"	18.3	26.2	1.43	539
$Ca(NO_3)_2 \cdot 4H_2O$	"	18.3	382.0	20.90	527

Initial Maximum emission wavelength of MA-NBD in CH_3CN before the addition of metal salts: 539 nm.

The Effect of Metal Salts on the Fluorescence Intensity of MA-NBD in 1:1 $CHCl_3$:MeOH: The fluorescence intensity of MA-NBD in 1:1 $CHCl_3$:MeOH is enhanced to a much smaller extent when certain salts of potassium, sodium and silver are added to the solution. The $F_{comp}/F_{MA\text{-}NBD}$ ratios are much smaller than those determined for the CH_3CN system, and as a consequence the LS-5 slit settings were 5 × 10 nm to improve the sensitivity of the method. Accompanying the change in intensity is a slight shift in the maximum emission wavelength from 537 nm for MA-NBD alone to 535 nm on complexation with the metal salts. There are a number of limitations to this system which is effective only under certain conditions. The most favorable MA-NBD concentration chosen was 3.5×10^{-7} mol/L MA-NBD in the 1:1 $CHCl_3$:MeOH solvent system. Solubilities of the metal salts are low in this solvent system containing fifty percent $CHCl_3$. The maximum change in fluorescence intensity at maximum complexation for MA-NBD with any of the salts produced a response of about 3 times the original intensity of the MA-NBD blank. The following ratios are reported: $F_{comp}/F_{MA\text{-}NBD} \geq 3.0$ for $AgClO_4$ and $AgNO_3$; $F_{comp}/F_{MA\text{-}NBD} = 2.0$ for NaCl; $F_{comp}/F_{MA\text{-}NBD} = 1.7$ for NaSCN; down to $F_{comp}/F_{MA\text{-}NBD} = 1.3$ for KCl and KSCN. In order to attain this maximum change attributed to the maximum complexation of MA-NBD with any of these metal salts, a very large concentration ratio of $[M^+]/[MA\text{-}NBD]$

was required, often greater than several thousand times the concentration of the ligand alone. This has been attributed to what appear to be small K_f constants, so that we essentially forced the maximum complexation between the metal cation and the MA-NBD to occur by adding a large excess of metal salt.

If a much smaller concentration of MA-NBD was held constant, a larger ratio of $[M^+]/[MA\text{-}NBD]$ is possible before exceeding the solubility of the metal salt in the solvent medium. The original fluorescence of the MA-NBD would be much lower, so that even with the three-fold enhancement of the intensity at maximum complexation seen with $AgClO_4$, the final maximum fluorescence would be lower and the already low sensitivity of the method under those conditions would be further sacrificed for only a slight increase in the concentration ratio of $[M^+]/[MA\text{-}NBD]$. If the fixed concentration of MA-NBD in the solution was increased, the original fluorescence intensity of the MA-NBD would be greater, and since the ratio, $F_{comp}/F_{MA\text{-}NBD}$, is expected to be the same - an advantage would be gained when the maximum complexation with the metal salt was attained. The intensity would be increased substantially and the sensitivity therefore improved. Because the maximum complexation can never be attained with the $> 10,000$ to 1 ratio of $[M^+]/[MA\text{-}NBD]$ since the metal salt would not be soluble enough in the 1:1 $CHCl_3$:MeOH medium to

provide that necessary large concentration ratio, a problem is posed. The 3.50×10^{-7} mol/L MA-NBD was therefore chosen as the fixed ligand concentration for these studies to off-set the metal salt solubility and the fluorescence response factors. The results for each metal salt titration appear in Tables 29 through 34, and a summary of all the important data features appears in Table 35.

When observing all six plots of fluorescence intensity vs. the molar concentration of these monovalent metal salts for MA-NBD in 1:1 $CHCl_3$:MeOH in Figure 20, the slopes increase sharply for the lower concentrations of $[M^+]$, but eventually level off, and - in some cases - start falling back towards the abscissa when the concentration is increased further. (No plots of fluorescence intensity vs. the log of molar concentration of the metal salts are shown as they provide no further insight into the system's behavior.) In the cases of NaCl and KCl, the fluorescence intensities reach their maxima but do not level off - this situation occurred when no further data points could be obtained, because the solubility of the metal salt in the 1:1 $CHCl_3$:MeOH medium was the limiting factor. The maximum solubility found for these salts in the 1:1 C:M solvent system was > 0.05 mol/L for NaSCN, 0.05 mol/L for KSCN, 0.008 mol/L for NaCl, 0.005 mol/L for KCl, > 0.052 mol/L for the NH_4SCN, about 0.009 mol/L for $AgClO_4$. Information on $AgNO_3$ was derived only from preliminary tests with it.

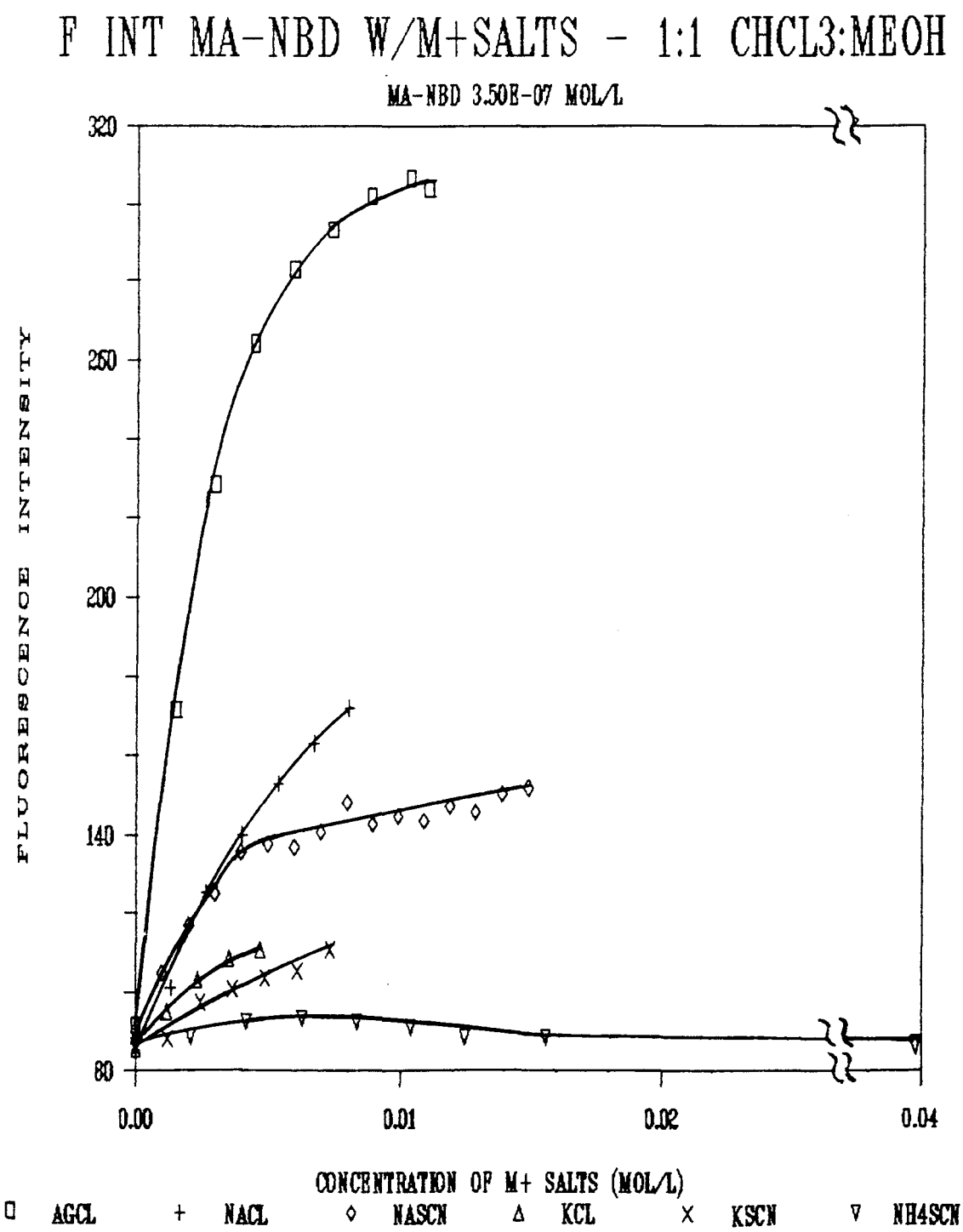

FIGURE 20. Fluorescence Intensity of MA-NBD with the Monovalent Metal Salts in 1:1 $CHCl_3$:MeOH.

Table 29: Fluorescence Intensity of MA-NBD w/ $AgClO_4$ in 1:1 $CHCl_3$:MeOH.

Conc $AgClO_4$ (Moles/L)	Log Conc $AgClO_4$	F Int Soln	Ratio Conc Ag^+/MA-NBD
0.00E+00	----	91.6	0
1.47E-03	-2.83	171.5	4190
2.93E-03	-2.53	228.5	8380
4.40E-03	-2.36	264.1	12600
5.87E-03	-2.23	282.5	16800
7.33E-03	-2.13	293.5	21000
8.80E-03	-2.06	302.2	25100
1.03E-02	-1.99	306.6	29300
1.10E-02	-1.96	304.2	31400

Concentration MA-NBD: 3.50E-07 M.

Table 30: Fluorescence Intensity of MA-NBD w/NaCl in 1:1 $CHCl_3$:MeOH.

Conc NaCl (Moles/L)	Log Conc NaCl	F Int Soln	Ratio Conc Na^+/MA-NBD
0.00E+00	----	85.4	0
1.33E-03	-2.88	101.2	3810
2.67E-03	-2.57	125.2	7620
4.00E-03	-2.40	140.0	11400
5.33E-03	-2.27	152.9	15200
6.67E-03	-2.18	163.0	19000
8.00E-03	-2.10	171.9	22900

Concentration MA-NBD: 3.50E-07 M.

Table 31: Fluorescence Intensity of MA-NBD w/KCl in 1:1 $CHCl_3$:MeOH.

Conc KCl (Moles/L)	Log Conc KCl	F Int Soln	Ratio Conc K^+/MA-NBD
0.00E+00	----	85.7	0
1.17E-03	-2.93	95.0	3330
2.33E-03	-2.63	103.2	6670
3.50E-03	-2.46	108.5	10000
4.67E-03	-2.33	110.9	13300
5.83E-03	-2.23	ppt	16700

Concentration MA-NBD: 3.50E-07 M.

Table 32: Fluorescence Intensity of MA-NBD w/ NaSCN in 1:1 $CHCl_3$:MeOH.

Conc NaSCN (Moles/L)	Log Conc NaSCN	F Int Soln	Ratio Conc Na^+/MA-NBD
0.00E+00	----	87.3	0
9.90E-04	-3.00	104.9	2830
1.98E-03	-2.70	117.0	5660
2.97E-03	-2.53	124.9	8490
3.96E-03	-2.40	135.5	11300
4.95E-03	-2.31	137.7	14100
5.94E-03	-2.23	136.9	17000
6.93E-03	-2.16	140.5	19800
7.92E-03	-2.10	148.0	22600
8.91E-03	-2.05	142.5	25500
9.90E-03	-2.00	144.5	28300
1.09E-02	-1.96	143.4	31100
1.19E-02	-1.93	147.0	33900
1.29E-02	-1.89	145.6	36800
1.39E-02	-1.86	150.4	39600
1.49E-02	-1.83	151.8	42400

Concentration MA-NBD: 3.50E-07 M.

Table 33: Fluorescence Intensity of MA-NBD w/KSCN in 1:1 $CHCl_3$:MeOH.

Conc KSCN (Moles/L)	Log Conc KSCN	F Int Soln	Ratio Conc K^+/MA-NBD
0.00E+00	----	86.5	0
1.22E-03	-2.92	88.2	3480
2.43E-03	-2.61	97.2	6950
3.65E-03	-2.44	100.7	10400
4.87E-03	-2.31	103.6	13900
6.08E-03	-2.22	105.4	17400
7.30E-03	-2.14	111.0	20900

Concentration MA-NBD: 3.50E-07 M.

Table 34: Fluorescence Intensity of MA-NBD w/ NH_4SCN in 1:1 CHC13:MeOH.

Conc NH_4SCN (Moles/L)	Log Conc NH_4SCN	F Int Soln	Ratio Conc NH_4^+/MA-NBD
0.00E+00	----	88.6	0
2.08E-03	-2.68	88.3	5940
4.16E-03	-2.38	92.4	11900
6.24E-03	-2.20	93.3	17800
8.32E-03	-2.08	92.5	23800
1.04E-02	-1.98	91.0	29700
1.25E-02	-1.90	88.5	35700
1.56E-02	-1.81	88.3	44600
7.00E-02	-1.15	87.0	200000

Concentration MA-NBD: 3.50E-07 M.

Table 35: Summary of Fluorescence Intensity Data for Metal Salt Complexes with MA-NBD in 1:1 $CHCl_3$:MeOH.

Metal Salt Tested	Conc MA-NBD (Mol/L)	F Int MA-NBD	Max F Int Complex	Ratio F Int (Complex/ MA-NBD)	Complex Max (nm)
$AgClO_4$	3.50E-07	91.6	306.6	3.4	535
$AgNO_3$	"	---	---	3.0	535
NaCl	"	85.4	171.9	2.0	535
NaSCN	"	87.3	151.8	1.7	536
KCl	"	85.7	110.9	1.3	535
KSCN	"	86.5	110.0	1.3	536
NH_4SCN	"	88.6	93.3	1.0	536

(Initial maximum emission wavelength of MA-NBD (3.50E-07 M) in 1:1 $CHCl_3$:MeOH, before addition of metal salts: 537 nm.)

Table 35: (Cont'd) Summary of Fluorescence Intensity Data for Metal Salt Complexes with MA-NBD in 1:1 $CHCl_3$:MeOH.

Metal Salt Tested	Conc MA-NBD (Mol/L)	Ratio F Int (Complex/ MA-NBD)	Ratio Conc. $[M^{n+}]/[MA\text{-}NBD]$ 1st[a]	Final[b]	Est. Detection Limits	K_f Formation Constant
AgClO4	3.50E-07	3.3	4190	29300	158.6 ppm	5.20E+02
AgClO4 (Est. for Lower Std:)	"		1430	29300	54.0 ppm	" "
AgNO3	3.50E-07	3.0	---	---	---	----
NaCl	"	2.0	3810	22900	30.6 ppm	3.30E+02
KCl	"	1.3	3330	13300	45.7 ppm	6.00E+02
NaSCN	"	1.7	2830	42400	22.8 ppm	----
KSCN	"	1.3	3480	20900	47.7 ppm	1.20E+02
NH4SCN	"	1.0	11900	17900	75.0 ppm	----

No complete calibration curve for $AgNO_3$ was completed in 1:1 $CHCl_3$:MeOH.

The solvent system was modified first to 1:3 $CHCl_3$:MeOH, and later to 25:65:10 $CHCl_3$:MeOH:H_2O, in attempts to increase the concentration range of the metal salts and extend the curves by increasing their solubility. The problem with decreasing the chloroform and increasing the methanol and H_2O concentrations is that the quantum efficiency of fluorescence for MA-NBD decreases considerably as reported earlier. There is also substantial evidence that the presence of the water decreases the intensity of the complex or prevents any complexation from occurring. (This phenomenon will be presented in next section.) The only salts tested were KCl and NaCl in all 3 solvent systems, the results are shown in Figures 21 and 22, where it can be seen that no advantage was achieved with these modifications which were made to improve solubility of the salts.

Along with the silver, sodium, and potassium salts tested, NH_4SCN was also included for comparison. The presence of NH_4SCN has virtually no effect on the intensity of MA-NBD in the chloroform:methanol system even at higher concentrations. This observation complies with the behavior of the NH_4^+ cation described in the literature reporting little evidence of its complexation seen with the 18-crown-6 size rings. Even more importantly, this provides

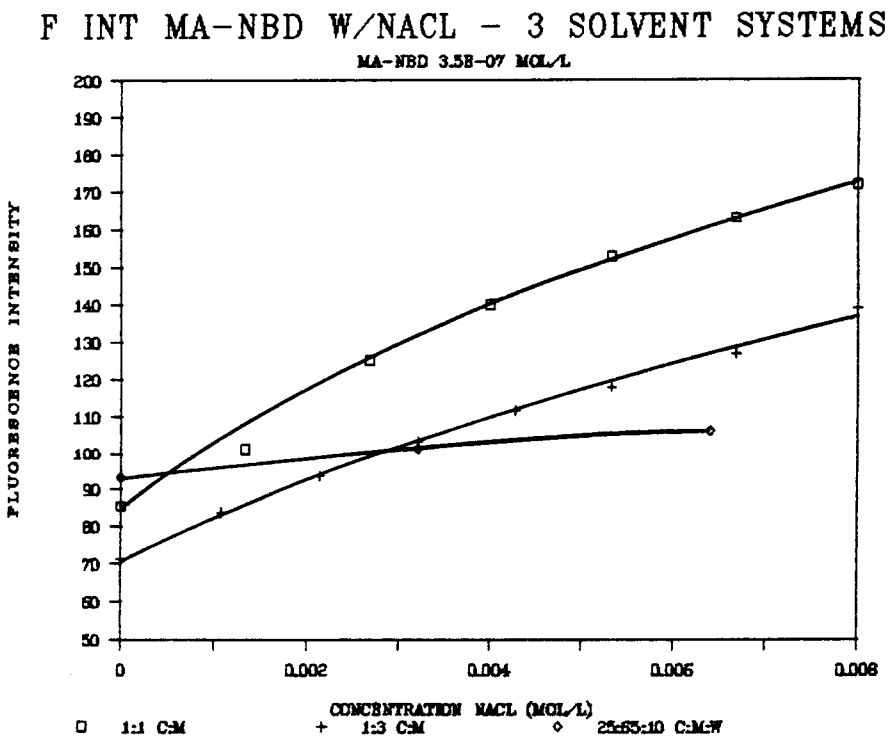

FIGURE 21. Fluorescence Intensity of MA-NBD in Three Solvent Systems with NaCl.

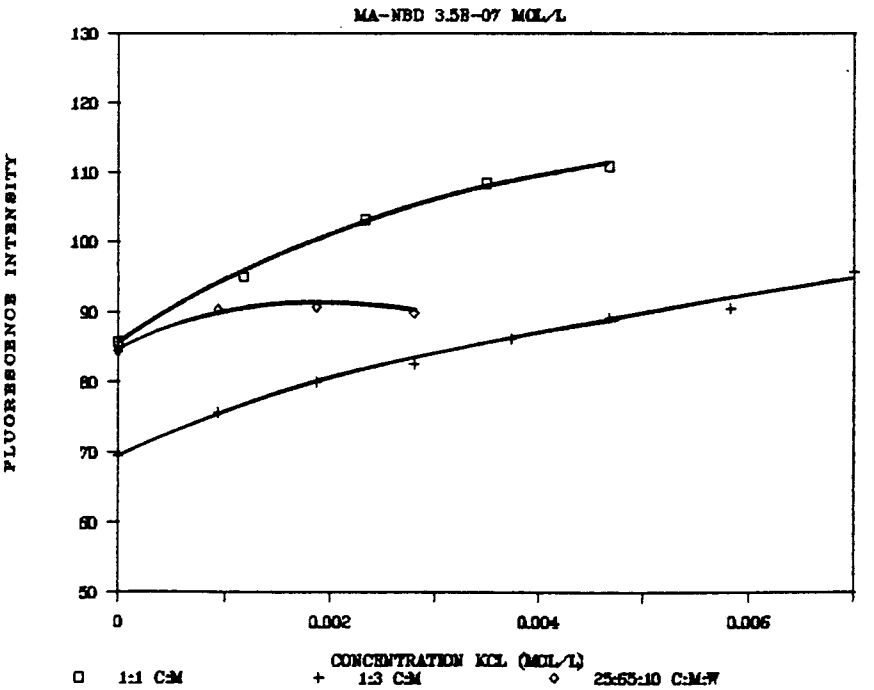

FIGURE 22. Fluorescence Intensity of MA-NBD in Three Solvent Systems with KCl.

support for the assumption that it is the Na^+, K^+ and other metal cations that are responsible for the change in fluorescence intensity - and not the presence of the SCN^- anion. (It would have been interesting to see the effect of AgSCN on the MA-NBD system since the silver perchlorate and nitrate salts had a large effect on the fluorescence and the thiocyanate anion appears to improve the solubility of the Na^+ and K^+ salts. Furthermore, the presence of the SCN^- anion seems to produce less change in the fluorescence intensity of MA-NBD than the other metals with perchlorate and nitrate anions. It was unfortunate, however, that the only AgSCN available to us was not a in the form of dry solid crystals, but somewhat moist crystals of AgSCN. As will be shown later, the presence of water adversely affects the results so that such a study of AgSCN is not available for comparison.

These studies of the change in fluorescence intensity of MA-NBD with added metal salts in 1:1 $CHCl_3$:MeOH were interesting, but not useful for analytical work, and therefore not further developed. The estimated detection limits at best, are in ppm range, and the largest determined K_f values were only about 5×10^2. Silver perchlorate produced the most promising curve and largest change in fluorescence intensity, but after the initial data was obtained, the use this metal salt in nonaqueous media was reconsidered. Because of the known explosive

tendencies of heavy metal perchlorates in organic solvents, further research with $AgClO_4$ was not pursued as high concentrations are required to attain maximum complexation. For the work reported in the previous section, higher concentrations of K-, Na-, Ca-, and Mg-perchlorates in CH_3CN were prepared, but these Group I A and II A metal perchlorates are not considered as unstable as the heavier silver compound.

Water Study

The Effect of H_2O on the Fluorescence of the Complex of $Ca(NO_3)_2 \cdot 4H_2O$ with MA-NBD in Acetonitrile: One of the main disadvantages of using either CH_3CN or the chloroform: methanol solvent systems for the studies of the effect of metal salts on the fluorescence of MA-NBD has been the poor solubility of those salts in the non-aqueous media.

As reported in the previous section concerning the results of the $CHCl_3$:MeOH solvent media, an attempt to add water to the system in order to improve the solubility of the salts like NaCl and KCl only served to decrease the fluorescence intensity of their solution with MA-NBD and diminished the sensitivity of a method already considered to have poor sensitivity. In contrast, the solubility of all of the metal salts were already greatly improved just by using acetonitrile as the solvent. For example, the metal salt providing the best enhancement of fluorescence of any salt

investigated was $Ca(NO_3)_2 \cdot 4H_2O$, and up to 0.09 mol/L was soluble in CH_3CN. A small amount of H_2O was added to a solution containing MA-NBD and $Ca(NO_3)_2 \cdot 4H_2O$ in CH_3CN in order to see if the solubility could be further improved. An unexpected and potentially useful response occurred which is described below. When the concentration of a solution of MA-NBD in CH_3CN in a medium sized test tube was large enough to observe its color, the solution was orange. When a small scoop of $Ca(NO_3)_2 \cdot 4H_2O$ crystals was added to the solution of MA-NBD the color immediately changed to an intense bright yellow. On the addition of one drop of deionized or HPLC grade H_2O to this solution, however, the color immediately reverted back to its initial orange color.

This behavior was found to be consistent and enabled the construction of a standard curve for the determination of the concentration of H_2O in acetonitrile. One of the standard curves is presented in Figure 23. The amount of water present in different brands of acetonitrile could then be determined as well as the amount in containers of leftover solvent that may have been contaminated by moisture after their initial use.

The study required the preparation of a reagent containing a fixed concentration of MA-NBD complexed with calcium nitrate, to which different standard amounts of H_2O were added and the resulting fluorescence measured. The

study focused on the determination of small concentrations of H_2O in samples of acetonitrile, therefore, the only way a change in the amount of water in the system could be detected was by ensuring that all reagent and H_2O standard solutions were prepared in the driest acetonitrile available - whether it be purchased directly from a manufacturer or prepared in the laboratory. The individual samples of acetonitrile to be tested also required the same concentrations of MA-NBD and calcium nitrate as the standards. The fixed concentration of MA-NBD must be associated with a fixed concentration of $Ca(NO_3)_2 \cdot 4H_2O$ high enough to approach the maximum complexation, and thus, the highest fluorescence intensity. The maximum allowable concentration of MA-NBD was fixed by two important factors. First, the concentration of MA-NBD in CH_3CN must not exceed 0.05 absorbance units or inner filtering of fluorescence was likely to occur. This prevented the concentration of MA-NBD from being greater than 1.9×10^{-6} mol/L based upon the results for the calculated molar absorptivity of MA-NBD in CH_3CN ($\epsilon_{484} = 2.62 \times 10^4$) presented in Table 4. Second, once maximum complexation with calcium nitrate is attained the fluorescence cannot be allowed to exceed 1000 fluorescence units, (Fixed Scale 1.00; slit settings 5 × 5 nm) based on the limits of the detector for the Perkin-Elmer LS-5. If the maximum complexation intensity was 1000, and that has been shown to be 21 times the initial fluorescence

intensity of the MA-NBD alone, the initial fluorescence of the MA-NBD solution before addition of the $Ca(NO_3)_2 \cdot 4H_2O$ could not be greater than about 47 fluorescence units; this corresponded to concentrations of MA-NBD less than 7.5×10^{-7} mol/L. (These values are based on the sensitivity of the Perkin-Elmer LS-5 spectrofluorometer during that period of time, as discussed and compared to initial data presented in Table 8 for MA-NBD in CH_3CN.)

The entire H_2O in acetonitrile study became an elaborate set of stringent preparations established in order to prevent contamination of the system by outside sources of moisture, e.g., humidity. The procedure - which was performed twice - is described in detail in the experimental section. The conditions of both of the studies were seriously affected by the excessive humidity present in the atmosphere at the time. The relative humidity of the laboratory was 85 % for the first study and 63 % for the follow-up study. This seasonal problem was also compounded by the close proximity of the chemistry department to Lake Michigan. The results for the fluorescence intensity of the MA-NBD/$Ca(NO_3)_2 \cdot 4H_2O$ standards with increasing percent of H_2O in CH_3CN are presented in Tables 36 and 37. The plot of the data from Table 37 is shown in Figure 23.

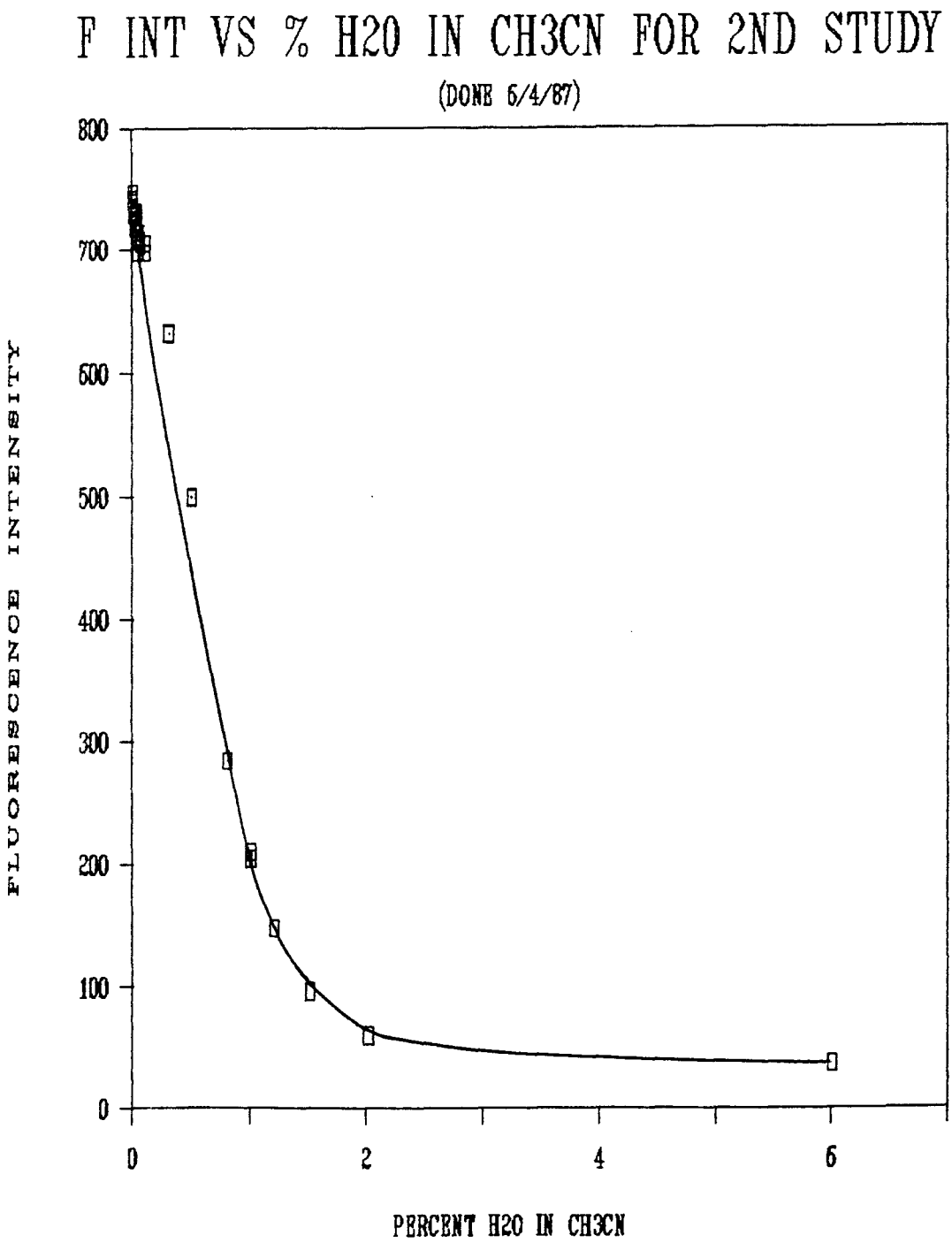

FIGURE 23. Calibration Curve for Percent H_2O in CH_3CN.

Table 36: Fluorescence Intensity vs % H_2O in Dry CH_3CN Standards for Calibration Curve for First H2O Study - (Done 7/21/86)

Std. #	Preparation of H_2O Std	Added Vol H_2O	Adjusted % H_2O*	F Int Soln	Max. F Int (nm)
1	No Added H_2O	0.000	0.047	705.0	527
2	No Added H_2O	0.000	0.047	694.7	527
3	0.020 mL 10% H_2O	0.002	0.057	679.2	527
4	0.060 mL 10% H_2O	0.006	0.077	670.9	527
5	0.120 mL 10% H_2O	0.012	0.107	641.7	527
6	0.200 mL 10% H_2O	0.020	0.147	641.7	527
7	0.600 mL 10% H_2O	0.060	0.347	506.0	527
8	1.000 mL 10% H_2O	0.100	0.547	382.7	527
9	0.160 mL 100% H_2O	0.160	0.847	218.9	529
10	0.200 mL 100% H_2O	0.200	1.047	162.5	529
11	0.240 mL 100% H_2O	0.240	1.247	120.4	530
12	0.300 mL 100% H_2O	0.300	1.547	76.5	535
13	0.400 mL 100% H_2O	0.400	2.047	51.6	535
14	1.200 mL 100% H_2O	1.200	6.047	35.8	537

Concentration MA-NBD - 6.33×10^{-7} mol/L
Concentration $Ca(NO_3)_2 \cdot 4H_2O$ - 3.94×10^{-4} mol/L

* (The % H_2O listed for each prepared standard has been adjusted for the 0.047 % H_2O in the stock CH_3CN used: Fisher HPLC grade Distilled from CaH_2 7/86, and for the 20 mL total volume for each standard.)

Table 37: Fluorescence Intensity vs % H_2O in Dry CH_3CN Standards for Calibration Curve for 2nd H2O Study - (Done 6/4/87)

Std. #	Preparation of H_2O Std	Added Vol H_2O	Adjusted % H_2O*	F Int Soln	Max. F Int (nm)
1	No Added H_2O	0.000	0.010	739.4	527
2	No Added H_2O	0.000	0.010	735.9	527
3	No Added H_2O	0.000	0.010	739.6	527
4	No Added H_2O	0.000	0.010	742.6	527
5	No Added H_2O	0.000	0.010	747.3	527
6	0.020 mL 10% H_2O	0.002	0.020	730.5	527
7	1.000 mL 0.4% H_2O	0.004	0.030	724.3	527
8	1.000 mL 0.4% H_2O	0.004	0.030	719.2	527
9	0.060 mL 10% H_2O	0.006	0.040	731.7	527
10	0.060 mL 10% H_2O	0.006	0.040	723.1	527
11	2.000 mL 0.4% H_2O	0.008	0.050	709.0	527
12	2.000 mL 0.4% H_2O	0.008	0.050	715.0	527
13	2.000 mL 0.4% H_2O	0.008	0.050	697.0	527
14	0.120 mL 10% H_2O	0.012	0.070	705.5	527
15	0.120 mL 10% H_2O	0.012	0.070	707.2	527
16	0.200 mL 10% H_2O	0.020	0.110	705.4	527
17	0.200 mL 10% H_2O	0.020	0.110	697.0	527
18	0.600 mL 10% H_2O	0.060	0.310	631.7	527
19	0.600 mL 10% H_2O	0.060	0.310	631.5	527
20	1.000 mL 10% H_2O	0.100	0.510	499.9	527
21	1.000 mL 10% H_2O	0.100	0.510	499.2	527

(Table continued on the following page.)

Table 37: Fluorescence Intensity vs % H_2O in Dry CH_3CN (Cont'd) Standards for Calibration Curve for 2nd H2O Study - (Done 6/4/87)

Std. #	Preparation of H_2O Std	Added Vol H_2O	Adjusted % H_2O*	F Int Soln	Max. F Int (nm)
22	0.160 mL 100% H_2O	0.160	0.810	284.5	527
23	0.200 mL 100% H_2O	0.200	1.010	209.0	529
24	0.200 mL 100% H_2O	0.200	1.010	204.1	529
25	0.240 mL 100% H_2O	0.240	1.210	147.3	530
26	0.300 mL 100% H_2O	0.300	1.510	95.6	535
27	0.400 mL 100% H_2O	0.400	2.010	59.5	535
28	1.200 mL 100% H_2O	1.200	6.010	37.0	537

Concentration MA-NBD - 7.04×10^{-7} mol/L
Concentration $Ca(NO_3)_2 \cdot 4H_2O$ - 7.72×10^{-4} mol/L

* (The % H_2O listed for each prepared standard has been adjusted for the 0.010 % H_2O in the stock CH_3CN used: Burdick & Jackson UV Grade Distilled in Glass Lot AP438, and for the 20 mL total volume for each standard.)

The fixed concentration of MA-NBD in all standards and samples for the first study was 6.33×10^{-7} mol/L and that of $Ca(NO_3)_2 \cdot 4H_2O$ was 3.94×10^{-4} mol/L prepared in previously purified and dried CH_3CN. This constitutes a concentration ratio of $[Ca^{2+}]/[MA\text{-}NBD]$ of 622, not high enough to ensure maximum complexation but enough to produce 90 % of the maximum fluorescence intensity for the complex. When the second study was performed, similar concentrations were used with 7.04×10^{-7} mol/L MA-NBD complexed with 7.72×10^{-4} mol/L $Ca(NO_3)_2 \cdot 4H_2O$ in dry CH_3CN. On this occasion the ratio of the $[Ca^{2+}]/[MA\text{-}NBD]$ was 1100, which is enough Ca^{2+} to ensure maximum complexation.

There was some difficulty in dissolving sufficient $Ca(NO_3)_2 \cdot 4H_2O$ to attain maximum complexation with the concentration of MA-NBD present in the stock standard. The acetonitrile used for the studies had to be the driest available at the time - whether obtained through the series of distillations reported in the experimental section or purchased directly from Burdick and Jackson. When the percentage of H_2O in CH_3CN used for the preparation of the standard and stock solutions was less than 0.05 %, the solubility of the $Ca(NO_3)_2 \cdot 4H_2O$ decreased at least twenty-fold, and an hour of periodic shaking was required for complete dissolution of the salt. For the first study, one of the calcium nitrate/MA-NBD stock standards was prepared the night before the actual experiment, and by the

following morning a considerable amount of salt had precipitated out of solution. For subsequent preparations, the salt was not dissolved in the MA-NBD acetonitrile stock solution until immediately prior to use.

The curves obtained from plots of the data from both studies are so reproducible that they could virtually be superimposed one upon the other, and only Figure 23 is shown. The results in Table 36 for the first study show the initial maximum fluorescence intensity before addition of H_2O to be 700 and the fluorescence at the end of the study - after the curve levels off around 6 % H_2O - to be 35.8. The results in Table 37 for the second study show the initial maximum fluorescence intensity before addition of H_2O to be 741 (the average of 5 standards) and the fluorescence at the end of the study - after the curve levels off around 6 % H_2O - to be 37.0. The fluorescence intensity ratios for the maximum fluorescence intensity of the complex over the final fluorescence intensity of the complex after 6 % H_2O addition ($F_{comp}/F_{comp+H2O}$) are 19.7 and 20.0, respectively. These two values are in close agreement to the ratio of maximum F_{comp}/F_{MA-NBD} = 21 consistently produced for the standard ratio for maximum complexation of $Ca(NO_3)_2 \cdot 4H_2O$ with MA-NBD in acetonitrile. The last column to the right in Tables 36 and 37 is the maximum emission wavelength obtained for each standard. The initial maximum emission wavelength for the

complex of MA-NBD and calcium nitrate is 527 nm. Each successively larger addition of H_2O continues to sharply decrease the fluorescence intensity, but it is not until 1.0 % H_2O is present that the wavelength starts to shift markedly. At this point the fluorescence intensity has fallen to only about 25 % of the original maximum readings for the complex. All further increases in the concentration of water continue to shift the falling emission maximum farther to the red until the final fluorescence intensity is only 36-37 at a λ_{max} of 537 nm. This emission intensity and wavelength are equal to the values observed for the same concentration of MA-NBD (about 7×10^{-7} mol/L) before complexation - in the absence of calcium nitrate - in spectral grade CH_3CN. All of these results are significant and lean towards an explanation that the H_2O added to the system is not just quenching the fluorescence intensity - but that the H_2O actually prevents the MA-NBD:$Ca(NO_3)_2 \cdot 4H_2O$ complex from forming or destroys the complex after it has already formed - and that competitive equilibria are the driving force for this determination.

The results of the CH_3CN samples tested in both studies are presented in Tables 38 and 39 and include the individual fluorescence intensities of the samples that were prepared in triplicate and the calculated average percent of water in each sample.

Table 38: Fluorescence Intensity and Calculated % H_2O of Acetonitrile Samples for 1st H_2O Study-(7/21/86)

Sample Tested	F Int	Avg F Int	Calc Avg % H_2O
1) Distilled CH_3CN (Prep.10/85)			
#1	537.9	542.7	0.354
#2	545.2		
#3	545.0		
2) Fisher HPLC Grade 860661 (Open 6/86)			
#1	569.1	574.2	0.294
#2	574.3		
#3	579.2		
3) Aldrich Gold Label 15,460-1 (Open 2/26/86)			
#1	661.2	667.7	0.109
#2	667.3		
#3	674.5		
4) B & J CH_3CN UV Grade AM814 (Open 2/26/86)			
#1	653.6	670.2	0.104
#2	677.8		
#3	679.1		

(Table continued on following page.)

Table 38: Fluorescence Intensity and Calculated % H_2O of Acetonitrile Samples for 1st H_2O Study-(7/21/86)

Sample Tested	F Int	Avg F Int	Calc Avg % H_2O
5) Eastman 488 - K 7 (Open - Date Unk. Min. 2 Years)			
#1	629.7	632.1	0.176
#2	634.5		
#3	---		
6) Aldrich Gold Label 5319EE (Open 7/86)			
#1	660.8	663.5	0.116
#2	660.5		
#3	669.1		

Table 39: Fluorescence Intensity and Calculated % H_2O of Acetonitrile Samples for 2nd H_2O Study - (6/4/87)

Sample Tested	F Int	Avg F Int	Calc Avg % H_2O
1) B & J CH_3CN UV Grade AP438 (Open 3/10/87)			
#1	729.1	717.9	0.071
#2	718.8		
#3	705.7		
2) Aldrich Sure-Seal 00318 LP (Open 3/10/87)			
#1	699.0	695.9	0.136
#2	697.6		
#3	691.2		
3) Distilled CH_3CN (Prep. 7/86)			
#1	754.2	726.1	0.046
#2	719.9		
#3	704.2		
4) Aldrich Gold Label 5319EE (Open 6/2/87)			
#1	667.8	670.5	0.213
#2	674.2		
#3	669.6		

(Table continued on following page.)

Table 39: Fluorescence Intensity and Calculated % H_2O of Acetonitrile Samples for 2nd H_2O Study - (6/4/87) (cont'd)

Sample Tested	F Int	Avg F Int	Calc Avg % H_2O
5) Aldrich Gold Label 5319EE (Open 7/86)			
#1	690.8	683.4	0.174
#2	683.7		
#3	675.8		
6) Eastman 488 - K 7 (Open - Date Unk. Min. 2 Years)			
#1	655.5	651.8	0.269
#2	650.2		
#3	649.6		
7) Fisher HPLC Grade 853136 (Open 6/86)			
#1	681.8	685.5	0.168
#2	690.4		
#3	684.4		
8) B & J CH_3CN UV Grade - AM814 (Open 2/26/86)			
#1	678.2	669.0	0.217
#2	673.1		
#3	655.3		

The percent H_2O was obtained using linear regression analysis and the calculations shown at the end of the experimental section. The fluorescence intensities of all the samples fell within the upper linear range of the standard curves so that such calculations apply. The fluorescence results for individual samples are quite consistent across both sets of studies.

The two common methods for the determination of small amounts of water in organic solvents are either Karl Fischer titration or gas chromatography using a Poropak column with a thermal conductivity detector. The gas chromatography method was used as a backup method of analysis for the first study and a modified Karl Fischer titration was performed on the samples from the second study. When the first MA-NBD/$Ca(NO_3)_2 \cdot 4H_2O$ in CH_3CN fluorescence study was completed, the remainder of the six acetonitrile samples and the dried CH_3CN that was used to prepare all standards and reagent solutions were sent to the Witco Chemical Corporation to be analyzed by the gas chromatographic method. In addition to the above leftover samples, six small vials containing a few milliliters taken earlier from each of the same samples were also sent. (The CH_3CN in these small vials was obtained at the same time the larger sample bottles had been filled from their original containers before the study was performed.) Unfortunately, Witco's laboratory could not analyze the samples

until one month after the fluorescence study. The samples had not been stored in a desiccator, and therefore were sitting around for four extremely humid weeks before analysis. The results from Witco's analysis are compared to those obtained by the fluorescence method in Table 40. Witco's results for percent H_2O in the leftover CH_3CN samples in the original bottles tested - marked "A" samples- are generally somewhat higher than our % H_2O values. An exceptionally large difference is shown for the first sample labelled 'CH_3CN - distilled 10/85'. (This sample was from another batch of previously purified and dried acetonitrile distilled eight months earlier - not the same dry solvent used for the study reagent preparations.) The H_2O content determined by Witco was 0.710 %. This was twice the amount - 0.354 % - reported by our fluorescence method. Four out of six of Witco's reported results for the previously unopened small vials, marked "B" samples, are significantly lower than their "A" sample results. These "B" sample results also do not correlate with our calculated percent H_2O values. In contrast, the dried CH_3CN used to prepare the standards and reagent solutions was reported by Witco as having the lowest concentration of H_2O - 0.047 %- a result we expected. All the remaining 200-300 mL of this solvent had been sent in the same gallon bottle - under dry nitrogen and argon - and with the septum cap tightly replaced. Thus, it was probably the best protected of all

Table 40: Results of 1st H_2O Study - Comparison of Calculated % H_2O in CH_3CN Samples to GC Method- (Done by Witco 8/21/86 - One Month after Fluorescence Method for 1st H_2O Study, 7/21/86)

CH_3CN Sample		Calc. % H_2O	GC Results A (Bottles)	GC Results B (Vials)
CH_3CN -	# 1	0.361	0.710	0.091
DIST. 10/85	# 2	0.349		
	# 3	0.349		
	Avg:	0.354		
FISHER HPLC GRADE				
Lot 860661				
Open 6/86	# 1	0.301	0.359	0.087
	# 2	0.294		
	# 3	0.297		
	Avg:	0.294		
ALDRICH GOLD LABEL				
Lot 5319EE				
Open 2/86	# 1	0.119	0.096	0.150
	# 2	0.109		
	# 3	0.092		
	Avg:	0.109		
BURDICK & JACKSON				
Lot AM814				
Open 2/86	# 1	0.135	0.202	0.067
	# 2	0.085		
	# 3	0.085		
	Avg:	0.104		
EASTMAN 488				
Lot K 7	# 1	0.181	0.190	0.242
(Unk. date)	# 2	0.171		
	Avg:	0.176		
ALDRICH GOLD LABEL				
Lot 5319EE				
Open 7/86	# 1	0.119	0.238	0.088
	# 2	0.123		
	# 3	0.104		
	Avg:	0.116		

Table 41: Comparison of GC Method to Karl Fischer Method for Determination of H_2O in CH3CN before 2nd H_2O Study, 1987.

CH_3CN Tested	% H2O By GC Method	% H2O By Karl Fischer Method
BURDICK & JACKSON UV Lot AP 438	0.006 - 0.007	0.0087
CH_3CN (Distilled from CaH_2 - 7/86)	0.060	0.0608
CH_3CN Standard 1	0.695	0.7130
CH_3CN Standard 2	0.182	0.1930

the samples from atmospheric moisture.

By the time the second water study was to be performed, a number of factors were reconsidered in the protocol based on the first H_2O study. From the first study it was obvious that too much time had lapsed between the outside analysis and the fluorescence analysis. We also had no quality control over what actually happened to the samples once they were sent to another site - or the laboratory preparations used there. It was therefore decided that the gas chromatographic determination of H_2O in the samples would also be performed "in house" immediately after the fluorescence study was completed.

The preparations for the second study began during late winter when the humidity was extremely low. The driest acetonitrile eventually used to prepare all stock and standard solutions for the second study was determined to be a fresh gallon of Burdick and Jackson UV grade acetonitrile, Lot AP 438. (Burdick and Jackson CH_3CN lists its solvent purity specifications, and % H_2O is always < 0.02 % by Karl Fischer titration.) On recommendations from a representative of the company we purchased a gallon of CH_3CN from one of the lots manufactured during the winter months when humidity in the plant was lowest. Such lots often contained less than 0.003 % H_2O, (or 30 ppm). After extensive preliminary testing of several sources of acetonitrile by our gas chromatography system, B & J Lot AP 438

was found to contain the lowest amount of water at 0.005 % H_2O. This was somewhat better than the level for Aldrich Sure Seal CH_3CN, Lot 00318 LP at 0.013 % H_2O. The remaining dried CH_3CN from the first study had increased its water content to 0.060 % H_2O from the earlier 0.047 % H_2O. In order to do this preliminary testing, 60 mL of each sample had been removed from their original containers and transferred to small rubber septum capped bottles via the stringent dry solvent transfer method described in the experimental section. To further validate the accuracy of our gas chromatographic analysis, four samples were tested, then sent to Witco for analysis by the Karl Fischer method. The results of those four samples tested, presented in Table 41, indicate both methods give comparable results. Immediately after these were obtained, however, the Sigma 3B thermal conductivity detector (TCD) overheated and produced no signal other than noise. Subsequent repairs made on the TCD by Perkin Elmer restored only limited sensitivity with continued noise in the signal.

The fluorescence results for the standard H_2O in CH_3CN curve are presented in Table 37 and the plot in Figure 23. The results for the individual fluorescence intensities, and the calculated average percent H_2O in each of the eight samples, are presented in Table 39. The triplicate fluorescence intensity results for most of the eight samples show reproducibility except for Samples 1, 3, and 8 that

produced large variations in their intensity measurements. The most significant common factor for the magnitude of relative deviations in the analysis is that samples producing very high fluorescence intensities and therefore the lowest % H_2O, (such as Samples 1 and 3), have the poorest precision. The experimental section explains in detail how the test tubes containing the samples were handled up through the time they were opened, and the solution immediately measured in a dried quartz fluorescence cuvette. The fluorescence signal was integrated every 15 seconds for two minutes and then scanned twice followed by one more integration. A decrease in the fluorescence intensity was observed, to some extent, for all the samples between the first and last integrations. After two minutes, most of the readings leveled off for the samples. The samples determined to contain the highest H_2O content began with the lower initial fluorescence intensities and a much smaller drop in successive readings was observed. Samples determined to contain the lowest H_2O content had extremely high initial fluorescence readings, however, that dropped rapidly - even before the integration mode could be activated - and continued to fall significantly for the first minute. The two trials with highest initial readings for Sample 3) "CH_3CN - distilled 7/86", fell from a fluorescence of 754 to 709 - and from 720 to 696 - within 1 minute. In contrast, Sample 2) "Aldrich Sure Seal", that

was determined to have a higher % H_2O content by the fluorescence method, started with fluorescence intensities of 699 that only fell to 694 in 1 minute. This same phenomenon was also observed with the standards. Therefore, the first (and highest) fluorescence readings obtained after the first integration were reported, rather than the readings that leveled off after 1 or more minutes had passed. This behavior caused those samples that contained the lowest % H_2O to have large variations from one trial to the next. Even though great effort was expended to treat every test tube sample the same way- those first seconds were crucial for those samples that had the lowest water content - and moisture was rapidly absorbed from the air and the cuvette walls.

Once the fluorescence study was completed, the gas chromatographic method was employed on the remaining CH_3CN samples after removal from the glove box. The sample containers had been recapped tightly as possible, and their necks wrapped in parafilm. Most had wired-on rubber septum caps from when they were initially extracted from their original containers by the dry solvent transfer method. Therefore, the samples were easily withdrawn with a small G.C. syringe while the bulk of the remaining solution was protected from further exposure to moisture. The small containers and flasks containing the eight acetonitrile samples were also placed into desiccators with drierite.

Table 42: Results of H_2O in Acetonitrile from 2nd Study: Fluorescence Results vs. Gas Chromatography After Partial Repairs to TCD.

	% H_2O Fluorescence	% H_2O G.C. Results
Sample 1) Burdick & Jackson - AP 438 Small 60 mL bottle removed from original container 3/10/87	0.071	0.033
Sample 2) Aldrich Sure Seal 00318 LP	0.136	0.021
Sample 3) Distilled CH_3CN Prepared 7/86	0.046	0.072
Sample 4) Aldrich Gold Label 5319 EE Open 6/2/87	0.213	0.136
Sample 5) Aldrich Gold Label 5319 EE Open 7/86	0.174	0.072
Sample 6) Eastman - K 7 Open date Unknown	0.269	0.152
Sample 7) Fisher - 853136 Open 6/86	0.168	0.057
Sample 8) Burdick & Jackson - AM814 Open 2/26/86	0.217	---
Burdick & Jackson - AP 438 Remaining solvent used to Prepare all Standards & Reagents	---	0.009

Table 43: Results of H_2O in Acetonitrile from 2nd Study: Fluorescence Results vs. Karl Fischer Results from Phoenix Chemical.

	% H_2O Fluorescence	% H_2O Karl Fischer
Sample 1) Burdick & Jackson - AP 438 Small 60 mL bottle removed from original container 3/10/87	0.071	0.011
Sample 2) Aldrich Sure Seal 00318 LP	0.136	0.040
Sample 3) Distilled CH_3CN Prepared 7/86	0.046	0.088
Sample 4) Aldrich Gold Label 5319 EE Open 6/2/87	0.213	0.152
Sample 5) Aldrich Gold Label 5319 EE Open 7/86	0.174	0.071
Sample 6) Eastman - K 7 Open date Unknown	0.269	0.182
Sample 7) Fisher - 853136 Open 6/86	0.168	0.112
Sample 8) Burdick & Jackson - AM814 Open 2/26/86	0.217	0.136
Burdick & Jackson - AP 438 Remaining solvent used to Prepare all Standards & Reagents	---	0.010
Aldrich Sure Seal 00318 LP Removed from original container After Water Study	---	0.017

Those expected to have the lowest water content were placed in a glass desiccator whose lid formed a tight seal, the remaining samples had to be placed into large nalgene desiccators that had less tightly fitting covers. No follow up analysis was proposed nor performed on the prepared samples in the test tubes with added MA-NBD/$Ca(NO_3)_2 \cdot 4H_2O$ reagent. These had already been exposed to the atmosphere when opened for fluorescence measurement. The backup gas chromatographic results, (taken as the averages of two or three injections), are reported with the fluorescence results in Table 42. Because the TCD had never been restored to its original sensitivity, and the baseline was often extremely noisy, the TCD results obtained were not trusted at the time.

About two weeks later, the samples were sent to Phoenix Chemical Laboratory, Inc. 3953 Shakespeare Avenue, Chicago, IL 60647, for analysis by Karl Fischer titration. Only 10 samples could be sent. They were delivered in their storage desiccators and their analysis was performed 18 days after the initial fluorescence study. The results were reported as ppm H_2O in CH_3CN and Table 43 lists those samples converted to percent H_2O (1 ppm = 0.0001 %) along with the fluorescence results. The fluorescence method results for the determination of % H_2O (with one notable exception for Sample 3) are all higher than the Karl Fischer results by an average of 0.078 ± 0.018 % .

A comparison of the results reported in Table 42 and Table 43, reveals that the results for % H_2O in the CH_3CN samples by G.C. - performed "in house" shortly after the fluorescence study - are similar to those obtained later by Phoenix Chemical. Most of the Karl Fischer titration results have slightly higher reported H_2O content than the gas chromatographic results, which is not unexpected as they were done two weeks apart.

The second fluorescence water study used more elaborate precautions to prevent contamination due to moisture in the atmosphere than had been used for the first study. Most of the percent H_2O results obtained by the fluorescence method are, therefore, perhaps lower than the first study results. The exceptions to this are for two samples (Eastman, and Burdick and Jackson AM 814) that were analyzed on both occasions. Their percent H_2O content was observed to have increased by approximately 0.10 % between the first and second study.

Some further discussion is warranted concerning the data presented in Table 43 and the lack of agreement seen between the fluorescence results and the Karl Fischer results for certain samples; notably Sample 2) Aldrich Sure Seal and Sample 3) the CH_3CN - distilled 7/86. The lowest percent H_2O determined by the fluorescence method was 0.046% - obtained for Sample 3) previously dried and distilled CH_3CN leftover from 7/86. The second lowest

percent H_2O according to the fluorescence method was 0.071% - obtained for Sample 1) 60 mL previously removed from the Burdick & Jackson AP 438 solvent that had been used for all standard and reagent preparations. According to the Karl Fischer method, the lowest percent H_2O was 0.010 % - also for the remaining Burdick & Jackson AP 438, and 0.011% - for Sample 1) containing the 60 mL removed also from the same B & J AP438. These results, however, were followed by 0.040 % H_2O for Sample 2) Aldrich Sure Seal, and 0.017 % H_2O for analysis on the remaining Aldrich Sure Seal solvent in its original container. The Burdick and Jackson AP 438 Sample 1) and remaining solvent results observed from both methods are not in agreement - but both methods report it to have the lowest % H_2O content. (It should be remembered that the five preparations of Standard #1 with no addition of H_2O can be considered as five more samples of Burdick & Jackson AP 438, and they also consistently produced the highest fluorescence corresponding to lowest water content for all of the samples. Based on the preliminary gas chromatographic studies and the Karl Fischer analysis, this solvent was considered to contain 0.010% H_2O, and all the other fluorescence results were corrected for that amount of H_2O in the added reagent.) Sample 3), the distilled CH_3CN from 7/86, provided the next lowest percent H_2O results based on the average of the next set of highest fluorescence readings. These readings were difficult to

obtain due to the rapid drop in fluorescence intensity observed after the initial extremely high readings - and the variations are apparent in Table 39 where the fluorescence results are presented for the triplicate preparations of this sample.) In comparison, Sample 2) Aldrich Sure Seal, provided more stable and lower fluorescence intensities and thus produced much larger percent H_2O (0.136%) results. The ranking of Sample 2) and Sample 3) results were reversed by the Karl Fischer method. According to analysis by Phoenix Chemical, Sample 2) Aldrich Sure Seal, produced the next lowest percent H_2O (0.040%) after Burdick & Jackson AP 438, and Sample 3) the distilled CH_3CN, was determined to contain much higher percent H_2O content (0.088%), though still favorably low.

It is possible that two competing factors are being measured by our fluorescence method. Not only does the amount of water in acetonitrile affect the fluorescence intensity but the purity of the solvents in terms of other contaminants. From all of the acetonitrile samples that were used directly from the manufacturer - our experience indicates the best two solvents for our metal salt with MA-NBD fluorescence work had been; 1) the Burdick & Jackson distilled in glass CH_3CN and; 2) the Fisher HPLC grade CH_3CN. In the solvent purification literature (89), other grades of CH_3CN, other than those made from the Sohio process, may have more impurities although they may have

provided less initial H_2O content. Aldrich Sure Seal acetonitrile is guaranteed to have less residual H_2O contamination than other grades of CH_3CN, and is recommended for organic reactions that could be very sensitive to trace water contamination. It is not, however, recommended as a spectral or fluorescence grade solvent. The distillation method used for purification and drying of acetonitrile is supposed to produce the best solvent for both spectroscopy and electroanalytical work. The remaining distilled CH_3CN from 7/86 (Sample 3) may not have been as dry as the Aldrich Sure Seal - but it was possibly the purest acetonitrile as far as other spectral impurities are concerned. The Karl Fischer titration method is specifically used for the determination of H_2O. Other impurities that might affect fluorescence intensity could be present and would not change the Karl Fischer titration results.

After completion of the study, the fluorescence blanks of all the acetonitrile samples were run at fixed scale settings of 1.00 and 5.00. The results of this experiment lend some validity to the above discussion, because the Burdick and Jackson solvents and the distilled CH_3CN from 7/86 give nearly flat baselines throughout. Fisher, followed by Eastman, produced the next best baseline, with some emission 500-535 nm occurring with the scale setting of 5.00, and all of the Aldrich samples produced the most

fluorescence emission in their blanks and Aldrich Sure Seal had the highest blank of all. Both Aldrich Gold Label samples had the same 500-535 nm emission observed for Fisher and Eastman, but in addition, had a larger new band from 540 nm increasing through 600 nm. The Aldrich Sure Seal blank had the same emission background as Aldrich Gold Label but with greater intensity. The Aldrich Sure Seal baseline never zeroed for the 5.00 scale setting, and it was the only sample to show residual emission above 570 nm - even using the fixed scale of 1.00. None of these blanks showed fluorescence at 527-540 nm for the same fixed scale setting of 1.00 used for the fluorescence study, so no blank corrections had to be made in the reported intensities. These results do show, however, that there are probably more trace impurities in the Aldrich Sure Seal and Aldrich Gold Label samples than in the others, and that Burdick and Jackson and the distilled CH_3CN appear to be free of impurities in the spectral range covered.

CONCLUSIONS

The synthesized crown structure, MA-NBD, has been found to be an effective metal sensitive fluorophore for use in nonaqueous solvents. The structure is special because the NBD fluorophore portion of the structure is directly attached to the nitrogen in the monoaza-18-crown-6 ring. When the metal cation is complexed within the crown ring of the MA-NBD, the effects are directly transferred to the fluorophore portion of the molecule. Therefore, the formation of the complex results in an enhancement of the fluorescence emission of the MA-NBD. The change in fluorescence intensity is directly related to the change in concentration of the complex formed with the metal cation as the concentration of metal salt is increased in solution. The values obtained for the formation constants of the 1:1 complexes between several metal cations and MA-NBD are not very large. They range from 1×10^2 to 6×10^4. The concentration ratios for $[M^{n+}]/[\text{MA-NBD}]$, at values greater than several thousand, were often necessary to force maximum complexation.

For the metal salts studied with MA-NBD in acetonitrile or the chloroform:methanol system, there is definitely an anion effect. In the acetonitrile system, perchlorates and nitrates produced the greatest enhancement of fluorescence intensity for the divalent metal cations.

The nitrates generally produced smaller changes in intensity than the perchlorates, except for the case of $Ca(NO_3)_2 \cdot 4H_2O$, which produced the greatest enhancement of all the metal salts studied. The alkali metal salts sodium and potassium produced weaker effects than any of the divalent metal salts, but the alkali metal perchlorates also produced a higher change in intensity than their nitrates, thiocyanates, and chlorides.

The formation constants, K_f, for all the metal salt complexes with MA-NBD are listed in Table 35 for the $CHCl_3$:MeOH system and in Table 27 for the CH_3CN system. Where the same metal cation appears in more than one salt and paired with a different anion, there is also a different value for the calculated K_f. The anion effect causes several differences in the fluorescence behavior of MA-NBD with a given metal. For the calcium nitrate tetrahydrate and the calcium perchlorate tetrahydrate salts, this anion effect is reflected by the difference in ratios of the maximum $F_{comp}/F_{MA\text{-}NBD}$ for the nitrate and perchlorate. The K_f values for the two calcium salts also differ by one order of magnitude. Similar variations are seen for the Mg^{2+} cation and its salts in CH_3CN, and for the Na^+ and K^+ cations with their salts in both the CH_3CN and $CHCl_3$:MeOH solvent systems.

The calculations used for determining the formation constant were originally presented in the experimental

section of the dissertation and involved the determination of the equilibrium concentrations of the relevant species and substituting them into the following equation:

$$K_f = [M^{n+} \cdot MA\text{-}NBD] \; / \; ([M^{n+}]\,[MA\text{-}NBD]) \qquad \text{(Eq.3)}$$

The value of the formation constant for the complex of the same metal cation and the same ligand (MA-NBD), according to the equation - should be a constant - and should not vary from salt to salt as the anion does not appear anywhere in the above equation. However, in reality, many competing equilibria occur simultaneously in solution. Several of these are shown in the equations below.

$$MX_n \overset{K_{ip}}{\rightleftharpoons} \underset{\text{Ion Pair}}{[M \text{ --- } X_n]} \overset{K_d}{\rightleftharpoons} M^{n+} + n\,X^-$$

$$M^{n+} + L \overset{K_f}{\rightleftharpoons} ML^{n+}$$

(Eq. 9)

In this equation, MX_n represents one of the metal salts with the metal cation, M^{n+}, with the anion, X^-, having a (- 1) charge; K_{ip} is the ion pair formation constant for the formation of a solvent separated ion pair [M---X_n]; K_d is the dissociation constant for the ion pair dissociating into free metal cation and anion; L is the ligand, which is MA-NBD here; K_f is the actual formation constant whose

magnitude depends only on the equilibrium concentrations of $[M^{n+}]$, [L] and complex formed $[M \cdot L^{n+}]$. An overall or total formation constant, K', is the combination of all three factors and is the actual "formation constant" that is being evaluated here. The other individual constants cannot be obtained individually through the method being used. The ion pair formation constant, K_{ip}, will vary with the anion and the solvent being used. The dissociation constant, K_d, will also vary because the extent of ion pair formation is different. The true formation constant, K_f, should not change with the anion or solvent being used, as it is still dependent only upon the equilibrium concentrations of the free metal cation, the ligand involved and the complex formed between them.

For the two magnesium perchlorate salts, anhydrous $Mg(ClO_4)_2$ and the hydrated $Mg(ClO_4)_2 \cdot 6H_2O$, major differences are seen in the steepness and changes in slope of the curves. The ratios of their maximum F_{comp}/F_{MA-NBD} are 11.0 for the anhydrous salt and only 3.0 for the hydrate. The overall formation constants reported in Table 27 for both salts do not appear to differ significantly, nor do the estimated limits of detection. The equilibria of all metal salts must also be affected by the presence or absence of any water of hydration. Anhydrous magnesium perchlorate is often recommended as a more effective desiccant than regular drierite (anhydrous $CaSO_4$). There

is a strong probability that the anhydrous $Mg(ClO_4)_2$ acts as a drying agent in the MA-NBD in acetonitrile solution which could account for its significantly higher ratio of maximum $F_{comp}/F_{MA\text{-}NBD}$ compared to the hydrated form of the salt. In consideration of the effect seen on fluorescence intensity when small amounts of H_2O are added to acetonitrile containing the complex of the already hydrated salt, $Ca(NO_3)_2 \cdot 4H_2O$ and MA-NBD, it would be interesting to follow the change in fluorescence intensity of the anhydrous magnesium perchlorate complex with MA-NBD in CH_3CN as water is added to the system.

The addition of water to solutions of MA-NBD and metal salts prevents further complexation from occurring and destroys most of the complexes already formed. It seems probable that the H_2O ligand complexes more strongly than the MA-NBD with the metal cations tested. This effect is most clearly seen in the CH_3CN medium. It enabled the construction of calibration curves for the concentration of water added to a system of MA-NBD complexed with $Ca(NO_3)_2 \cdot 4H_2O$, and the subsequent development of a method for the determination of small amounts of water in different sources of acetonitrile. The water study was performed twice and produced remarkably reproducible calibration curves for water in acetonitrile. The fluorescence results for samples prepared in triplicate were generally in close agreement, but the percent H_2O

determined by this method for the acetonitrile samples did not correlate closely with the amount of water, in those same samples, determined by the two standard methods of water determination in organic solvents, Karl Fischer titration and gas chromatography. In theory the new analytical method should work, but there are many variables inherent in the system which are difficult to control. First of all, the prevention of water contamination from the atmosphere and the equipment is extremely difficult when the laboratory has such high levels of humidity during the summer months and the only dry zone is a regular sized glove box. Secondly, even if the sample, standard, and reagent preparations successfully avoid contamination from outside moisture, use of an open quartz cuvette allows enough time for water to be absorbed even when the cuvette is capped. Residual water probably adheres to the quartz walls even when the cuvette is considered dry. The use of a flow injection system where all solutions are transferred through syringes or a series of valves, pumps, and teflon tubing would assure that no atmospheric moisture could come into contact with the solutions whose fluorescence is to be measured. Even if these conditions are successfully controlled, the fact remains that different samples of acetonitrile possess different inherent impurities along with the traces of water to be determined. Both of these contribute additive factors that can cause measurable

changes in fluorescence intensity. Although water is recognized as the primary source of any decreasing fluorescence intensity, the other impurities can have a marked effect on the system.

SPECTRA

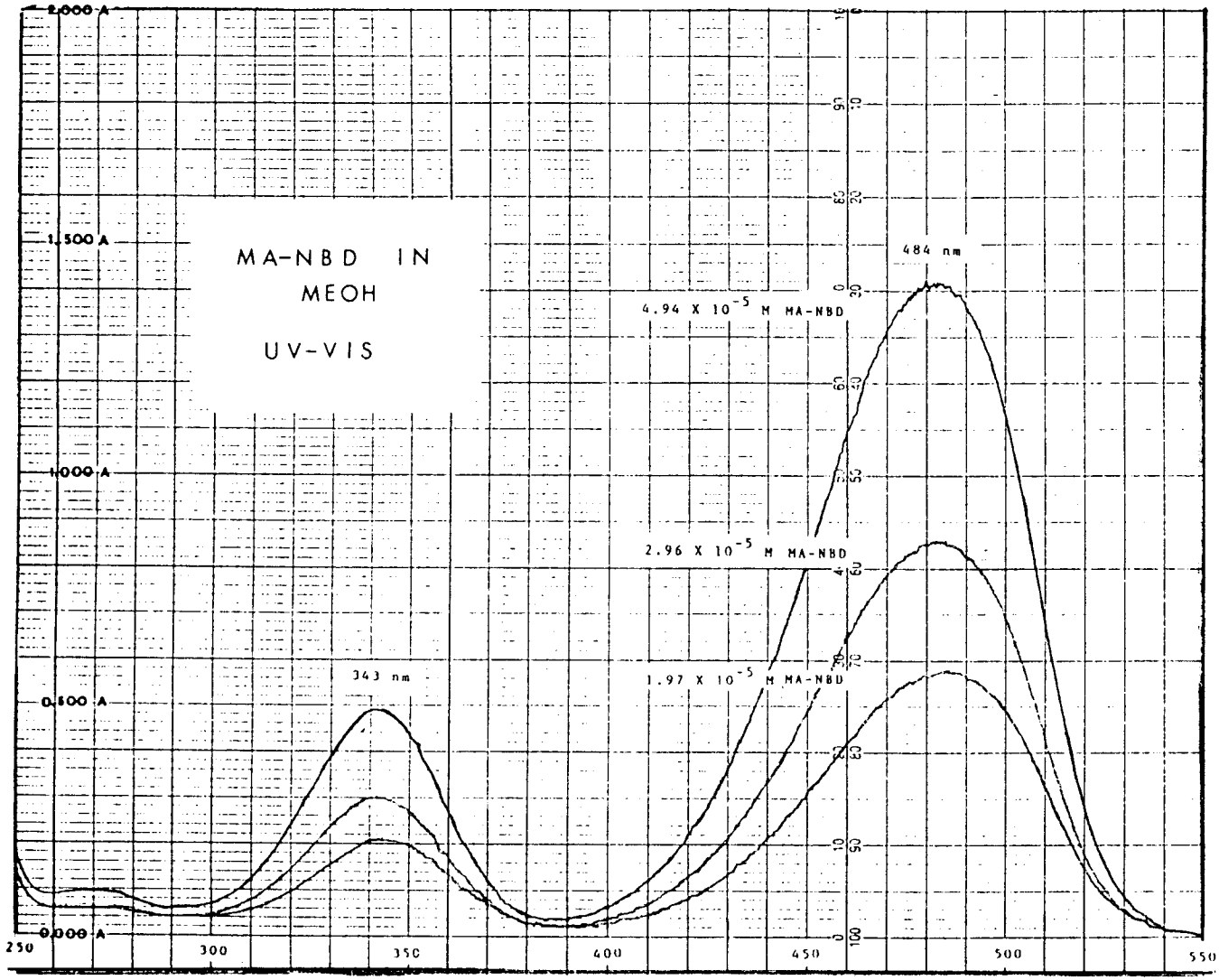
MA-NBD IN
MEOH
UV-VIS
2.000 A
1.500 A
1.000 A
0.500 A
0.000 A
250
300
350
400
450
500
550
343 nm
484 nm
4.94 X 10^-5 M MA-NBD
2.96 X 10^-5 M MA-NBD
1.97 X 10^-5 M MA-NBD

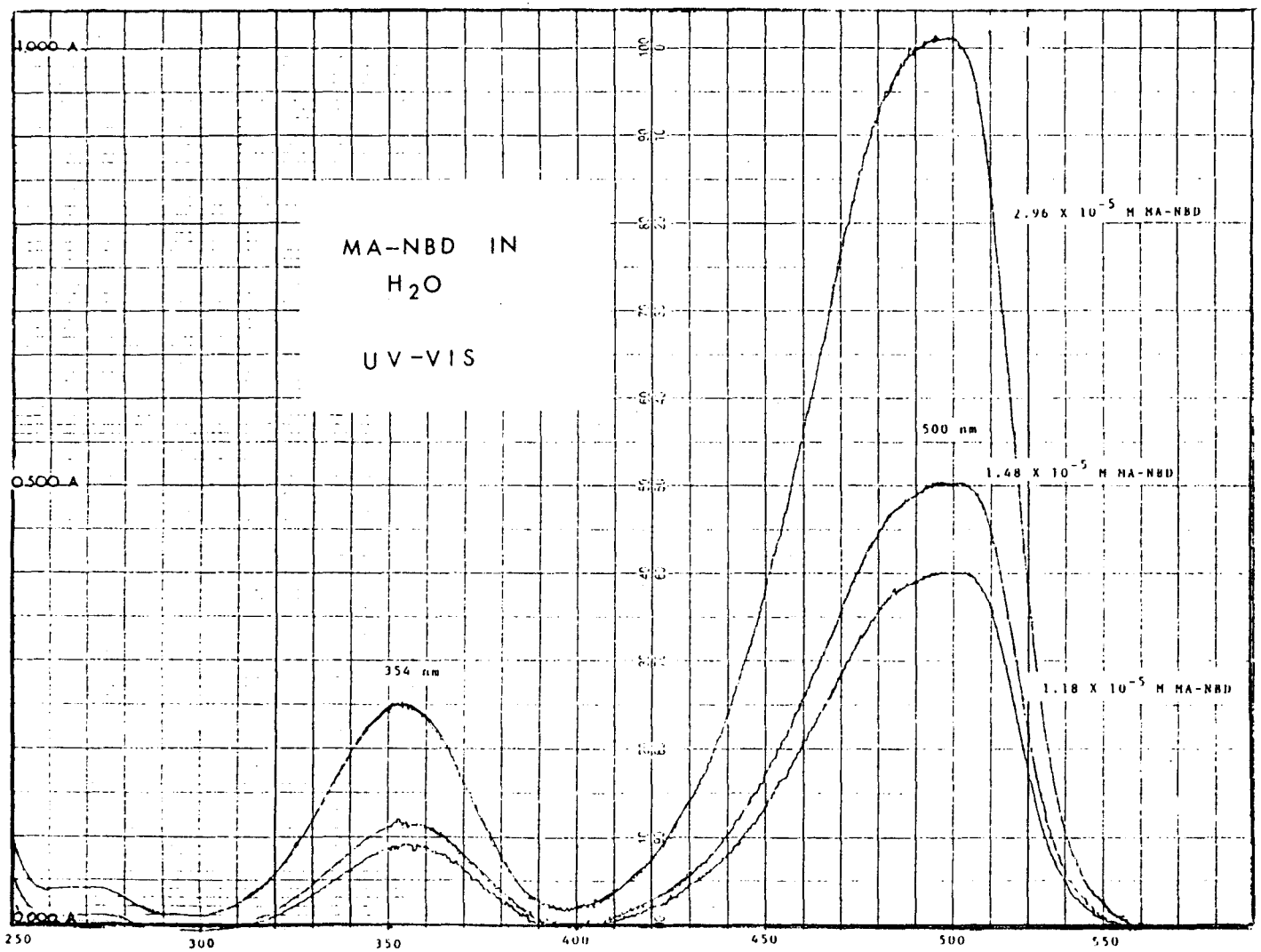
MA-NBD IN
H_2O
UV-VIS
1.000 A
0.500 A
0.000 A
354 nm
500 nm
2.96 X 10^{-5} M MA-NBD
1.48 X 10^{-5} M MA-NBD
1.18 X 10^{-5} M MA-NBD
250
300
350
400
450
500
550

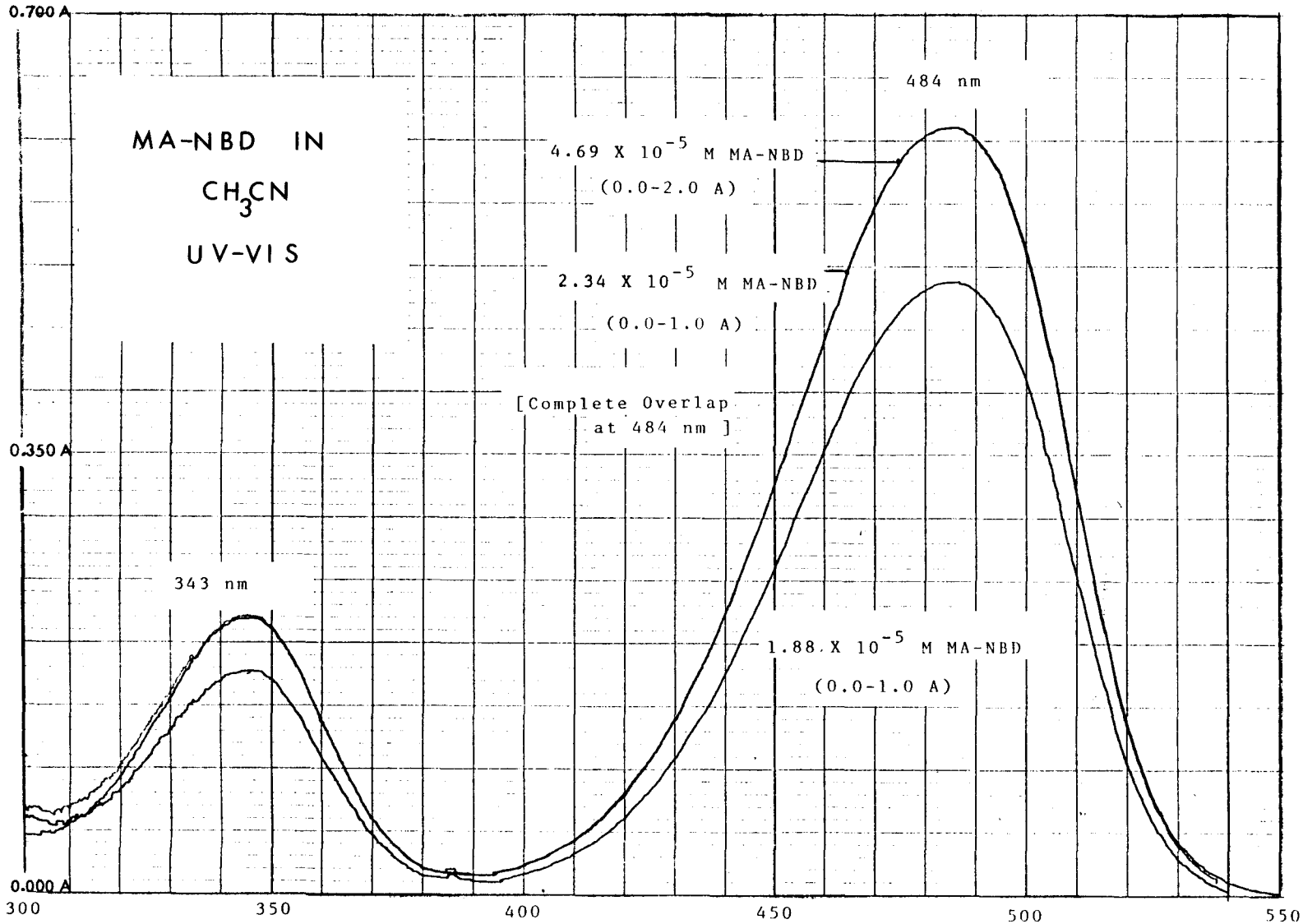
0.700 A
0.350 A
0.000 A
MA-NBD IN
CH3CN
UV-VIS
484 nm
4.69 X 10-5 M MA-NBD
(0.0-2.0 A)
2.34 X 10-5 M MA-NBD
(0.0-1.0 A)
[Complete Overlap
at 484 nm]
343 nm
1.88 X 10-5 M MA-NBD
(0.0-1.0 A)
300
350
400
450
500
550

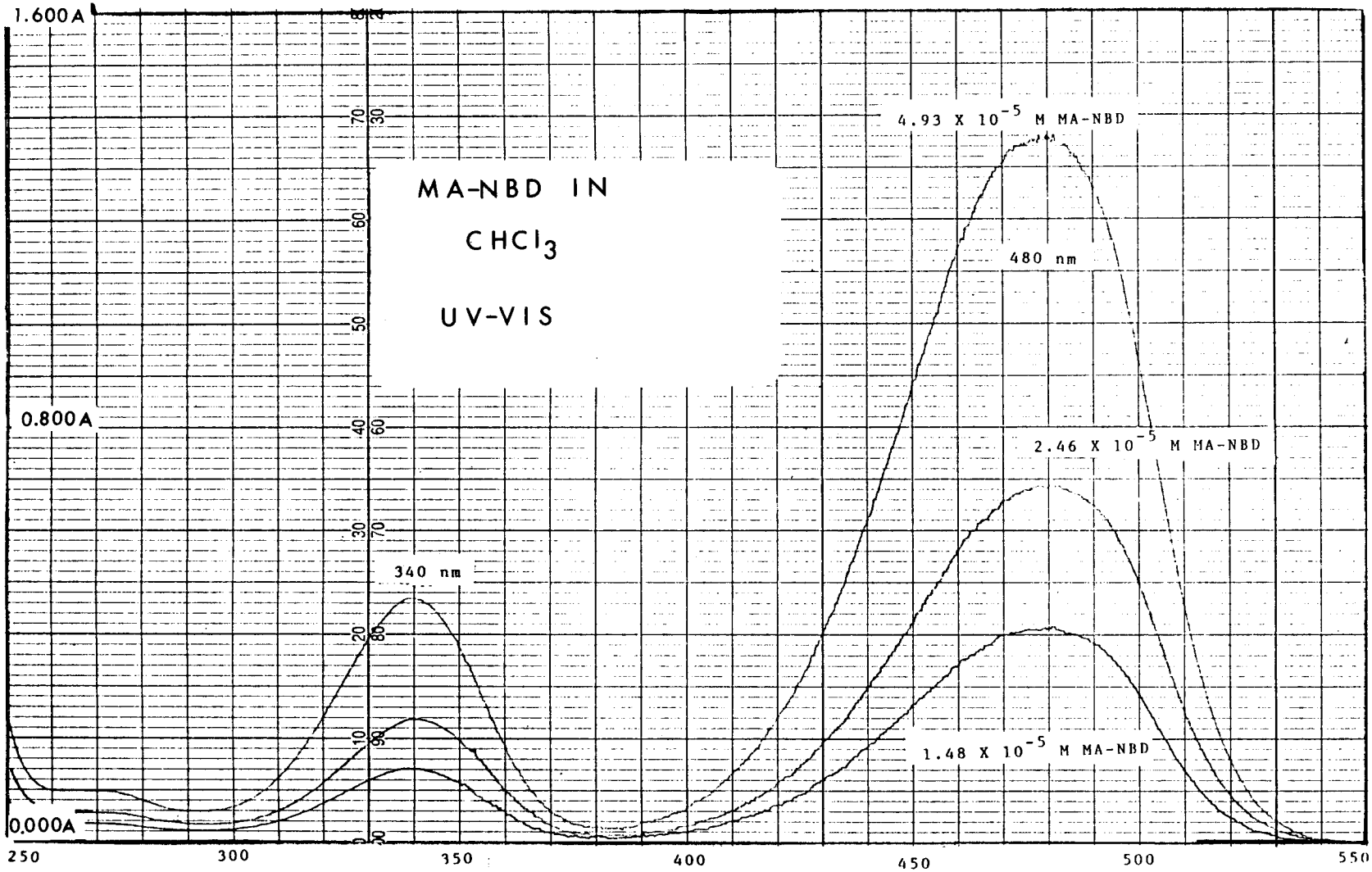
1.600A
0.800A
0.000A
MA-NBD IN
CHCl3
UV-VIS
4.93 X 10-5 M MA-NBD
480 nm
2.46 X 10-5 M MA-NBD
340 nm
1.48 X 10-5 M MA-NBD
250
300
350
400
450
500
550

MA-NBD in MeOH

Excitation and Emission Spectra

P.E. LS-5 Spectrofluorometer

Response: 2
Slits: 5 X 5 nm
Scan Speed: 120 nm/min

Excitation Scan: 540 nm emission fix.
320 - 520 exc.
Fixed Scale: 1.5 X

Emission Scan : 475 nm excitation fix.
500 - 600 nm emission
Fixed Scale: 1.5 X

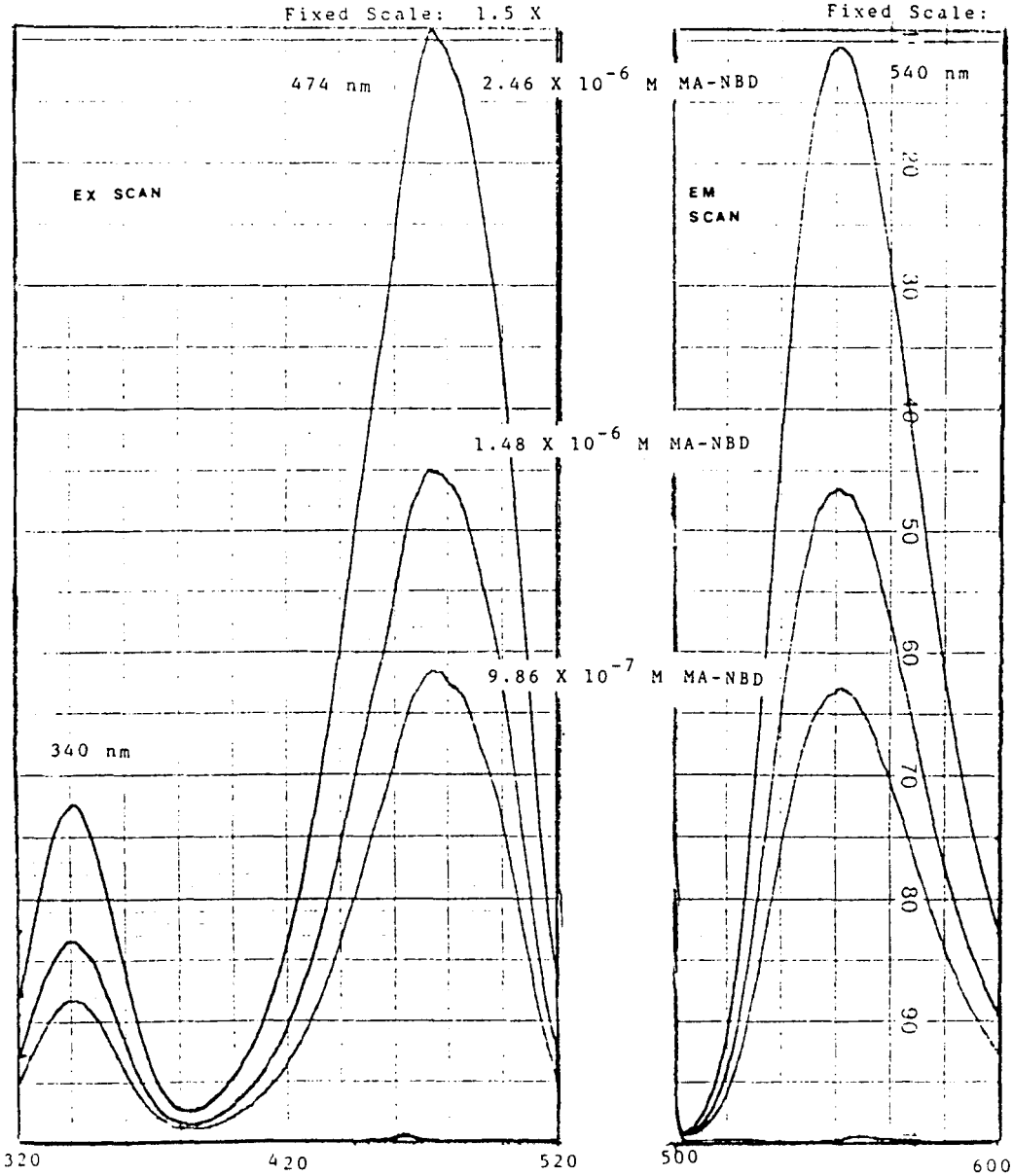

MA-NBD in H_2O

Excitation and Emission Spectra

P.E. LS-5 Spectrofluorometer
Response: 2
Slits: 5 X 5 nm
Scan Speed: 120 nm/min

Excitation Scan: 540 nm emission fix.
320 -520 exc.
Fixed Scale: 2.0 X

Emission Scan:
470 nm excitation fix
500 - 600 nm emssion
Fixed Scale: 2.0 X

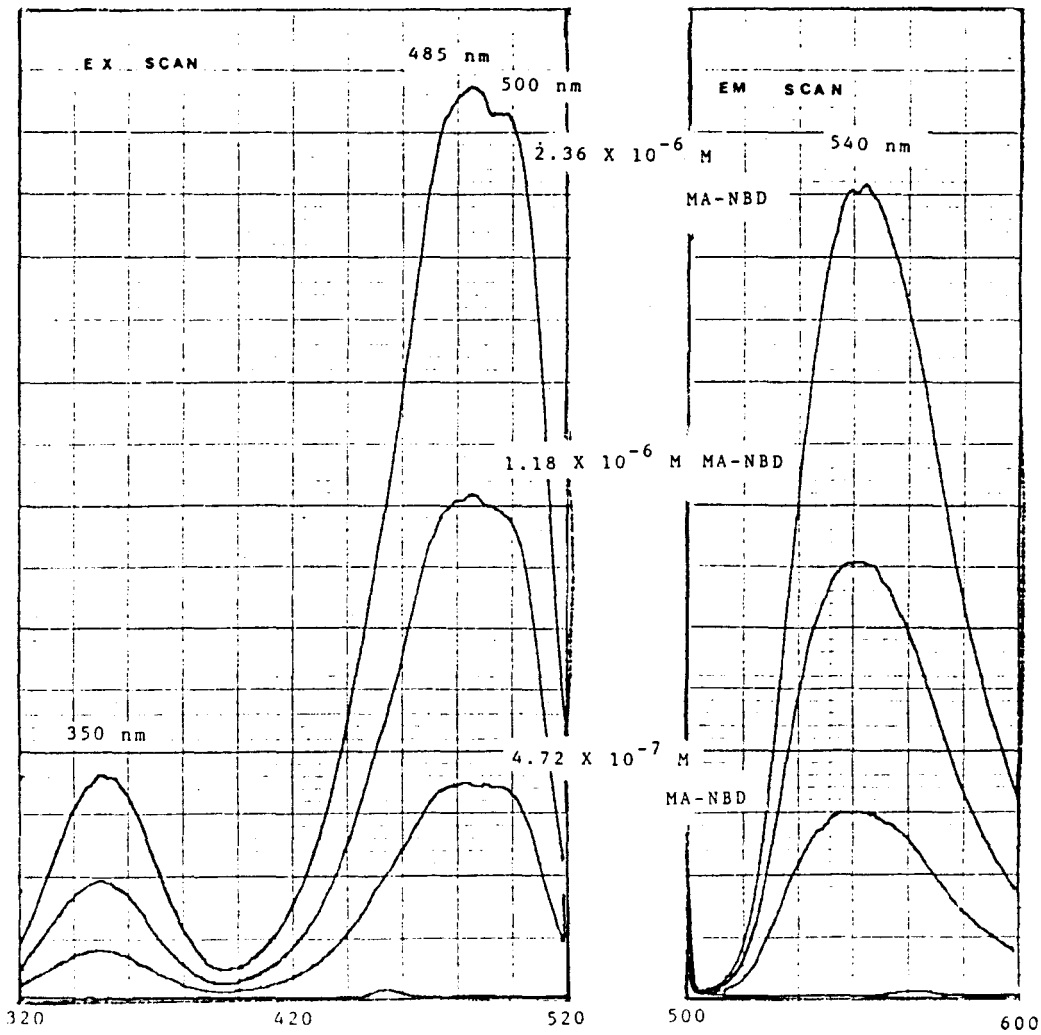

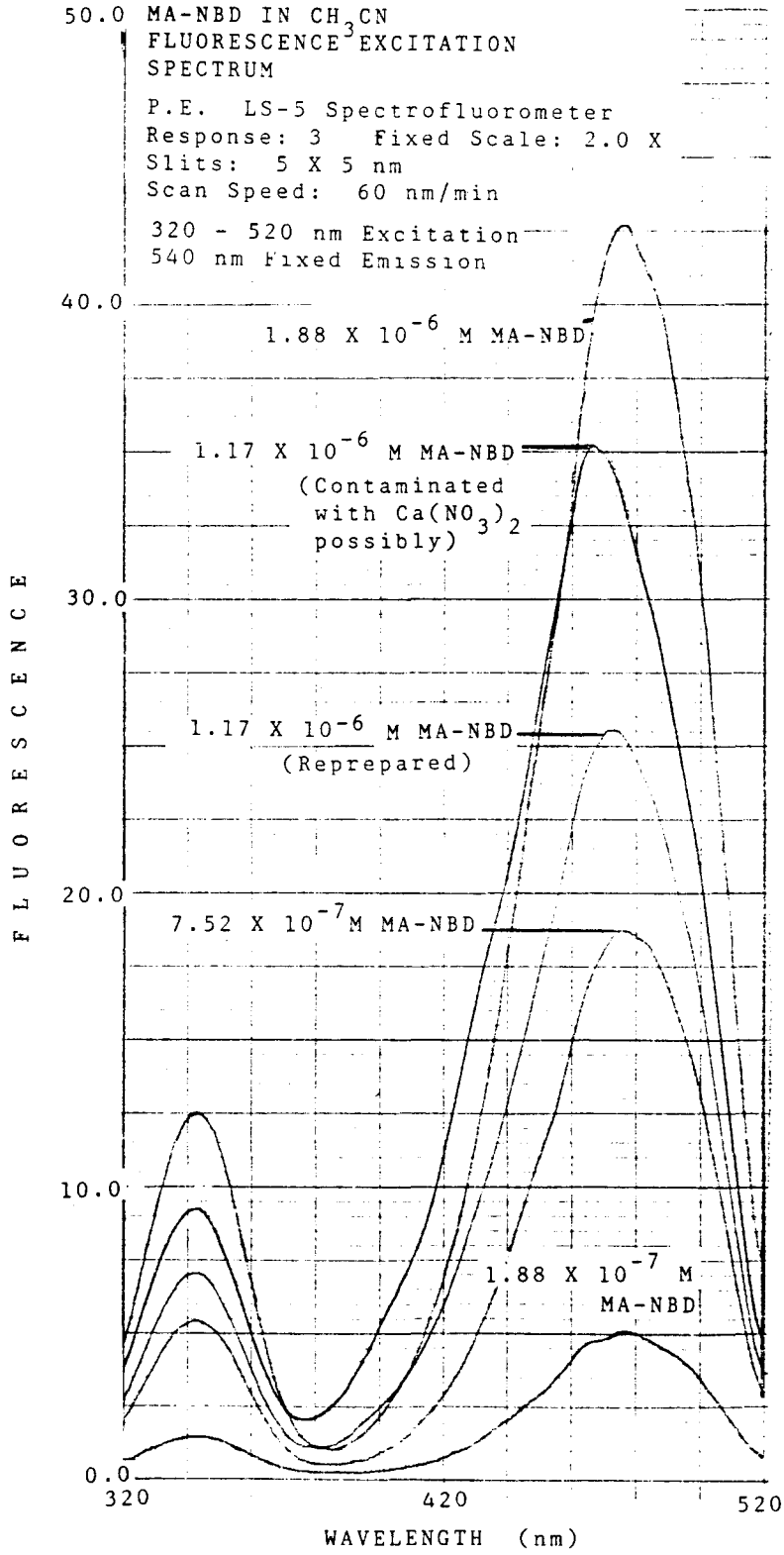
50.0
MA-NBD IN CH_3CN
FLUORESCENCE EXCITATION SPECTRUM
P.E. LS-5 Spectrofluorometer
Response: 3 Fixed Scale: 2.0 X
Slits: 5 X 5 nm
Scan Speed: 60 nm/min
320 - 520 nm Excitation
540 nm Fixed Emission
40.0
1.88×10^{-6} M MA-NBD
1.17×10^{-6} M MA-NBD
(Contaminated with $Ca(NO_3)_2$ possibly)
30.0
1.17×10^{-6} M MA-NBD
(Reprepared)
20.0
7.52×10^{-7} M MA-NBD
10.0
1.88×10^{-7} M MA-NBD
0.0
320
420
520
FLUORESCENCE
WAVELENGTH (nm)

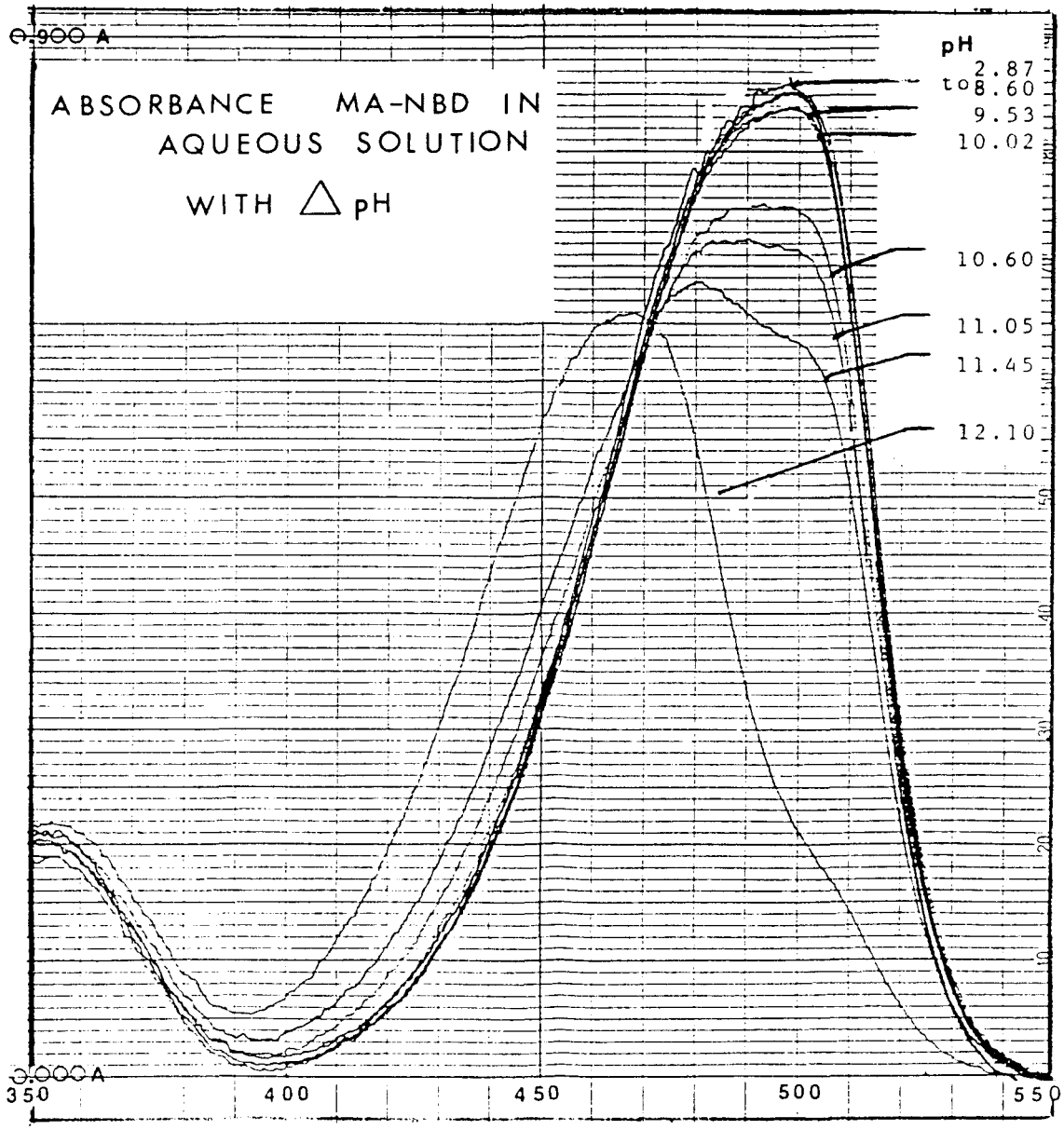
0.900 A
ABSORBANCE MA-NBD IN AQUEOUS SOLUTION
WITH △ pH
pH
2.87 to 8.60
9.53
10.02
10.60
11.05
11.45
12.10
0.000 A
350
400
450
500
550

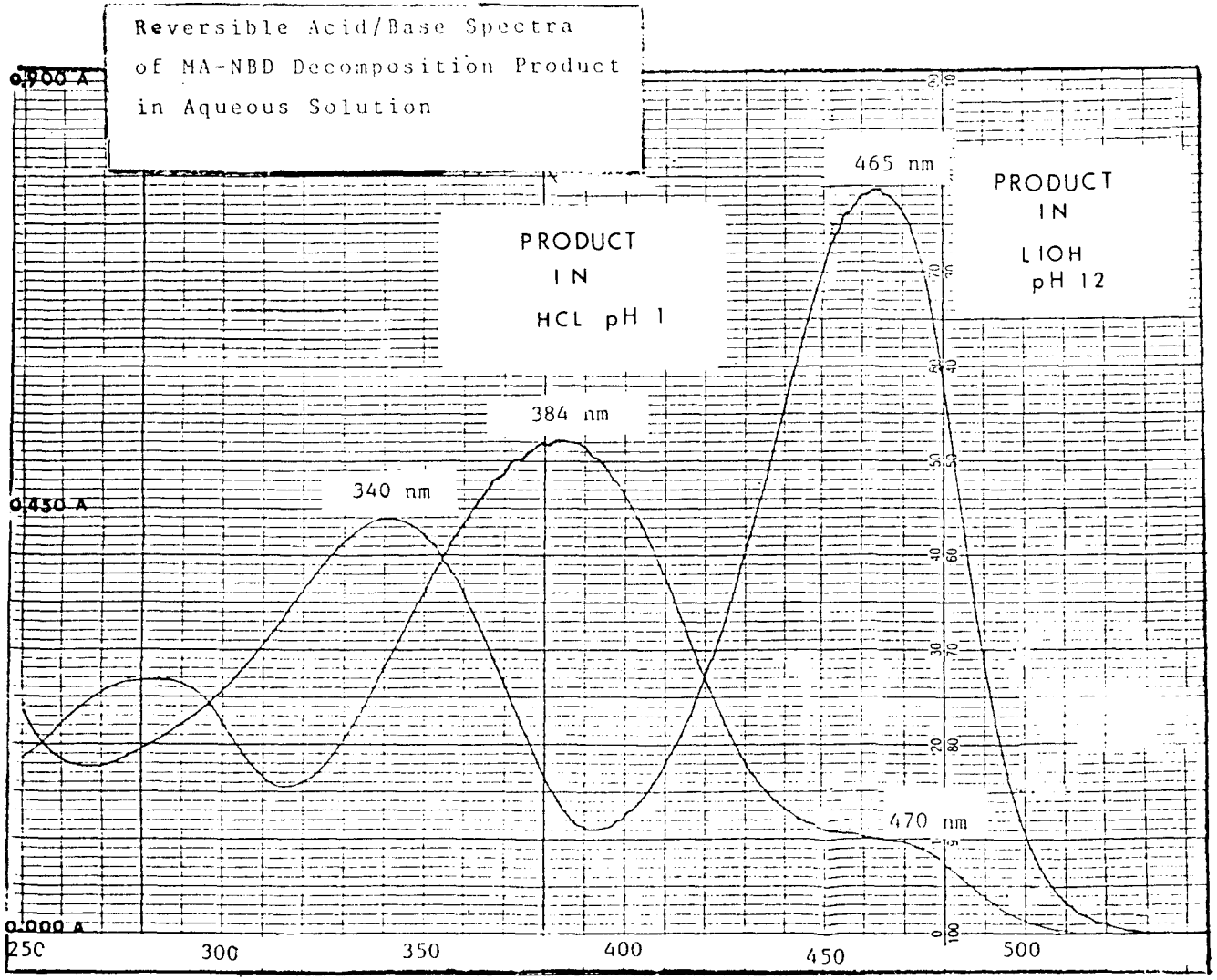
Reversible Acid/Base Spectra
of MA-NBD Decomposition Product
in Aqueous Solution
0.900 A
0.450 A
0.000 A
PRODUCT
IN
HCL pH 1
PRODUCT
IN
LIOH
pH 12
465 nm
384 nm
340 nm
470 nm
250
300
350
400
450
500

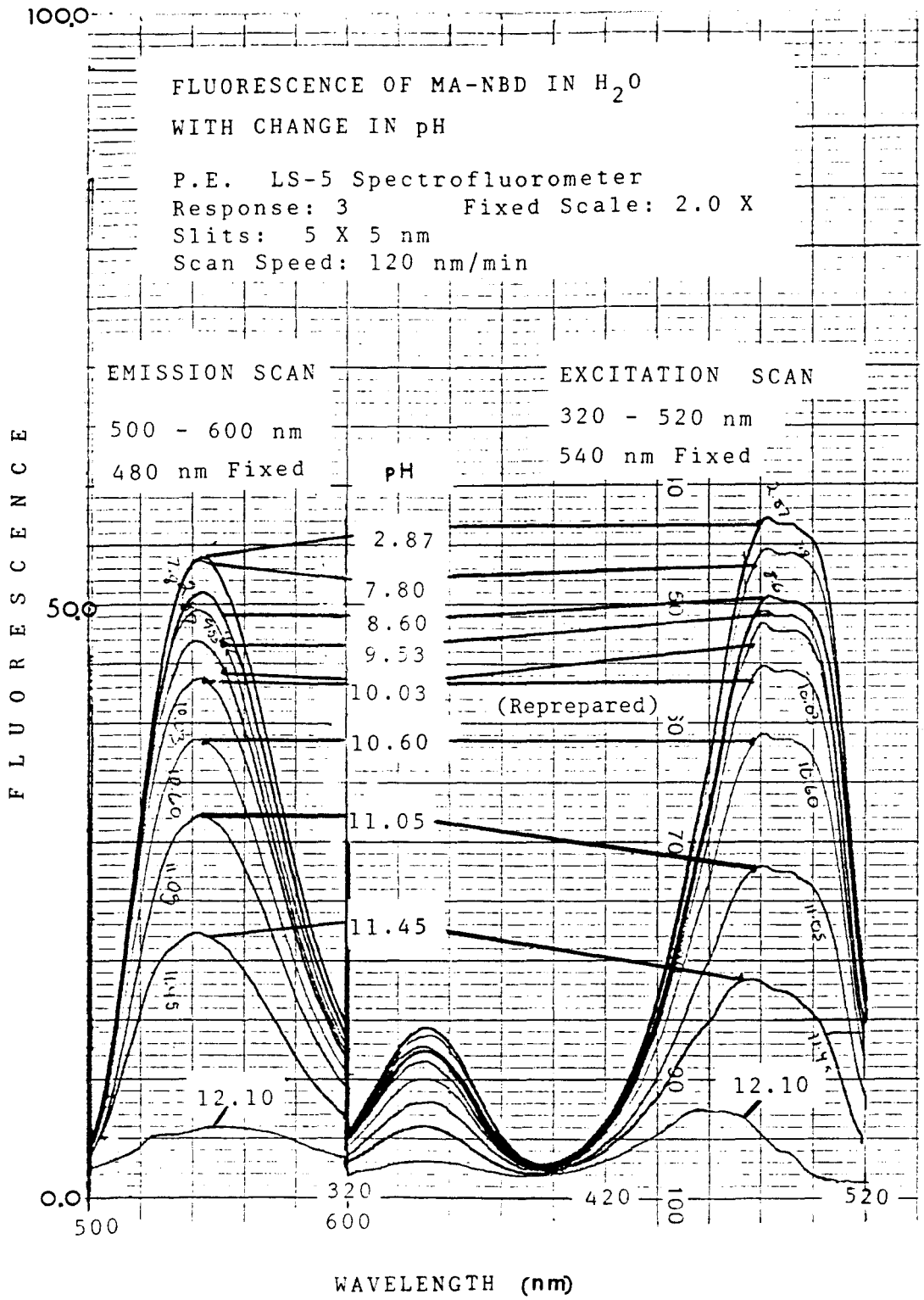
FLUORESCENCE OF MA-NBD IN H_2O
WITH CHANGE IN pH
P.E. LS-5 Spectrofluorometer
Response: 3 Fixed Scale: 2.0 X
Slits: 5 X 5 nm
Scan Speed: 120 nm/min
EMISSION SCAN
500 - 600 nm
480 nm Fixed
EXCITATION SCAN
320 - 520 nm
540 nm Fixed
pH
2.87
7.80
8.60
9.53
10.03
(Reprepared)
10.60
11.05
11.45
12.10
100.0
50.0
0.0
500
600
320
420
520
FLUORESCENCE
WAVELENGTH (nm)

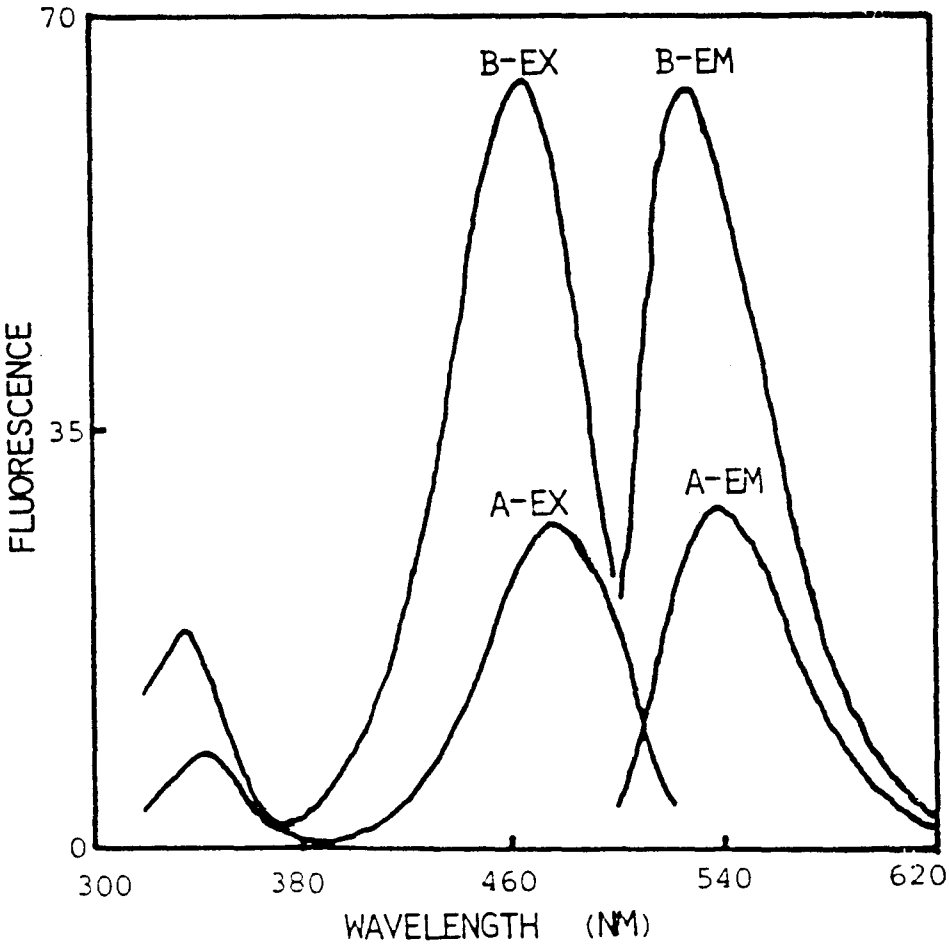

A - UNCOMPLEXED MA-NBD

B - COMPLEXED MA-NBD (F_{INT} X .10)

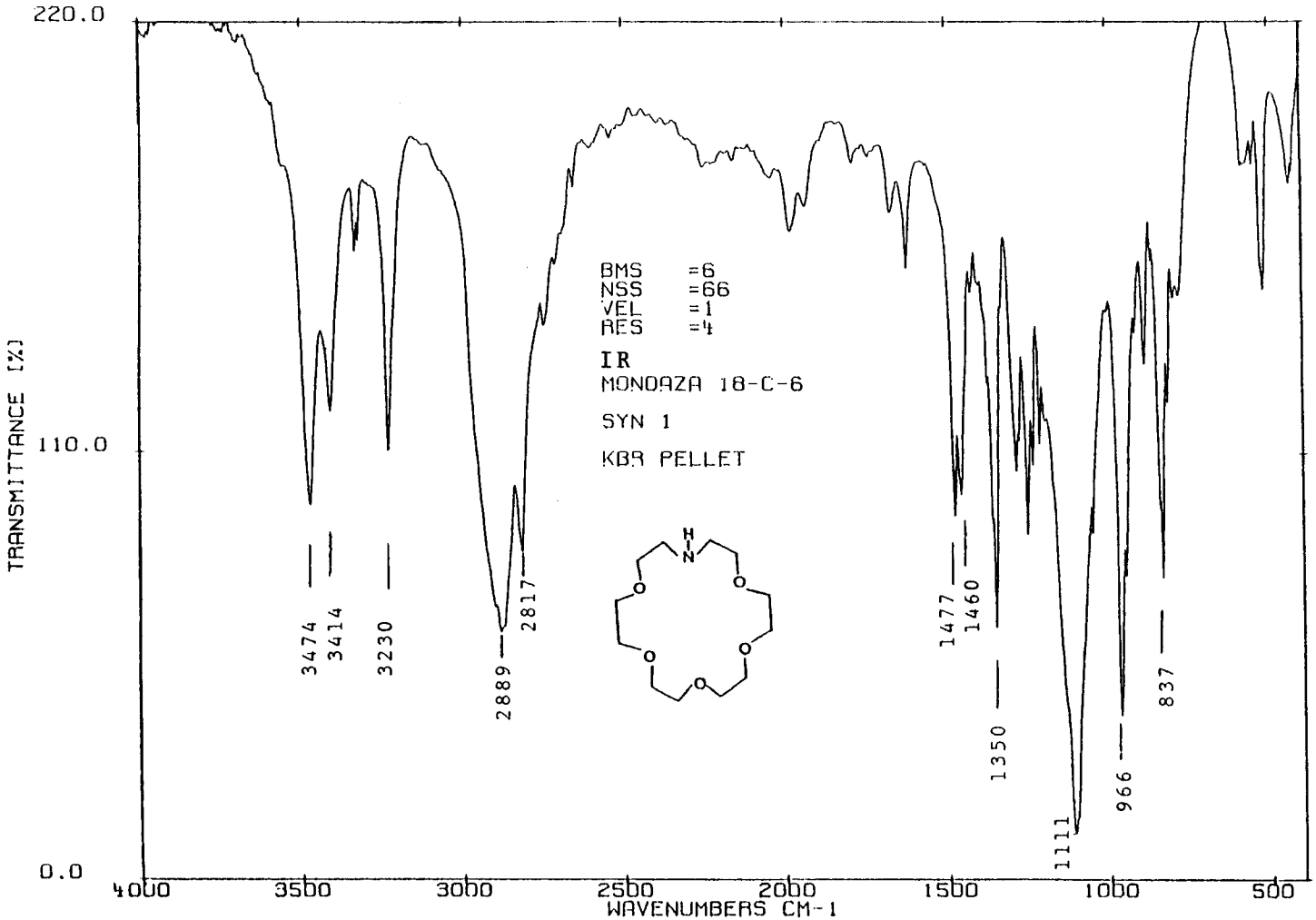
220.0
110.0
0.0
TRANSMITTANCE [%]
4000
3500
3000
2500
2000
1500
1000
500
WAVENUMBERS CM-1
BMS =6
NSS =66
VEL =1
RES =4
IR
MONOAZA 18-C-6
SYN 1
KBR PELLET
3474
3414
3230
2889
2817
1477
1460
1350
1111
966
837

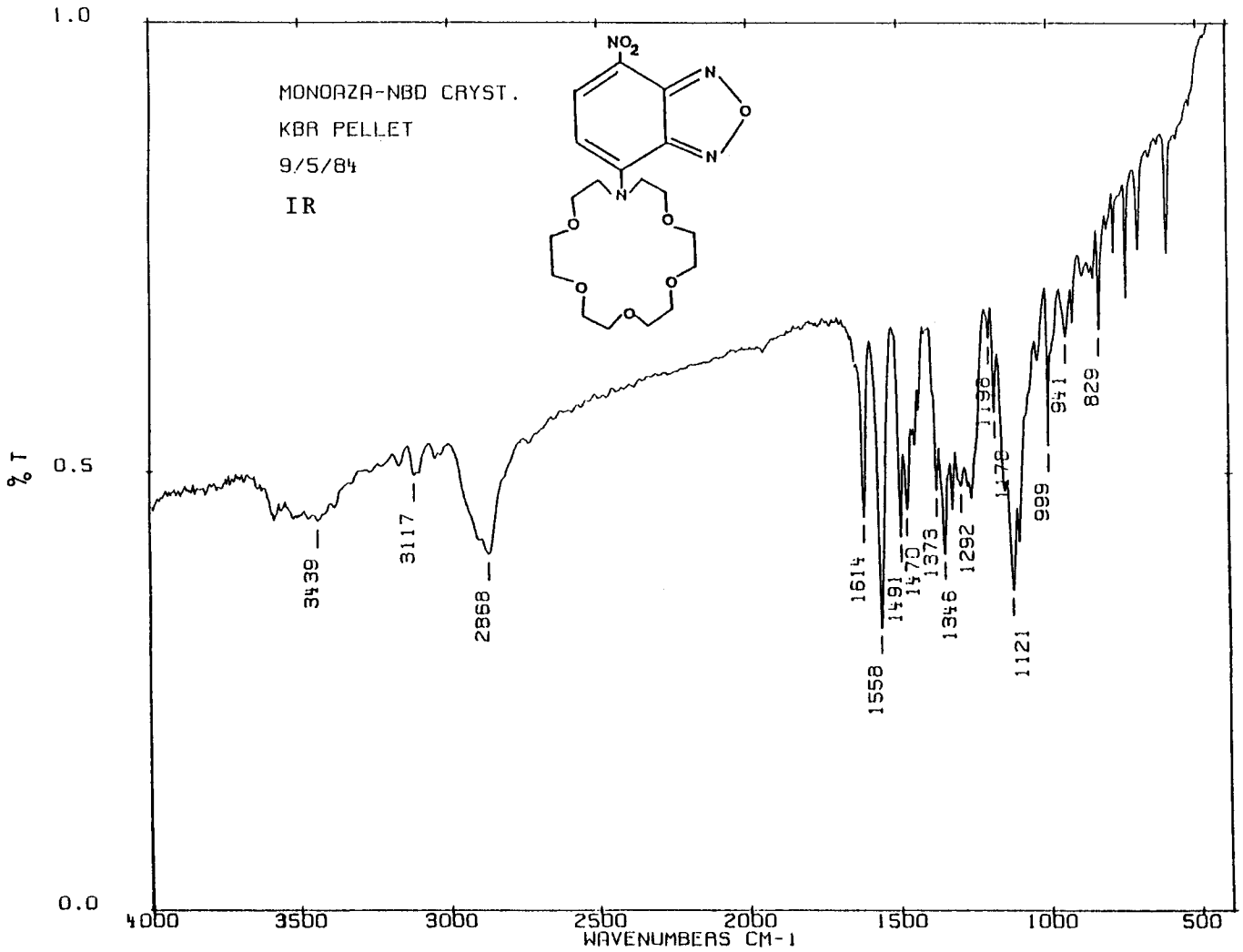
MONOAZA-NBD CRYST.
KBR PELLET
9/5/84
IR
NO2
N
O
N
N
O
O
O
O
O
O
1.0
0.5
0.0
% T
4000
3500
3000
2500
2000
1500
1000
500
WAVENUMBERS CM-1
3439
3117
2868
1614
1558
1491
1470
1373
1346
1292
1198
1170
1121
999
941
829

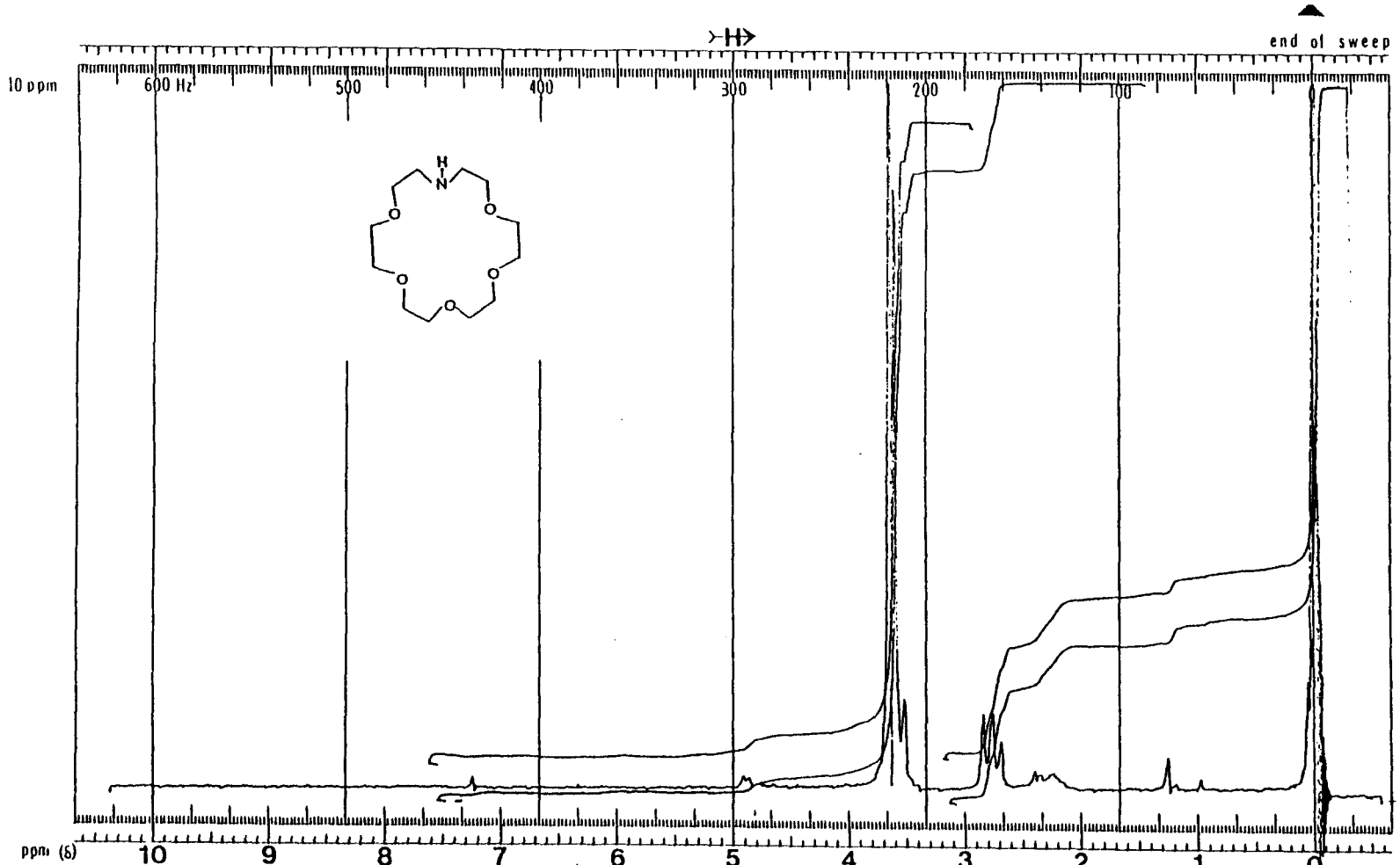

SPECTRUM AMPL 3.0 x 100 SWEEP TIME 5 min SAMPLE: MONOAZA-18-C-6 OPERATOR

FILTER 0.05 SWEEP WIDTH 10 ppm or Hz DATE 3/27/84

RF POWER 0.05 END OF SWEEP 0 ppm or Hz SOLVENT: $CDCL_3$ SPECTRUM NO

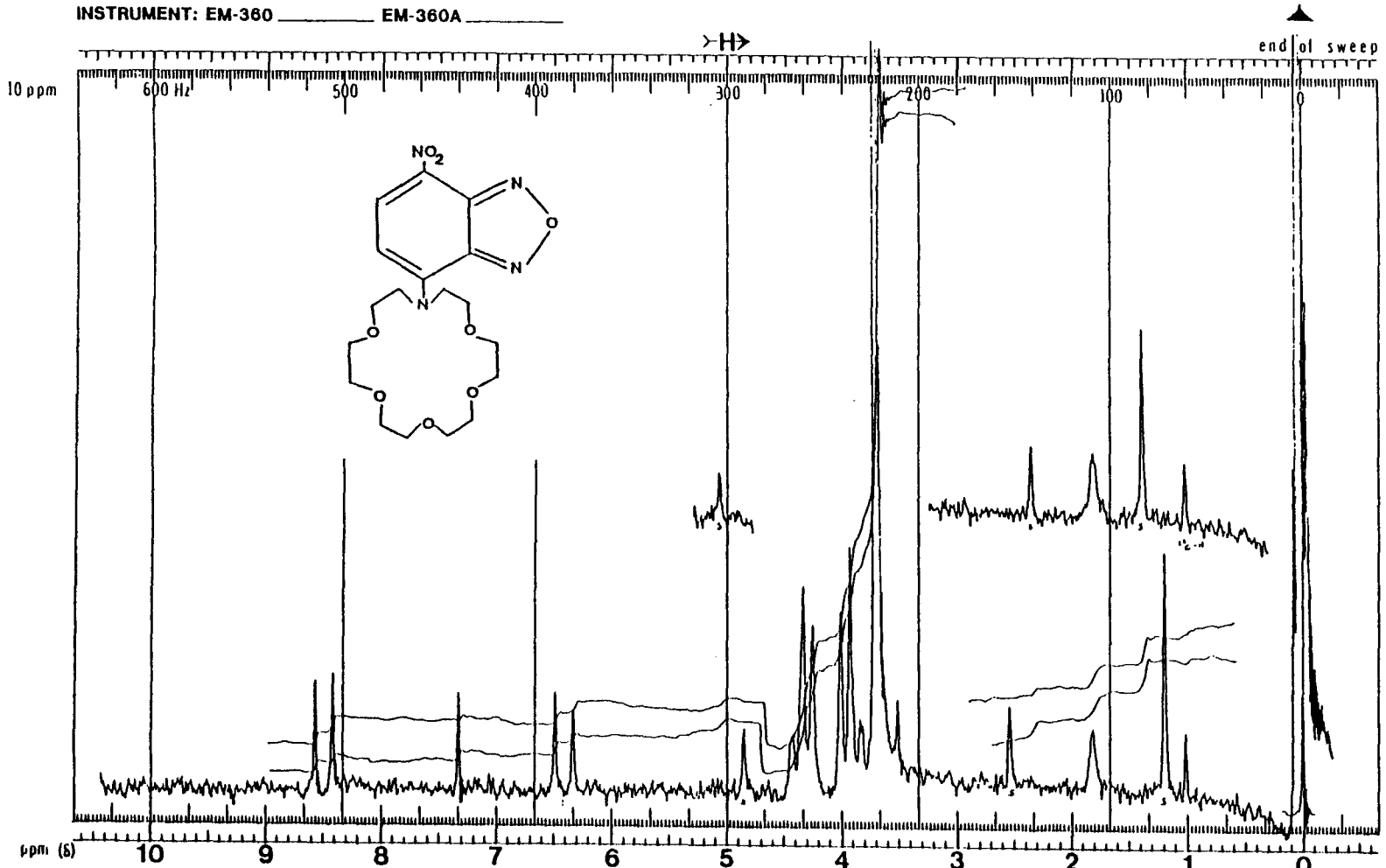
INSTRUMENT: EM-360 _____ EM-360A _____
10 ppm
600 Hz
500
400
300
200
100
0
end of sweep
NO2
N
O
N
N
O
O
O
O
O
O
ppm (δ)
10
9
8
7
6
5
4
3
2
1
0
SPECTRUM AMPL. 10 x 100
SWEEP TIME 5 min
SAMPLE: MA - NBD
OPERATOR
FILTER 0.2
SWEEP WIDTH 10 ppm or Hz
DATE 9/6/89
RF POWER 0.1
END OF SWEEP 0 ppm or Hz
SOLVENT: CDCl3
SPECTRUM NO

BIBLIOGRAPHY

1. Christensen, J. J.; Eatough, D. J.; Izatt, R. M., Chem. Rev. (1974), 74, 352-384.

2. Izatt, R. M.; Nelson, D. P.; Rytting, J. H.; Haymore, B. L.; Christensen, J. J., J. Amer. Chem. Soc. (1971), 93(7), 1619-1623.

3. Busch, D. H., Acc. Chem. Res. (1978), 11, 392-400.

4. Yoshio, M.; Nogouchi, H., Anal. Lett. (1982), 15(A15), 1197-1276.

5. Pedersen, C. J., J. Amer. Chem. Soc. (1967), 89(26), 7017-7036.

6. Christensen, J. J.; Hill, J. O.; Izatt, R. M., Science (1971), 174, 459-467.

7. Pedersen, C. J., J. Amer. Chem. Soc. (1970), 92, 386-390.

8. Frensdorff, H. K., J. Amer. Chem. Soc. (1971), 93, 600-606.

9. Izatt, R. M.; Rytting, J. H.; Nelson, D. P.; Haymore, B. L.; Christensen, J. J., Science (1969), 443.

10. Izatt, R. M.; Terry, R. E.; Haymore, B. L.; Hansen, L. D.; Dalley, N. K.; Avondet, A. G.; Christensen, J. J., J. Amer. Chem. Soc. (1976), 98, 7620-7625.

11. Izatt, R. M.; Terry, R. E.; Nelson, D. P.; Chan, Y.; Eatough, D. J.; Bradshaw, J. S.; Hansen, L. D.; Christensen, J. J., J. Amer. Chem. Soc. (1976), 98, 7626-7630.

12. Frensdorff, H. K., J. Amer. Chem. Soc. (1971), 93, 4684.

13. Pedersen, C. J.; Frensdorff, H. K., Angew. Chem. Int. Ed. Engl. (1972), 11(1), 16-25.

14. Pedersen, C. J., Fed. Proc. (1968), 27, 1305.

15. Pedersen, C. J., J. Amer. Chem. Soc. (1970), 92, 391-394.

16. Bourgoin, M.; Wong, K. H.; Hui, J. Y.; Smid, J., J. Amer. Chem. Soc. (1975), 97, 3462-3467.

17. Sinta, R.; Rose, P.S.; Smid, J., J. Amer. Chem. Soc. (1983), 105, 4338-4343.

18. Takeda, Y., Bull. Chem. Soc. Jpn. (1981), 54, 526-529.

BIBLIOGRAPHY, CONT.

19. Takeda, Y., Bull. Chem. Soc. Jpn. (1981), 54, 3727-3730.

20. Hasegawa, Y.; Suzuki, K.; Sekine, T., Chem. Lett. (1981), 1075-1078.

21. Hogan Esch, T. E.; Smid, J., J. Amer. Chem. Soc. (1969), 91, 4580-4581.

22. Wong, K. H.; Konizer, G.; Smid, J., J. Amer. Chem. Soc. (1970), 92, 666-670.

23. Sumiyoshi, H.; Nakahara, K.; Ueno, K., Talanta (1977), 24, 763-765.

24. Takagi, M.; Ueno, K., "Topics in Current Chemistry", Host-Guest Complex Chem. III., Boschke, F.L., Ed., Springer-Verlag: New York, 1984: pp 39-65.

25. Takagi, M.; Nakamura, H.; Ueno, K., Anal. Lett. (1977), 10(13), 1115-1122.

26. Ungaro, R.; El Haj, B.; Smid, J., J. Amer. Chem. Soc. (1976), 98, 5198-5202.

27. Mallinson, P. R.; Truter, M. R., J. Chem. Soc., Perkin Trans. II. (1972), 1818-1823.

28. Nakamura, H.; Takagi, M.; Ueno, K., Talanta (1979), 26, 921-927.

29. Nakamura, H.; Takagi, M.; Ueno, K., Anal. Chem. (1980), 52, 1668-1671.

30. Pacey, G. E.; Bubnis, B. P., Anal. Lett. (1980), 13(A12), 1085-1091.

31. Pacey, G. E.; Wu, Y. P.; Bubnis, B. P., Analyst (1981), 106, 636-640.

32. Bubnis, B. P.; Steger, J. L.; Wu, Y. P.; Meyers, L. A.; Pacey, G. E., Anal. Chim. Acta (1982), 139, 307-313.

33. Yamashita, T.; Nakamura, H.; Takagi, M.; Ueno, K., Bull. Chem. Soc. Jpn. (1980), 53, 1550-1554.

34. Nakamura, H.; Nishida, H.; Takagi, M.; Ueno, K., Bunseki Kagaku (1982), 31, E131-E134.

35. Nakamura, H.; Nishida, H.; Takagi, M.; Ueno, K., Anal. Chim. Acta (1982), 139, 219-227.

BIBLIOGRAPHY, CONT.

36. Kaneda, T.; Sugihara, K.; Kamiya, H.; Misumi, S., Tett. Lett. (1981), 22, 4407-4408.

37. Nakashima, K.; Nakatsuji, S.; Akiyama, S.; Kaneda, T.; Misumi, S., Chem. Lett. (1982), 1781-1782.

38. Shinkai, S., J. Amer. Chem. Soc. (1982), 104, 1967.

39. LeMoigne, J.; Gramain, P., J. Coll. Inter. Sci. (1977), 60, 565-567.

40. Nishida, H.; Tazaki, M.; Takagi, M.; Ueno, K., Mikrochim. Acta (1981), 1, 281-287.

41. Nakatsuji, Y.; Kobayashi, H.; Okahara, M.; Matsushima, K., Chem. Lett. (1982), 1571-1574.

42. Nakamura, H.; Sakka, H.; Takagi, M.; Ueno, K., Chem. Lett. (1981), 1305-1306.

43. Nishida, H.; Katayama, Y.; Katsuki, H.; Nakamura, H.; Takagi, M.; Ueno, K., Chem. Lett. (1982), 1853-1854.

44. Shiga, S., Bunseki Kagaku (1983), 32, E293.

45. Takagi, M.; Tazaki, M.; Ueno, K., Chem. Lett. (1978), 1179-1182.

46. Tazaki, M.; Nita, K.; Takagi, M.; Ueno, K., Chem. Lett. (1982), 571-574.

47. Uechi, T., Acta Crystallogr. (1982), B38, 433.

48. Dix, J. P.; Vogtle, F., Angew. Chem. Int. Ed. Engl. (1978), 17, 857-859.

49. Dix, J. P.; Vogtle, F., Chem. Ber. (1980), 113, 457-470.

50. Dix, J. P.; Wittenbrink-Dix, A.; Vogtle, F., Naturwiss. (1980), 67, 91-93.

51. Dix, J. P.; Vogtle, F., Chem. Ber. (1981), 114, 638-651.

52. Sousa, L. R.; Larson, J. M., J. Amer. Chem. Soc. (1977), 99, 307-310.

53. Shizuka, H.; Takada, K.; Morita, T., J. Phys. Chem. (1980), 84, 994-999.

BIBLIOGRAPHY, CONT.

54. Kina, K., Doctoral Thesis, Kyushu Univ. 1981.

55. Sanz-Medel, A.; Blanco Gomis, D.; Garcia Alverez, J. R., Talanta (1981), 28, 425-430.

56. Wolfbeis, O. S.; Offenbacher, H., Monatsh. Chem. (1984), 115, 647-654.

57. Steger, J. L.; Pacey, G. E., "Fluorescent Detection of Alkali Metals Using Crown Ethers", presented at the 15th Central Regional ACS meeting in Oxford, Ohio, 1983, Abstract #21.

58. Steger, J. L., "The Application of Crown Ethers in the Fluorometric Determination of Alkali Metals", Dist. Abstr. Int. 45 (8), (1984), DA8425434.

59. Skoog, D. A.; West, D. M., "Principles of Instrumental Analysis" 2nd Ed., Saunders College: Philadelphia, 1980.

60. Parker, C. A., "Photoluminescence of Solutions", Elsevier Publishing Co., LTD: Amsterdam, 1968.

61. Lakowicz, J. R., "Principles of Fluorescence Spectroscopy", Plenum Press: New York, 1983.

62. Bowen, E. J.; Wokes, F., "Fluorescence of Solutions", Longman, Green and Co.: London, 1953.

63. Jablonski, A., Z. Physik. (1935), 94, 38-46.

64. Seiler, N.; Demisch, L., Chapter 2 in "Handbook of Deriviatives for Chromatography", Blau, K.; King, G., Eds., Heyden: London, 1977.

65. Weber, G., Biochem. J. (1952), 51, 155-167.

66. Patacki, G., "Techniques of TLC in Amino Acid and Peptide Chemistry", Ann Arbor Science: Ann Arbor, 1968.

67. Cassidy, R. M.; LeGay, D. S.; Frei, R. W., J. Chromatogr. Sci. (1974), 12, 85.

68. Frei, R. W.; Lawrence, J. F., Chromatogr. (1973), 83, 321.

69. Udenfriend, S.; Stein, S.; Bohlen, P.; Dairman, W.; Leimgruber, W.; Weigele, M., Science (1972), 178, 871-872.

70. Toome, V.; Manhart, K., Anal. Lett. (1975), 8, 441-448.

BIBLIOGRAPHY, CONT.

71. Watanabe, Y.; Iami, K., Anal. Chem. (1983), 55, 1786.

72. Stein, S.; Bohlen, P.; Dairman, W.; Udenfriend, S., Arch. Biochem. Biophys. (1973), 155, 213-220.

73. Roth, M., Anal. Chem. (1971), 43, 880-882.

74. Gehrke, C. W., J. Chromatogr. (1979), 162, 293.

75. Hodgin, J. C., J. Liquid Chrom. (1979), 2(7), 1047.

76. Dunges, W., Chromatographia (1976), 9, 624.

77. Dunges, W., Anal. Chem. (1977), 49, 442.

78. Ghosh, P. B.; Whitehouse, M. W., Biochem. J. (1968), 108, 155.

79. Dal Monte, D.; Sandri, E.; Mazzaracchio, P., Bollettino (1968), 26, 165-180.

80. "NBD-Chloride", Regis New Product News, 1971; (Regis Chemical Co., 8210 Austin Ave., Morton Grove, IL 60053).

81. Price, N. C., Oxford University, Oxford England; Regis Applications Bulletin: "Applications of the Fluorogenic Reagent NBD Chloride: A Survey".

82. Monforte, J.; Bath, R. J.; Sunshine, I., Clin. Chem., (1972), 18, 1329-1333.

83. Brewster, J.H.; Ciotti, C.J., J. Amer. Chem. Soc., (1955), 6214.

84. Maeda, H.; Nakatsuji, Y.; Okahara, M., J.C.S. Chem. Comm., (1981), 471-472.

85. Gokel, G.W.; Dishong, R.A.; Schultz, R.A.; Gatto, V.J., Synthesis, (1982), 997-1012.

86. Maeda, H.; Furuyoshi, S.; Nakatsuji, Y.; Okahara, M., Tetrahedron. (1982), 39, 3358-3362.

87. Ahnoff, M.; Grundevik, I.; Arfwidsson, A.; Fonselius, J.; Persson, B.A., Anal. Chem., (1981), 53, 485-489.

88. Kolthoff, I.M.; Stenger, V.A.; Belcher, R., Volumetric Analysis, Interscience: New York: 1942-1957.

89. Walter, M.; Ramaley, L., Anal. Chem., (1973), 45, 165-166.

BIBLIOGRAPHY, CONT.

90. Aldrich Technical Information Bulletin, AL-134. Aldrich Chemical Company, 1983.

91. Aboderin, A.A.; Semakula, R.E.K.; Boedfield, E.; Kenner, R.A., FEBS. LETT., (1973), 34, 90-94.

APPROVAL SHEET

The dissertation submitted by Shelley A. Krause has been read and approved by the following committee:

Dr. Kenneth W. Street, Jr., Director
Assistant Professor, Analytical Chemistry,
Kent State University

Dr. Bruno Jaselskis
Professor, Analytical Chemistry, Loyola

Dr. Carl E. Moore
Professor Emeritus,
Analytical Chemistry, Loyola

Dr. David S. Crumrine
Associate Professor, Organic Chemistry, Loyola

Dr. John R. Ferraro
Professor Emeritus,
Physical Chemistry, Loyola

The final copies have been examined by the director of the dissertation and the signature which appears below verifies the fact that any necessary changes have been incorporated and that the dissertation is now given final approval by the Committee with reference to content and form.

The dissertation is therefore accepted in partial fulfillment of the requirements for the degree of Doctor of Philosophy.

August 7, 1989
Date

Kenneth W. Street Jr.
Director's Signature